DELFT UNIVERSITY OF TECHNOLOGY
Master Sustainable Energy Technology

MASTER THESIS

Valorization of coffee processing mill residues for bioenergy to support coffee processing

A technoeconomic study of Robusta coffee in Wayanad

August 16, 2024

AUTHOR Ben Jansen Verplanke *(5651751)*

SUPERVISOR Dr. Ir. Ralph Lindeboom
DAILY SUPERVISOR Sandra Iglesias Guerrero

Preface

This report was written by a student from the Technical University of Delft completing his master's program in Sustainable Energy Technology. The main focus of the master's curriculum is system integration to connect technology to socioeconomic benefits. The curriculum, which was divided into program tracks, focused on the following tracks: biomass, energy storage, and economics. The aim of this thesis is to combine the biomass and economics tracks while also covering the storage track. The choice for a technoeconomic study was based on the conviction that technology can never become successful without taking its economic and social value into account. The potential of technology should therefore be assessed not only in terms of its technical merits, but also in terms of socioeconomic factors.

This thesis combines an interest in sustainable technology, a passion for coffee, and a wish to keep enjoying a cup of joe in the future. Enjoying coffee should never compromise a fair price for the coffee producer, a sustainable method of coffee cultivation, nurturing valuable agricultural land with respect to nature, and a carbon-negative approach to the processing of coffee. I sincerely hope that the findings discussed in this work will benefit future research, and, more importantly, could benefit the Climate Smart Coffee Program in Kerala resulting in a more sustainable form of coffee processing in the future.

The reader was assumed to have basic knowledge on biomass conversion processes, electrochemistry, and the economic assessment of energy projects. Readers who would like to obtain background information on the subject and learn more about coffee as a crop, how it is processed, the types of biomass residues produced and their current uses, and the sustainability issues of the coffee value chain are invited to read Chapter 2 first. Readers who prefer to dive into the research sections directly can start their reading at Chapter 3.

My gratitude goes to my daily supervisor, Sandra Iglesias, for her support and patience during the months writing this thesis. Furthermore, this research would not have been possible without the data collected by Sandra on coffee processing in the Wayanad district in Kerala, India. I would like to thank my supervisor, Ralph Lindeboom, for his help in structuring the research and his input of new ideas and approaches to my research. Moreover, a special thanks should be given to Chaitanya Joglekar for his help with the chemical process modeling in Aspen Plus, which was still new to me. Additionally, I would like to thank Luis Cutz for his input during the kick-off of the thesis project and his role in the thesis committee and John Posada for his role in my thesis committee. Finally, credits should be given to my girlfriend, Sanne, for supporting me in starting this master's degree study 7 years after finishing my bachelor's program. Allowing me to quit my job and make a complete switch toward a subject I am more passionate about and being there for me every step on the way toward the completion of this thesis project.

I hope you enjoy reading my thesis research.

Haarlem, August 1st, 2024
Ben Jansen Verplanke

Abstract

Coffee is a beverage that millions of people around the globe enjoy on a daily basis. Although coffee consumption is becoming increasingly popular, the cultivation of coffee is under threat of: climate change, economic inequality in the coffee value chain, and unsustainable coffee cultivation and processing. Studies predict that all land currently used for the cultivation of Arabica coffee might become unusable by 2080 because of the sensitivity of the crop to changes in temperature, humidity, and the amount of UV irradiation. A shift is needed in the coffee value chain to ensure the livelihood of the current 25 million smallholder coffee farmers responsible for 70 to 80% of coffee production worldwide. The Climate Smart Coffee Program in the state of Kerala in India focuses on making coffee cultivation and processing more resilient, sustainable, and economical in the future. This is accomplished by conducting research on more sustainable agriculture (such as agroforestry to preserve and nurture valuable land) and reduce carbon emissions and waste generation during the processing of coffee.

The focus of this study is on the use of biomass residues produced during the processing of coffee to meet the energy needs of coffee processing units in the Wayanad district in Kerala. The goal is to make the processing of coffee less carbon-intensive, produce less waste, improve the quality of the coffee, and make coffee processing less energy dependent. This study presents a technoeconomic analysis for a novel approach to the use of these coffee processing mill residues (CPMRs) by using a combination of gasification to produce syngas, a solid-oxide fuel cell (SOFC) to transform the syngas into electricity and heat, and the use of an afterburner to further optimize the energy efficiency of the biomass plant. The biomass plant's goal is to replace the current energy need of the processing units: electricity from the grid and liquefied petroleum gas (LPG).

The results of the technoeconomic model show that the biomass plant produces enough electricity and heat to cover the energy needs of the coffee processing unit that supplies the biomass material. With an hourly feed rate of 1295 kilograms of biomass material the plant produced 2,681 kW of electricity with an electrical efficiency of 41% and an overall system efficiency of 62%. The financial analysis of the biomass plant yielded a capital expenditure of $ 24.1 million, or 8,984 $ per kWh of electricity generated. The levelized cost of electricity (LCOE) of the plant was 0.45 $/kWh. A sensitivity analysis revealed that by optimizing the operating conditions of the biomass conversion plant, the LCOE could be decreased to 0.35 $/kWh. Improving the capacity factor would have the most substantial effect on the costs of the system, increasing the days of operation from 90 in the base model to 300 could result in an LCOE as low as 0.12 $/kWh.

List of abbreviations

Abbreviation	Definition	Abbreviation	Definition
CAGR	Compounded average growth rate	MSW	Municipal solid waste
CapEx	Capital expenditures	NPV	Net present value
CCE	Carbon conversion efficiency	OpEx	Operational expenditures
CEPCI	Chemical Engineering Plant Cost Index	O&M	Operation and maintenance
CGE	cold-gas efficiency	PEM	Proton exchange membrane
CHP	Combined heat and power	ROA	Real options analysis
CPMR	Coffee processing mill residue	S/B	Steam/biomass
DCF	Discounted cash flow	SMR	Steam methane reforming
EAF	Electric arc furnace	SOFC	Solid-oxide fuel cell
ER	Equivalence ratio	TC	Total costs
FC	Fixed carbon	UV	Ultraviolet
LCOE	Levelized cost of electricity	VM	Volatile matter
LPG	Liquefied petroleum gas	WACC	Weighted average cost of capital
LHV	Lower heating value	WGS	Water-gas shift
HHV	Higher heating value		

Contents

1 Introduction

The cultivation and consumption of coffee are prone to change in the coming decades due to climate change. Large land areas currently used for coffee cultivation could become unusable due to a changing climate with reports that all agricultural land used for the cultivation of Arabica coffee could disappear by 2080. (Davis, Gole, Baena, & Moat, 2012) The majority of coffee in the world is produced by smallholder coffee farmers: approximately 70 to 80% of coffee is produced by over 25 million smallholder farms. (Barreto Peixoto, Silva, Oliveira, & Alves, 2023) Climate change is a direct threat to the lively hoods of these farmers and their local communities, which are dependent on the revenues generated from coffee cultivation. On the demand side, the market for coffee has experienced steady growth, with a 2.7% on average growth in worldwide coffee consumption between 2012 and 2021. (Wu et al., 2022) Without intervention, these two opposing trends substantially change the coffee market, with the highest costs being paid by the coffee farmers through the loss of their livelihoods.

The effects of climate change on coffee cultivation have been observed in the district Wayanad in the state of Kerala in India. Extremer weather is becoming more prevalent in the form of droughts and extreme heat. These conditions are expected to further intensify with climate change. (NLWorks, 2023) Low prices for coffee, low coffee quality due to difficulties in process control, and decreasing popularity of coffee farming due to human development and historic policy decisions all lead to a situation that could be described as an agricultural crisis within Kerala. (Seufert, Austin, Badami, Turner, & Ramankutty, 2023) To enable a future for the coffee farmers in Wayanad, which are resilient to climate change and price fluctuations in both the energy market and the coffee market, an integral transition to more sustainable coffee cultivation and processing needs to be made. Both ecological, environmental, social, and financial sustainability need to be achieved to become more resilient in the future. A sustainable coffee industry will allow for continued coffee consumption in the future with fair prices for coffee farmers and cultivation that maintains the fertility of agricultural land. (P. V. Aravind et al., 2022)

The use of bioenergy in the coffee value stream could help improve waste management, decrease carbon emissions, improve process control, support local communities in terms of their energy needs, and decrease outside dependencies on the electricity grid. The use of bioenergy is one of the pathways for India toward a net-zero future. Due to high feedstock availability, favorable policies, and high levels of political support, the use of biomass for electricity generation and biofuels is expected to grow substantially in the coming decades. (IEA, 2024) India produces over 840 million tonnes of agricultural waste per year. A large portion of this waste is already used, for example for domestic fuel. However, these residue streams are still underutilized resources that could be used for the benefit of local communities through better valorization of this biomass. (Cardoen, Joshi, Diels, Sarma, & Pant, 2015) The Climate Smart Coffee Program is a government-supported program focused on making the complete coffee value chain more resilient in the future. The program combines circular agroforestry, coffee cultivation, sustainable coffee processing, and future-proof energy systems to create a climate-resilient coffee industry to help and support smallholder coffee farmers in the Wayanad region. (NLWorks, 2023)

The aim of this study, in support of the Climate Smart Coffee Program, is to create a technical and economic blueprint to improve the usage and handling of coffee processing mill residues (CPMRs) from Wayanad by proposing a strategy to cover the energy needs of coffee processing units and, when available, to support local communities in terms of their energy needs. Using biomass residues produced during coffee processing could decrease the energy dependency of coffee farmers and coffee processing plants, increase coffee quality, increase bottom-line profitability, and improve their ecological footprint by reducing carbon emissions and waste generation. The outcome of this feasibility study shows the potential of biomass residues pro-

duced during coffee processing for the generation of energy and the economic viability of such a biomass conversion process.

This report is presented in the following structure. In Chapter 2, background information is presented to broaden the understanding of the biomass produced during the processing of coffee, its potential for energy production, its current uses, and the sustainability issues currently seen in the coffee industry. Additionally, the current energy consumption during coffee processing in Wayanad is discussed. Second, Chapter 3 describes the methodology of how the CPMR from coffee processing in Wayanad was converted into useful energy products and which assumptions were made while creating the model for this biomass conversion. Moreover, the economic model used to assess the financial viability of the biomass plant was described. Chapter 4 presents the results of the biomass conversion process with the outcomes of the technical and financial modeling. Furthermore, a sensitivity analysis was performed on a set of input parameters to test the validity of these models and optimize the technical and economic performance of the biomass plant. After the results section, the assumptions and results of this study are critically assessed in Chapter 5. The conclusions and recommendations of this research are presented in Chapter 6.

2 Background information

This chapter aims to provide the readers with background information on the production of coffee and its environmental and social challenges. With this information, the reader will be better equipped to understand the aims of this study and the assumptions that were made to create the technoeconomic model for the use of biomass residues produced during the processing of coffee beans to produce bioenergy.

In Section 2.1, information is provided on coffee as an agricultural crop and how this crop is transformed into the popular beverage that is consumed worldwide. In Section 2.2, more information is given about coffee as a commodity and the size of the worldwide coffee market and that of India and Kerala. Section 2.3 provides an overview of the different processing methods used in the coffee value chain. In Section 2.4, the biomass residues produced during the processing of coffee in Wayanad are discussed and the following section covers the current uses for these biomass residues. In Section 2.6, the energy use of coffee processing in Wayanad can be found. Sustainability issues related to the processing of coffee are covered in Section 2.7. The subsequent section (Section 2.8) provides more information on the Wayanad district in Kerala and the aims of the Climate Smart Coffee Program. In the final section of this chapter (Section 2.9), knowledge gaps were identified for the conversion of coffee processing residues to energy products.

2.1 Coffee

The term "coffee" refers to the beverage made from an extraction of roasted and ground seeds from the cherry of a coffee plant, also known as the *genus Coffea*. Coffee as a crop is cultivated in approximately 80 countries and is consumed as a drink on a daily basis all over the globe. (Murthy & Madhava Naidu, 2012) Coffee drinking originated in Ethiopia and coffee as a beverage has been consumed for at least 10 centuries. (Cruz-O'Byrne, Piraneque, Aguirre, & Ramirez-Vergara, 2020; Said, Abdullah, Ismail, Hasan, & Othman, 2023) There are over 100 species of *Coffea* plants from Latin America, Africa, and Asia. The main species are Arabica and Robusta, which are the only species that are commercially cultivated and traded for coffee making in the world's coffee markets. Liberica and Excelsa are well known species as well.(Febrianto & Zhu, 2023; Wu et al., 2022; Cruz-O'Byrne et al., 2020; Dong, Hu, Chu, Zhao, & Tan, 2017)

To transform the fruit from the coffee plant into the final coffee product, the following steps can be identified: coffee cultivation, coffee processing, roasting, grinding, and coffee preparation. All steps have an impact on the quality of the cup and the style of coffee that the end user wants to enjoy. (Febrianto & Zhu, 2023)

2.1.1 Anatomy of the coffee cherry

To make coffee from the fruit of the coffee plant, the fruit flesh and other layers of material need to be removed from the coffee beans inside the fruit which is done during coffee processing. The coffee cherry consists of an outer skin layer (exocarp), a fruit pulp layer (mesocarp), a pectin layer (also called the mucillage or parenchyma), and a parchment layer (endocarp). (Cruz-O'Byrne et al., 2020; National Coffee Association of U.S.A., Inc., 2023; Bastian et al., 2021; de Melo Pereira et al., 2019) After removing all these layers from the coffee, the green coffee bean is left. This green coffee is the coffee that is usually seen as the traded commodity on the world market. (International Coffee Organization, 2024) Silver-skin, also called the testa, epidermis or integument, is the single byproduct of the roasting process. (Martuscelli, Esposito, Di Mattia, Ricci, & Mastrocola, 2021; de Melo Pereira et al., 2019) An illustration of the anatomy of the coffee fruit is shown in Figure 1. Understanding the anatomy of coffee fruit is important for understanding the different biomass residues generated during coffee processing,

the challenges in the disposal of these residues, and their potential for conversion into useful (energy) products.

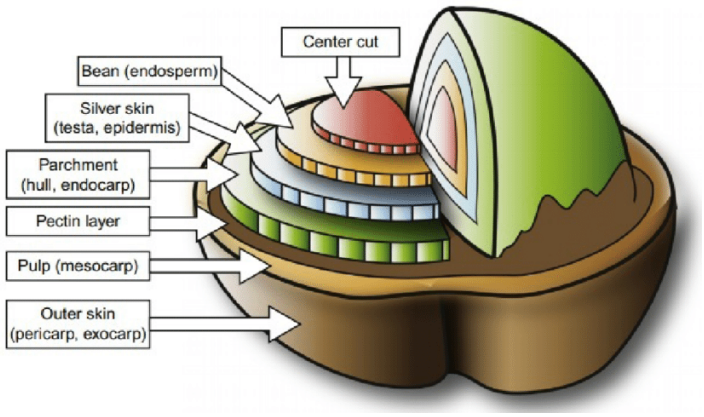

Figure 1: Illustration of the anatomy of a coffee cherry as published by Cruz-O'Byrne et al.. The outer skin, pulp, pectin layer, and parchment are removed during coffee processing to create the green coffee bean. The silver-skin is later removed during coffee roasting. (Martuscelli et al., 2021)

2.1.2 Differences between Arabica and Robusta

The main coffee species, Arabica and Robusta, have different chemical compositions. The composition is dependent on these intrinsic factors, genetic aspects within different varieties, and extrinsic factors such as the environment in which the coffee is cultivated, the soil, coffee roasting, storage of the coffee, and the preparation of the coffee (like espresso, filter coffee, and French press). (Wu et al., 2022; Várady, Tauchen, Fraňková, Klouček, & Popelka, 2022) Arabica coffee is grown at relatively high altitudes, whereas Robusta grows well at lower altitudes as well. Furthermore, Robusta plants tend to be more resistant to pests and UV rays which could help Robusta coffee plants adapt to climate change better than Arabica coffee plants. This is mainly because of their higher antioxidants contents, as shown in Table 1. Arabica is generally seen as the higher quality coffee product due to its lower acidity, higher sweetness, and more complex aromas in the cup caused by a wider variety of volatile compounds than Robusta coffee. (Wu et al., 2022)

2.1.3 Analysis of the coffee beans

People drink coffee due to the effects of the bioactive compounds in coffee beans, from which caffeine is the most studied compound. (Wu et al., 2022) The occurrence of these bioactive compounds has a substantial effect on the taste of the coffee endproduct and therefore has been thoroughly analyzed for the two main coffee species.

The drinking of coffee is associated with a multitude of health benefits due to the bioactive compounds naturally contained within the green coffee beans. These bioactive compounds can be roughly divided into phenolic compounds, alkaloids, and diterpines. (Wu et al., 2022; Várady et al., 2022) Phenolic compounds such as chlorogenic acids and gallic acid are natural antioxidants that help plants protect themselves against environmental threats, like microbes, UV radiation, insects and other plants. (Kumar & Goel, 2019) Green coffee beans are rich in phenolic compounds and approximately 6 to 10% of their dry mass is composed of chlorogenic acids. Among the alkaloids in green coffee beans, caffeine and trigonelline are the most common. Caffeine, a xanthine alkaloid, is a psychostimulant that antagonizes adenosine receptors within the brain, inhibiting the activity of adenosine molecules. The binding of adenosine onto the receptors of neurons is one of the mechanisms in the human body to induce sleep. (Janissen

& Huynh, 2018) Blocking these receptors with caffeine therefore causes a delayed reaction toward sleepiness and thereby improves fatigue and cognitive activity in the brain. (Wu et al., 2022) For an overview of the differences in the chemical composition of Arabica and Robusta, see Table 1.

Table 1: Occurrence of bioactive compounds (in gram/100 grams of coffee beans) in Arabica and Robusta coffee beans based on the work of Wu et al.. Robusta coffee has higher chlorogenic acid and caffeine contents than Arabica coffee. Arabica has a higher lipid content.

Coffee species	**Arabica**	**Robusta**
	average content in g/100 g	
Nutrients		
Soluble carbohydrates	9–12.5	6–11.5
Protein	9.8	9.5
Lipids	16.5	10
Water	8-12	8-12
Fiber	46-53	35-44
Minerals	4.2	4.4
Bioactive compounds		
Chlorogenic acids	6.5	10
Caffeine	0.8-1.4	1.7-4.0
Kahweol	0.7-1.1	-
Trigonelline	0.6-1.2	0.3-0.9

Numerous studies have linked the regular consumption of coffee with a reduced risk of diseases, such as Parkinson's disease, type 2 diabetes, cardiovascular disease and some types of cancer, due to the bioactivity of these phenolic and alkaloid compounds. (Wu et al., 2022) Other types of compounds are found within green coffee beans that have been linked to negative health effects, like diterpines, from which cafestol and kahweol are usually the main diterpines found in the coffee bean. These compounds are associated with increased cholesterol levels. Robusta coffees generally have lower kahweol contents than Arabica coffees do, as shown in Table 1. Caffeine consumption can also have negative side effects when it is consumed excessively. High caffeine consumption increases the risk of intestinal problems and negative cardiovascular side effects. (Wu et al., 2022)

2.1.4 Coffee quality

One of the goals of this study was to improve coffee quality together with the bottom-line profitability and environmental footprint of coffee processing. A clear definition of what high-quality coffee entails does not yet exist. It is a combination of the physical properties of the coffee bean, its chemical composition and the sensory experience of the coffee by the end-user. (Poisson, Blank, Dunkel, & Hofmann, 2017) Physical properties are related mostly to physical defects in the coffee bean, the size of the coffee bean and the uniformity of its size and shape. Coffee beans with few defects and contamination with other organic materials are generally considered physically high-quality coffee. This is influenced by coffee cultivation, harvesting,

processing, and storage of the coffee bean. (Febrianto & Zhu, 2023) The sensory experience of the coffee is the most important trait of the coffee product. The quality of the coffee is ultimately distilled toward this goal and all the different steps in the coffee-making process that influence the sensory experience are important for understanding coffee quality and improving it. Arabica is seen as qualitatively better coffee than Robusta because of its more flavorful aroma. The chemical composition of Arabica highlights this difference in quality. Research revealed that high-quality coffee generally has higher sucrose and acid contents, higher cafestol contents; and lower contents of caffeine, protein and chlorogenic acid. (Febrianto & Zhu, 2023) When looking at the earlier analysis of the chemical differences between Arabica and Robusta green coffee beans in Table 1, it becomes clear why Arabica is the winner in the coffee quality contest. Coffee brews made with Arabica are characterized by fruity notes and greater sweetness, while Robusta brews are more bitter and heavily bodied.

Since coffee quality is the main parameter that determines the coffee price, coffee producers would be wise to spend a considerable amount of effort in improving their coffee quality. This is especially true for Robusta coffee since this coffee species is lower in contents which generally make coffee drinking the pleasant experience it is. However, not all is lost for Robusta coffees. Coffee processing and roasting have a substantial effect on the chemical composition of the beans and could therefore benefit Robusta coffees, producing high-quality Robusta or 'fine Robusta'. Fine Robusta is the Robusta equivalent of the term 'specialty coffee', which is used for high-quality Arabica. (Febrianto & Zhu, 2023)

2.2 Coffee market

As mentioned earlier, only Arabica and Robusta coffees are cultivated and traded on a commercial scale. In the world coffee market, 60.5% of coffee exports were Arabica coffee and 39.5% were Robusta in 2023. (International Coffee Organization, 2024) Coffee is generally traded per bag of coffee where a bag contains 60 kilograms of green coffee beans. (USDA Foreign Agricultural Service, 2024) Over 90% of all traded coffee consists of green coffee beans, 0.6% of roasted coffee, and 8.8% of soluble coffee. The total coffee production is estimated to be 178 million bags of coffee by 2024, a 5.8% increase compared with the previous year. (International Coffee Organization, 2024) The largest coffee producing country is Brazil with a market share of 39.2% in 2023. India is number 7 on the list of coffee producing countries with a market share of 3.6% and a production of 6.1 million bags of coffee in 2023. (USDA Foreign Agricultural Service, 2024) Approximately 125 million people in the world are dependent on coffee cultivation for their livelihoods. (Barreto Peixoto et al., 2023)

In India, most coffee produced is Robusta coffee with a domestic market share of 78.7%. The state of Kerala is the second largest producer of coffee in India. Almost all of the coffee cultivated in Kerala is Robusta coffee, accounting for 95.1% of agricultural land used for the cultivation of coffee. (Foreign Agricultural Service, 2023) Robusta coffee was expected to yield approximately 1200 kilograms of coffee per hectare in India, whereas Arabica yielded just 360 kilograms per hectare in the 2022/2023 season. (Foreign Agricultural Service, 2023) In the district of Wayanad, only Robusta coffee is cultivated. Wayanad is the largest coffee-producing district in Kerala, with a total coffee production of approximately 61,000 tons in 2022, more than 17% of the total coffee production in India. (Ministry of Commerce and Industry, 2022) This share in India's coffee market shows the economic importance of the Wayanad district, even though Wayanad is just a small region (see Figure 16 in the Appendix).

The coffee market in India is estimated to grow substantially in the coming years with an expected compounded average growth rate (CAGR) of 9.87% until 2033. This growth is partly due to the growth of coffee consumption in the domestic market, exports are expected to grow as well. (Custom Market Insights, 2024)

2.3 Coffee processing

Coffee processing is used for sorting, depulping, and grading of the coffee cherries to convert the cherry to the green coffee bean. This green coffee bean is the end product of coffee processing. When coffee is mentioned as a commodity for trading, this green coffee bean is usually referred to. (de Melo Pereira et al., 2019; Febrianto & Zhu, 2023) Coffee processing is one of the main factors in obtaining a qualitatively high end-product, partly by eliminating damaged coffee beans, thereby increasing the overall bean quality. (Várady et al., 2022) The processing of coffee cherries can be broadly categorized into three main approaches: dry processing, wet processing, and semidry processing. (de Melo Pereira et al., 2019; Febrianto & Zhu, 2023; Said et al., 2023) Other emerging technologies are becoming more popular in search of a better and more distinguished sensory experience while drinking coffee.

Approximately 80% of Arabica and 20% of Robusta coffee are wet processed in India. The remaining coffee is processed through the dry process. (Foreign Agricultural Service, 2023) In the district of Wayanad, the dry process is the main processing method. (Iglesias, 2023) Figure 2 shows an overview of the coffee processing steps that are deployed in Wayanad both for dry and wet processing to obtain green coffee beans. This green coffee is subsequently roasted and ground to obtain the final product of the processing units in Wayanad: ground coffee. As mentioned earlier, most of the traded coffee on the world's coffee markets consists of green coffee beans. The roasting and grinding of coffee is usually not performed in the coffee processing unit but in the country or region of consumption.

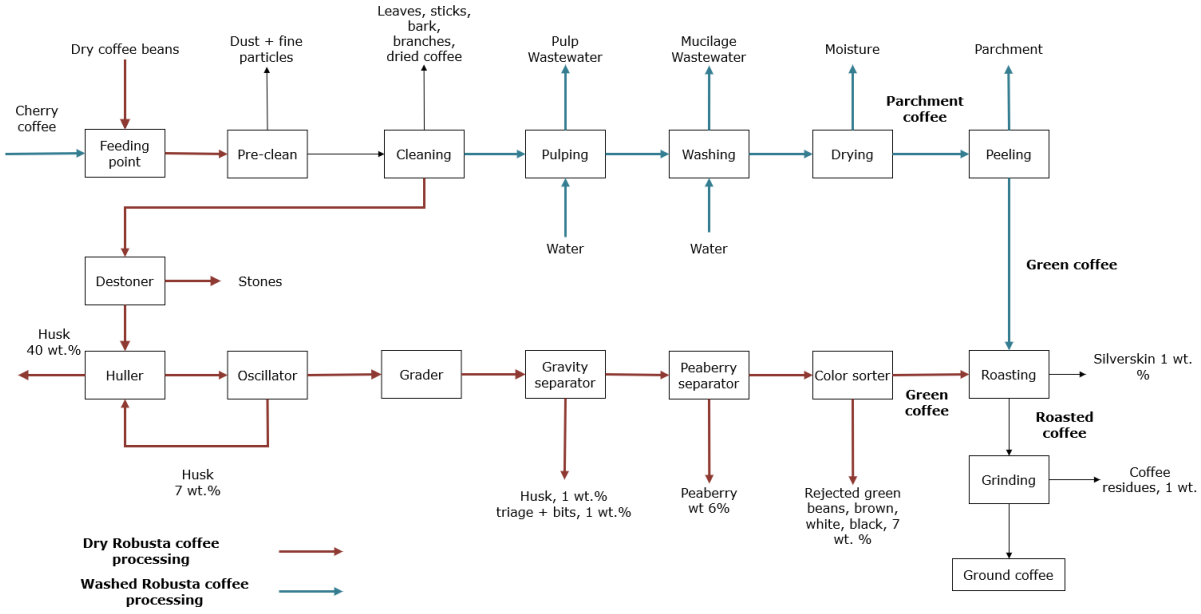

Figure 2: Detailed process flow of the dry and wet coffee processes from the coffee processing units in the Wayanad region of Kerala, India. (Iglesias, 2023)

In the following sections, the dry and wet processing methods are further described. For more information on the semidry process and more emerging processing technologies, see the Appendix.

2.3.1 Dry process

During dry processing, also called natural processing, the harvested coffee cherries are dried either naturally by the sun or by machine drying before the start of processing. This dry method is used most often since it is the least complex and least expensive processing method. Fur-

thermore, natural drying of harvested cherries is often the only available drying technique for smallholder coffee farmers. This method requires only the availability of sunlight and sufficient airflow to dry cherries. (Wu et al., 2022; Dong et al., 2017) The duration of drying is dependent on the ambient environment and can last up to 4 weeks. (Febrianto & Zhu, 2023) This step may seem arbitrary, but the drying method has a substantial effect on the bioactive components and volatiles in the green coffee beans.

The natural drying method has a substantial disadvantage. Drying exposes coffee cherries to contaminants, like dust or litter, as well as to birds, insects, rodents and fungi which can damage coffee beans. (Dong et al., 2017) Due to these environmental influences, high-quality coffee is usually difficult to obtain with the dry process. (Bastian et al., 2021) Other drying techniques, like hot air drying and freeze drying, could be used to improve process control. (Dong et al., 2017) When energy is more abundant and less expensive, sophisticated drying methods could become financially realistic. This could result in less damage to the coffee cherries during drying and therefore a higher quality end-product. Also, drying can be faster when these more advanced drying methods are used. (Wu et al., 2022)

After drying, the coffee fruit is removed from the coffee bean to obtain the green coffee bean via a process called hulling. In this process all layers of the coffee fruit (skin, pulp, mucillage and parchment) are removed from the coffee seed. (Várady et al., 2022) The residue obtained through hulling is called the coffee husk, which is the main residue produced during the dry processing of coffee as shown in Figure 2. Hulling is difficult when coffee fruit has a high moisture content. A moisture content that is too low could fracture the coffee bean during hulling. Therefore, coffee cherries are usually dried until they reach a moisture content between 10 to 15%. (Bastian et al., 2021)

2.3.2 Wet process

The wet process, also called the washed process, is often used for high-quality Arabica coffees. The process involves multiple steps that have higher technological requirements than the dry process has and is therefore more cost intensive. First, the coffee cherries are mechanically depulped to remove the skin and the pulp from the coffee fruit, leaving the mucilage and the parchment layer on the coffee bean. Depulping can be performed effectively only when the skin and pulp are ripened enough; otherwise, they cannot be easily disconnected from the rest of the coffee bean. Therefore, only the best and most ripe coffee cherries can be used, adding to the quality of the coffee end-product. The mucilage on the depulped coffee bean is then fermented until the mucilage is degraded by fermentation. This usually takes up to 2 days. This fermentation can take place with naturally occurring microorganisms or with an added culture. Sometimes fermentation is done under dry conditions, but in other cases, the coffee beans are submerged under water. (Febrianto & Zhu, 2023) After fermentation, the coffee beans are washed to remove the remains of the mucilage layer; hence, the process name. Wet parchment coffee, the name for the coffee bean with the parchment later still on the bean, remains after washing the coffee beans. The parchment coffee is then dried, which is comparable to the drying in the dry process. After drying the parchment is removed through hulling. (Várady et al., 2022; Febrianto & Zhu, 2023; Wu et al., 2022) This whole process is substantially faster than the dry process and is usually executed in 8 to 10 days, where the drying step is the most time-consuming. Compared with the dry process, the wet process results in more flavor and acidity in coffees. (Bastian et al., 2021) This process also produces completely different biomass residues from which organic waste water is the main product, as shown in Figure 2.

2.4 Byproducts from coffee processing

The end product of coffee processing, the green coffee bean, consists of only 18% of the weight of the harvested coffee cherry, and around 50 to 55% of the coffee cherry on a dry weight basis. (Adams & Dougan, 1987) The remaining dry weight contributes to the byproducts produced during processing. These residues produced during coffee processing and roasting are often called coffee processing mill residues (CPMRs) in the literature. (Said et al., 2023) In this section, the different byproducts of the dry process are discussed since most of the coffees in Wayanad are processed through the dry process. The waste streams are based on the detailed process flow of coffee processing in the Wayanad district in Kerala, India, by Iglesias, as shown in Figure 2.

Table 2: Process steps during the dry processing of Robusta coffee in Wayanad, India based on the work of Iglesias.

Process step	**Residue**	**Weight (kg/h)**	**wt%**	**Current use**
	Dried coffee cherries	2.600	100	
Precleaning	Leaves, branches & dust	0.025	0.96	-
Cleaning	Rejected coffee cherries	0.180	6.92	Instant coffee
Hulling & Oscillation	Husk	1.000	38.46	Fertilizer, animal bedding, briquettes, fuel
Gravity separation	Husk	0.010	0.38	See above usage
	Triage and bits	0.012	0.46	Instant coffee
Color sorting	Rejected green beans	0.170	6.54	Instant coffee
Peaberry separation	Peaberries	0.150	5.77	Instant coffee
	Green coffee beans	1.052		
Roasting	Silver skin	0.032	1.23	Composting
Grinding	Ground coffee residues	0.020	0.77	Composting
	Ground coffee	1.000		

2.4.1 Leaves & branches

Little is known about the amount of leaves and branches that are produced as residues in the literature. This residue is considered a contamination of the green coffee bean; therefore, removal of this material is essential for high-quality coffee. (Klingel et al., 2020) Due to the lack of data and the low volumes produced, this waste stream is disregarded within the scope of this research. It could be assumed that this waste stream could be used for direct combustion at the coffee processing plant. In Wayanad, approximately 1% of the weight of the dried coffee cherries contains leaves, branches, bark and dust and is removed during precleaning, as shown in Table 2.

2.4.2 Coffee husk

During the dry process, the coffee cherries are hulled to remove the different layers of the coffee fruit, leaving unwashed green coffee beans as the main product. The biomass produced is called the coffee husk, which contains dried coffee skin, pulp, mucilage and a parchment layer. All these layers are removed from the green coffee beans within one process step. Multiple studies reported a yield of approximately 12% coffee husk on a dry weight basis. (Alves, Rodrigues, Antónia Nunes, Vinha, & Oliveira, 2017; Janissen & Huynh, 2018) However, an analysis of the coffee processing units in Wayanad by (Iglesias, 2023) revealed that these units yielded around 42% of coffee husks during hulling. This value is not on a dry weight basis but is still substantially greater than the numbers reported in literature.

Coffee husk still contains relatively high fractions of bioactive compounds such as caffeine, chlorogenic acids and tannins. When released into the environment, these compounds could have a toxic effect on natural life. (Janissen & Huynh, 2018)

2.4.3 Defective green beans

Coffee beans that are too brown, black or white are removed from the green coffee beans. (Iglesias, 2023) These defective green beans have a somewhat different chemical composition than nondefective green beans. (Franca & Oliveira, 2008) The color of the defective bean is an indicator of the defect that is present in the coffee bean. Black and sour beans (often brown) are associated with fermentation problems, whereas white coffee beans tend to be immature coffee beans. Black beans cause heavy flavors and a sour taste, while white beans cause cup astringency. Since coffee quality is closely related to the chemical composition of beans, it is no surprise that the chemical composition of these defective green beans is (somewhat) different from that of nondefective ones. (Franca & Oliveira, 2008; Alves et al., 2017)

There is a market for these defective green beans to be used for other coffee products, such as instant coffee. (Iglesias, 2023) Therefore, the economic and environmental need for the use of this byproduct for the generation of energy products is lower than that for, for example, coffee husk.

2.4.4 Peaberries

The last cleaning step of the dry process aims to remove peaberries from the green coffee beans. In regular coffee cherries, two embryos are formed that, after fertilization, grow out to become the coffee beans (as shown in Figure 1). In a peaberry, only one of these embryos further develops into a coffee seed. (Fu et al., 2023) These peaberries have a distinct round shape, or peashape, hence their name, because they are not flattened at the side of the other coffee bean during growth. However, peaberries are smaller than regular coffee beans. These peaberries are removed from green coffee beans because of the market demand for consistent-looking coffee beans. These peaberries are often seen as waste, but this is changing. Peaberry coffee has shown outstanding tasting scores and is therefore becoming more relevant for commercial coffee products. (Duque-Dussán, Figueroa-Varela, & Sanz-Uribe, 2023) Peaberries generally have a natural occurrence of approximately 5 to 7% of the total harvested coffee cherries for both Arabica and Robusta coffee, so removing those as waste would incur a substantial loss. (Duque-Dussán et al., 2023; Fu et al., 2023) In the Wayanad district, peaberries constitute 5.77 wt% to the harvested and dried coffee. Just like defective green beans, peaberries are currently used for the production of different types of coffee products, including instant coffee. (Iglesias, 2023)

2.4.5 Silver-skin

Silver-skin is the sole byproduct produced during coffee roasting. During the roasting process, other products are also formed, but these are volatile and are released into the air. The silver-skin is tightly connected to the coffee bean and is therefore not detached from the bean during hulling. During roasting, the silver-skin does not expand like the coffee bean and therefore detaches from the bean and falls off. (Alves et al., 2017) Silver-skin is easy to extract from roasted coffee beans and relatively stable compared with other processing residues due to its low moisture content of around 7%. (Borrelli, Esposito, Napolitano, Ritieni, & Fogliano, 2004) In Wayanad, the silver-skin contributes 1.23% to the weight of the coffee cherry. (Iglesias, 2023) A low moisture content makes the silver-skin usable for direct combustion. However, the moisture content varies throughout literature. This is probably due to the intensity of roasting (light, medium, or dark), among other factors. (Janissen & Huynh, 2018)

2.5 Current utilization of coffee processing residues

All biomass byproducts from the coffee processing plants in Wayanad are being used. The main byproduct, coffee husk, is currently used as fertilizer, animal bedding, briquettes and other domestic fuel. (Iglesias, 2023) The uses of the different residues is summarized in Table 2. The use and/or disposal of coffee husk in the dry process is generally seen as the most challenging residue since it is the largest byproduct in weight that does not have a profitable use yet, and its direct disposal causes environmental problems. (Oliveira & Franca, 2015)

There are other concerns about the disposal of CPMR due to the caffeine, polyphenol, and tannin contents of many of the byproducts. (Janissen & Huynh, 2018; Alves et al., 2017) Although all of these compounds have been related to health benefits for humans, these compounds are also used by coffee plants as protection mechanisms against microorganisms (see section 2.1.2). When released into the environment, caffeine and tannins are toxic to (water) animals, plants, fungi and bacteria and can result in abnormal growth and reduced fertility within animals. Tannins have low biodegradability and therefore tend to remain in the environment for a long period of time. (Janissen & Huynh, 2018) Hence, the CPMR should preferably not be disposed directly into the environment to prevent ecological damage and environmental pollution. Fortunately, the CPMR already has a wide variety of uses and has grown passed the traditional, inefficient, uses such as animal feed, compost, and fertilizer. (Janissen & Huynh, 2018)

For coffee husk, a wide array of uses can be identified. (Oliveira & Franca, 2015) Below, an overview of the main uses of coffee husk, including the traditional forms of processing currently performed in Wayanad, as others like the production of bioenergy, is given.

2.5.1 Composting

Since coffee husk is high in minerals and has a relatively high lignin content, composting is considered the most cost-effective way to process coffee husk. (Hoseini, Cocco, Casucci, Cardelli, & Corti, 2021; Oliveira & Franca, 2015) Composting is a technique currently used to dispose of silver-skin and ground coffee residues in Wayanad (see Table 2). However, the direct use of these residues on agricultural land (silage) is limited by the high contents of phenolic compounds, caffeine, and tannins in the biomass material. Caffeine inhibits the growth of bacteria and other microorganisms responsible for degrading the biomass into compost. For the composting of high amounts of CPMR to be successful, the material first needs to be detoxicated to reduce caffeine and tannin concentrations. (Hoseini et al., 2021; Arya, Venkatram, More, & Vijayan, 2022) Detoxification has been successfully performed using certain fungal strains that feed on the caffeine and tannins. The composting of agricultural land is important for preventing soil erosion, maintaining and improving the soil itself and helps keep the soil porous,

which is important for allowing water and other nutrients to easily reach the roots of the coffee plants. Coffee husk has been successfully used as silage in mushroom beds, especially for shiitake mushrooms. However, even in mushroom beds, the efficacy of husk silage increases with fungal detoxification to decrease caffeine and tannin contents. (Hoseini et al., 2021) In addition to composting, coffee husk can also be pyrolyzed to convert the husk into charcoal: biochar. Biochar could be used to improve soil quality and reduce soil acidity. Agricultural land in the tropics tends to be quite acidic and low in certain minerals. Biochar from coffee husks can address both issues. (Hoseini et al., 2021)

2.5.2 Animal feed

Coffee husks, together with other byproducts from coffee processing, have been used as animal feed for a long time. The use of these residues has the benefits of reducing waste and decreasing food competition among other crops. Additionally, CPMR still contains large amounts of nutrients like protein, carbohydrates, and minerals. (Hoseini et al., 2021) However, the toxicity of many of the residues limits their use for animal feed, limiting the amount of, for example, coffee husk that could be included in livestock feed without impacting the quality of the feed. (Oliveira & Franca, 2015).

2.5.3 Solid fuel

Currently, coffee husk is used as a solid fuel in the form of briquettes and for direct combustion in Wayanad. Coffee husk has a calorific value of around 16 MJ/kg, which could make it a potential candidate for direct combustion. Direct combustion is the easiest form of processing of coffee husk for bioenergy. (Saenger, Hartge, Werther, Ogada, & Siagi, 2001) However, the direct combustion of coffee husk has its disadvantages, which are mainly high NO_x and CO_2 emissions. (Janissen & Huynh, 2018; Oliveira & Franca, 2015) Direct combustion is often performed in multiple steps while first producing briquettes through carbonization or pyrolysis of the biomass. Coffee waste could produce briquettes with 70% less processing cost and 80% higher energy density than unprocessed biomass. (Murthy & Madhava Naidu, 2012) The briquettes are subsequently used to produce heat through (co-)firing them in a heat furnace. The direct combustion of coffee husks presents challenges with respect to high emissions of pollutants. The high ash content and the low melting temperature of the ash content in coffee husk also lead to corrosion and other damage to the combustion furnace. (Oliveira & Franca, 2015)

2.5.4 Ethanol

The cellulose, hemicellulose, and lignin contents of coffee husk are similar to those of crops used for the production of bioethanol, such as sugarcane bagasse. (Hoseini et al., 2021) Bioethanol is already a widely used fuel replacement mixed with petroleum. However, for bioethanol to become a competitor for traditional fuels, the price should decrease and the issues around its competition with food production should be addressed. Coffee husk is a readily available and inexpensive feedstock and has a high carbohydrate content that allows for successful ethanol production. (Oliveira & Franca, 2015)

Gouvea, Torres, Franca, Oliveira, and Oliveira (2009) used acid hydrolysis and subsequent fermentation on coffee husk and reported that the yields were disappointing, probably due to high concentrations of caffeine and tannins in the coffee husk. Like for any microbial treatment of the coffee husk, detoxification of the biomass material would greatly improve the microbial activity and therefore the yield of the desired end-product.

2.5.5 Food industry

As mentioned earlier, coffee is a rich source of bioactive compounds like polyphenols and caffeine. Additionally, byproducts like coffee husk are rich in dietary fiber, such as cellulose, lignin, and minerals. Dietary fibers are important for a balanced diet and reduce the risk for gastrointestinal diseases and obesity. Coffee husk has also been shown to be used to extract anthocyanins, which can be used as pigments for food coloring. (Hoseini et al., 2021; Oliveira & Franca, 2015)

2.5.6 Chemicals

Most chemicals are currently products from the petrochemical industry and therefore based on crude oil. To decrease the dependency on crude oil, other synthesis routes for these chemicals need to be explored. Through fermentation, coffee husks has proven to be a good feedstock for the production of citric acid and gibberellic acid. (Hoseini et al., 2021) Through fermentation pathways, coffee husks can be used to produce enzymes such as pectinase, amylase, and caffeinase. (Murthy & Madhava Naidu, 2012) Coffee husk has also been shown to be a cost-effective option for removing pollutants from industrial wastewater as an alternative to high-cost activated charcoal. (Hoseini et al., 2021) Hejna (2021) showed the potential for the use of coffee byproducts to create (biodegradable) polymers. The antimicrobial properties of CPMR could enhance the protection of biodegradable forms of polymers due to its high concentrations of antioxidants. Furthermore, owing to the high cellulose, lignin, and protein contents of coffee husk, this byproduct could be suitable as a filler for wood polymer composites and as a plasticizer for these composites.

2.5.7 Materials

Coffee husk has been shown to be a useful product in the production of particle boards by substituting up to 50 percent of the wood material with coffee husk. Additionally, the use of coffee husks in the ceramic industry has been studied by adding coffee husks to a clay mixture. This improved the strength of the clay material studies. (Oliveira & Franca, 2015)

2.5.8 Biofuels

In literature, most research on the utilization of coffee husks for bioenergy has focused on the conversion of husks to syngas via either gasification or pyrolysis. Pyrolysis results in biogas, bio-oil, and biochar fractions. The sizes of these fractions are dependent on reaction parameters like temperature. Setter et al. (2020) reported that for the slow pyrolysis of coffee husk, the bio-oil fraction increased with increasing temperature, whereas the biochar fraction decreased. The pyrolysis of coffee husks produced a larger gas fraction than did the other fractions of end products, and this fraction seemed to increase with higher pyrolysis temperature. Compared to conventional pyrolysis, the pyrolysis through microwave treatment resulted in the production of more gas and a lower oil fraction. Additionally, this pyrolysis pathway produced more hydrogen in the syngas than using an electrical furnace, where CO_2 was the main product. (Oliveira & Franca, 2015) The gasification of coffee husk was found to be an appropriate technique for the low-cost production of biogas to be used directly on farms to reduce their dependency on fossil fuels. (Bonilla, Gordillo, & Cantor, 2019) Pala, Wang, Kolb, and Hessel (2017) created a computer model that showed promising results for the use of different types of biomass, including coffee husk, for gasification and Fischer-Tropsch pathways. de Oliveira, da Silva, Martins, Pereira, and da Conceição Trindade Bezerra e Oliveira (2018) concluded from their gasification experiments using coffee husk in Brazil that the process had good energy efficiency and that this waste-to-energy conversion should be further explored to support the energy needs

of the coffee-producing value chain and to positively impact both the costs and the sustainability of coffee production.

Through anaerobic digestion, which involves the microbial conversion of organic matter under anaerobic conditions, biogas can be produced, which is a mixture of methane and carbon dioxide. This process is sometimes referred to as biomethanation as well. (Oliveira & Franca, 2015) The biogas produced from CPMR could be used for roasting, and the waste heat from the roasting process could be used to predry the waste before further processing or drying the coffee mechanically for greater process control and to obtain higher-quality coffee. Coffee husk resists conversion to biogas through anaerobic digestion due to its acidic pH (4.3) and the presence of different toxic compounds, like polyphenols and caffeine. (Oliveira & Franca, 2015; Passos, Cordeiro, Baeta, de Aquino, & Perez-Elvira, 2018) Therefore, pretreatment is advised to increase biogas production. Jayachandra, Venugopal, and Anu Appaiah (2011) treated coffee husks with a thermophilic fungus to lower the acidity of the coffee husk material. This resulted in a biogas yield higher than that from fermented cow dung. This is due to the favorable composition of coffee husk, which has high carbohydrate and protein contents, resulting in a good C/N ratio for anaerobic digestion. (Aristizábal-Marulanda, Chacón-Perez, & Cardona Alzate, 2017) dos Santos, Adarme, Baêta, Gurgel, and de Aquino (2018) used ozonification as a pretreatment before anaerobic digestion of coffee husk to break down lignin and, to a lesser degree, hemicellulose but reported that the toxicity of the coffee husk caused inactivity of the microbial organisms responsible for anaerobic digestion. Using either powdered activated carbon or a two-step digestion process that separates the acidogenic and methanogenic stages yielded better results. Baêta et al. (2017) used a steam explosion pretreatment to improve the biodegradability and bioavailability of the biomass material for anaerobic digestion. Combined with the use of a combined heat and power system (CHP), they reported a yield of 0.59 kWh per kilogram of coffee husk.

For an alternative utilization process to be valid, it needs to be cost-effective and improve the environmental and ecological footprint compared with more traditional forms of handling, such as direct disposal, combustion, or animal feed. (Murthy & Madhava Naidu, 2012)

2.6 Energy consumption during coffee processing

To understand how CPMR could be used to generate energy for use in coffee processing, first, a good understanding of the total energy use during coffee processing and the type of energy sources used should be acquired. The energy use during the dry process in Wayanad was studied by Iglesias (2023). The process uses electricity for different processing steps, such as hulling, grading, and grinding. Roasting is the most energy intensive step of the coffee processing in Wayanad, which uses two different energy sources: liquefied petroleum gas (LPG) and electricity. (Iglesias, 2023) LPG is used to heat the coffee roasting drum, the apparatus used for roasting of green coffee. The heat required for roasting is dependent on the roasting temperature, which is typically between 180 and 250 °C, and the duration of roasting, between 7 and 20 minutes. The roasting process converts green coffee beans in light, medium, or dark roasted coffees. (Myhrvold, 2023) In total the process requires 291.2 Wh of electricity and 0.09 kilograms of LPG per kilogram of ground coffee produced. (Iglesias, 2023) A total overview of the energy use per dry process step is shown in Table 3.

2.7 Sustainability challenges in coffee processing

The sustainability of the coffee value chain is under pressure in social, economic, and environmental terms. (Barreto Peixoto et al., 2023) Environmental factors such as climate change, unsustainable land management, the use of harmful pesticides, and noncircular use of coffee residues have the potential to completely erase coffee cultivation in certain areas of the world.

Table 3: Energy use during coffee processing per processing step for the dry process in Wayanad based on the work of Iglesias (2023). Two types of energy carriers are used in the process: electricity and LPG. The energy use is normalized toward the production of 1 kilogram of ground coffee per hour.

Process step	**Energy use**	**Energe source**
Precleaning	1.0 Wh	Electricity
Cleaning	2.2 Wh	Electricity
Hulling	19.5 Wh	Electricity
Oscillation	1.3 Wh	Electricity
Gravity separator	8.6 Wh	Electricity
Destoner	1.9 Wh	Electricity
Color sorting	7.4 Wh	Electricity
Peaberry separation	3.0 Wh	Electricity
Grading	1.6 Wh	Electricity
Roasting	168.2 Wh	Electricity
	0.09 kg	LPG
Grinding	76.5 Wh	Electricity
Total	***291.2 Wh***	***Electricity***
	0.09 kg	***LPG***

(Poltronieri & Rossi, 2016) Coffee production throughout the world is under pressure due to rising temperatures and other changes in weather caused by increased greenhouse gas concentrations in the atmosphere. Coffee-producing regions like Wayanad already experience increased temperatures and intensified periods of drought. (NLWorks, 2023) Prospected changes in weather and climate could affect 80% of crops and 60% of the cultivated land in Colombia. In Ethiopia, increasing temperatures already kill Arabica coffee plants at a substandard rate. (Poltronieri & Rossi, 2016) Arabica coffee is especially sensitive to climate change due to the small range in temperature, humidity and other climate factors in which it can grow. (Barreto Peixoto et al., 2023) High and low temperatures affect the ripening of the cherry and could result in lower quality coffee beans. Models on the impact of climate change on Arabica coffee show that production could decrease between 65 and 100% by 2080 in the current regions where the crop is being grown. (Davis et al., 2012) Additionally, increases in average temperature and extreme temperatures increase the susceptibility of coffee plants to pests that damage the coffee plants. (Poltronieri & Rossi, 2016) Robusta plants are less susceptible to pests and UV radiation than Arabica due to their higher antioxidant and caffeine content, as mentioned earlier, but this does not mean that Robusta plants are immune to climate change.

Economic inequality still threatens coffee production and processing. Global crises such as the COVID-19 pandemic have worsened this inequality and made it more visible. Global coffee prices have been increasing in recent decades with increased consumption all over the world, but coffee farmers barely see any results of these increased prices due to an unfair profit distribution in the coffee chain and increased prices of labor and fertilizer, among other factors. Among the approximately 125 million people who are dependent on coffee cultivation for their

livelihoods, 50-100 million live below the poverty line. (Barreto Peixoto et al., 2023) Improving profitability for coffee farmers seems difficult in the current model since differentiation in the coffee product that allows for higher consumer prices mainly occurs in the cup and not in the green beans that are sold on international markets. Therefore, high-quality coffee beans are often still sold at commodity market prices. (Barreto Peixoto et al., 2023)

Coffee farmers are rarely involved in setting floor market prices. They are left out of the coffee value chain governance, giving more power to coffee roasters and distributors who ultimately profit from low green coffee prices. (Barreto Peixoto et al., 2023) This allows for coffee prices that do not include the real cost of producing coffee, including its negative externalities such as carbon emissions and social injustice. Owing to the high level of poverty among coffee farmers, social problems like poor working conditions, child labor, hunger, and gender inequality are the norm in a substantial part of coffee cultivation. (Barreto Peixoto et al., 2023)

2.8 Wayanad & the Climate Smart Coffee Program

Wayanad is a district in the southwestern Indian state of Kerala. Wayanad has one of the strongest agricultural sectors of all districts in Kerala but is also poorer than most other districts. Wayanad is one of the districts of Kerala with the highest elevation (1000 meters above sea level). (Seufert et al., 2023) Kerala is a unique region in India due to its high level of human development, despite its low economic growth. The factors influencing this level of development are a high level of gender equality and universal public education since the 1800s. Since the 1950s, effective policies by leftist governments in Kerala have resulted in active participation for most of the economy of the state, thereby reducing socioeconomic inequalities. In the 1960s, with the Land Reform Act, lands in Kerala were redistributed from wealthy land owners to poorer citizens, which created a large number of smallholders farmers, which is still seen to this day. (Seufert et al., 2023)

However, farming in Kerala is under pressure. In the last three decades, land prices and labor costs have increased, and interest in farming has decreased due to a shift in labor to higher education jobs, emigration to the Middle East, or skilled laborers moving to other, higher paying industries. (Seufert et al., 2023) Rising costs and more limited availability of workers have an impact on coffee quality as well. Farmers feel the need to reduce the number of times the coffee cherries are being harvested, which results in a less selective harvesting with respect to the ripeness of the cherries. Also, less attention and time are being paid to the drying of the coffee cherries. (Foreign Agricultural Service, 2023) Climate change already results in more extreme weather conditions in the form of droughts and extreme heat. In the 2022/2023 season, the amount of rainfall in Wayanad during winter decreased with 61% compared with its normal values. (Foreign Agricultural Service, 2023) Coffee plants are sensitive to these changes in conditions. Robusta, the main coffee variety in Kerala, is more dependent on regular rainfall since the plants are rooted less deeply than Arabica coffee plants are, which requires more irrigation for Robusta during the growing season. (Foreign Agricultural Service, 2023) Climate change therefore poses a risk for the livelihood of the many coffee farmers in the region. (NLWorks, 2023)

Kerala has one of the most developed agroforestry systems in the world. This system has been developed through large-scale community involvement. Having this support from the community should make it easier to further develop agroforestry systems toward environmentally friendly innovations in the form of carbon sequestration and carbon-neutral coffee cultivation and processing. The goal for further development would be to achieve carbon neutrality or even negative emissions while increasing welfare and protection against the negative effects of climate change and doing so in a manner that is socially accepted by local communities. (P. V. Aravind et al., 2022)

The Climate Smart Coffee Program aims to conserve, restore, and improve agricultural land where coffee is cultivated. Simultaneously, carbon is sequestered through the use of biochar and other soil-improving biomass. Emissions of greenhouse gases are reduced by the production of biofuels and the use of these biofuels for the processing of coffee, for which this study aims to support the program. The ultimate goal of the program is to increase the profits of coffee farmers, increase the quality of coffee, lower carbon emissions during cultivation and processing of coffee, and increase sustainable land use to mitigate the negative effects of climate change. (NLWorks, 2023)

2.9 Knowledge gaps

Substantial research has already been conducted on the conversion of CPMR to energy products. However, no specific research has been conducted on the Wayanad district in Kerala, India. Although extensive research has been performend on the gasification of coffee husks and, to a lesser degree, anaerobic digestion of coffee husks, to the best of our knowledge, no research has been done on the integral valorization of coffee husks to support the energy needs of coffee processing units. In such a coffee processing facility, two different energy carriers are required (LPG and electricity), and residual heat could theoretically be used for drying the biomass material or mechanical drying of the coffee cherries to improve process control and increase coffee quality by decreasing the fraction of defective cherries with fermentation issues. Additionally, when biomass is converted to syngas or biogas, limited research has been done on converting this gas to electricity in a cost-effective way. Finally, little is known about the economic viability of the biomass conversion pathways described in the literature.

3 Methodology

This chapter presents the methodology used to create the technical and economic blueprint of a biomass conversion system that transforms the biomass residues from the coffee processing units in Wayanad into useful energy products. In Section 3.1, the biomass type and availability of the biomass power plant are discussed. The overall process design of transforming these residues into energy products is covered in Section 3.2. Based on this process design, the different process steps were modeled using Aspen Plus V12 ® to understand the potential of CPMR and optimize the energy output of the biomass plant. These process steps are discussed in Sections 3.3 to 3.7. In the final section of the methodology, to understand the economic viability of the biomass conversion process, a description of the financial model for the biomass power plant can be found (see Section 3.8).

3.1 Biomass availability

The availability of coffee processing residues is dependent on when the processing of dried coffee cherries takes place. This processing of coffee cherries is dependent on the harvest and monsoon season. In the period between December and February, Robusta coffee is generally harvested and dried before the seasonal rains start at the end of March. (Foreign Agricultural Service, 2023) Processing is performed during work hours, and it is assumed that coffee is being processed in the harvest season, between 8.00 and 18.00, 7 days per week. This results in a total operational period of 900 hours per year (90 days x 10 hours) for the coffee processing plant.

In Wayanad, approximately twenty coffee processing plants serve more than 20.000 (smallholder) coffee farmers. The throughput of dried coffee cherries in these processing plants ranges from 1.5 to 12 tonnes per hour (see Figure 18 in the Appendix). (Iglesias, 2023) The assumption was made that the larger the coffee processing unit is, the more economies of scale could be achieved in the energy conversion process. The Perfetto Naturals plant in Panaram has a capacity of 8 tons of dried coffee cherries per hour, a relatively large coffee throughput. Therefore, the coffee throughput of Perfetto Naturals was used to determine the biomass feedstock availability in this study.

From the literature summarized in Chapter 2 and the data on coffee processing in Wayanad from Iglesias (2023), the conclusion could be drawn that the coffee byproduct with the greatest potential for more sustainable and profitable reuse would be coffee husk. Coffee husk has a wide range of uses, but almost all these uses have limitations and the recycling of coffee husk is seldom profitable. Additionally, it is by far the residue with the highest yield by weight, which makes it the residue with the highest potential for energy production (see Table 2 in Chapter 2).

As described in Section 2.4, for every kilogram of ground coffee, a total of 2.6 kg of dried coffee cherries are needed. In the processing of these cherries, a total of 1.01 kg of coffee husk is produced. A total throughput of 8 tonnes of dried coffee cherries per hour would result in coffee husk production of 3.1 tonnes per hour and 31 tonnes per day (with the assumption of 10-hour work days).

3.2 Process design

Coffee processing plants in Wayanad use two energy carriers: electricity and LPG. The aim of the biomass power plant is to use coffee husks from the coffee processing unit to cover the energy consumption of dry coffee processing, including roasting and grinding. Dry coffee processing in Wayanad requires a total of 291.2 Wh and 0.09 kilograms of LPG for the roasting of coffee

per kilogram of ground coffee. With the throughput of the selected processing unit of 8 tonnes of dried cherries producing a total of 3.08 tonnes of ground coffee per hour, the energy need would amount to 896 kWh of electricity and 277 kilograms of LPG per hour of operation.

To produce the required energy output, a multistep conversion process was deemed necessary. Single step conversion of biomass to electricity does exist using lignin electrolysis, but this technique was deemed nonviable for processing units in Wayanad owing to the immaturity of the technology and low energy conversion efficiencies. (Liu, Liu, Gogoi, & Deng, 2020) Due to the generally low moisture content of the produced coffee husk, the material was already dried before the coffee processing starts, the production of syngas through gasification was deemed the best biomass conversion technique. For other biomass conversion techniques, such as anaerobic digestion or hydrothermal liquefaction, a biomass feedstock with a relatively high moisture content is generally more advantageous. Furthermore, the high caffeine and antioxidant content of the coffee husk inhibit the activity of microbes used during anaerobic digestion. Pyrolysis has been used on coffee husks but generally yields a liquid fraction that is deemed less suitable for further conversion to electricity.

To generate electricity from the syngas, a solid-oxide fuel cell (SOFC) was chosen. Since both the gasification and the SOFC work at higher temperatures, this would benefit heat integration and system efficiency. Another advantage of using an SOFC for syngas is that an SOFC is not as selective toward the compounds in syngas as a proton exchange membrane (PEM) electrolyser. (Radenahmad et al., 2020) Syngas is a mixture of hydrogen and carbon monoxide gas, among other molecules like methane and hydrogen sulfide, and the SOFC is able to reform methane and carbon monoxide, producing hydrogen gas that can be subsequently oxidized to produce electricity. Therefore, an SOFC is better fitted to maximize the power production from syngas than a PEM electrolyser is.

To maximize the gasification-SOFC efficiency, this study uses a five-step conversion process. First, whether the biomass should be preprocessed before gasification was assessed. Second, the coffee husk will be transformed to syngas via gasification. Third, the syngas is cleaned to prepare the gas for injection into the SOFC. In the fourth step, the syngas is fed into an SOFC to produce the required electricity. Finally, the flue gas from the SOFC will be led through an afterburner to produce additional heat. This heat in the flue gas is subsequently used in a network of heat exchangers to supply heat for the coffee roasting drum, replace the need for LPG, and supply heat for the input streams of the gasifier and SOFC. This process is visualized in the block-flow diagram (BFD) in Figure 3.

The biomass conversion plant is assumed to operate for 24 hours a day, unlike the coffee processing unit, which operates only 10 hours a day. The difference in operating hours is due to the selection of an SOFC. SOFCs need a warm-up period before they are operational. This heating of the SOFC should be gradual due to the ceramic nature of its electrolytes. Heating the SOFC too quickly could cause thermal shock to the electrolyte and damage it. This means that operating an SOFC has limits with respect to its flexibility in operation. (Hami & Mahmoudimehr, 2023) With the assumption that the biomass plant operates during the same period (harvest season) as the coffee processing plant, the coffee husk availability would be 31 tonnes a day. Since the biomass plant runs continuously for 24 hours a day, the biomass feedrate is 1295 kilograms per hour.

In the following sections (3.3 - 3.7), the design assumptions that lay the foundation for the biomass conversion model are further discussed.

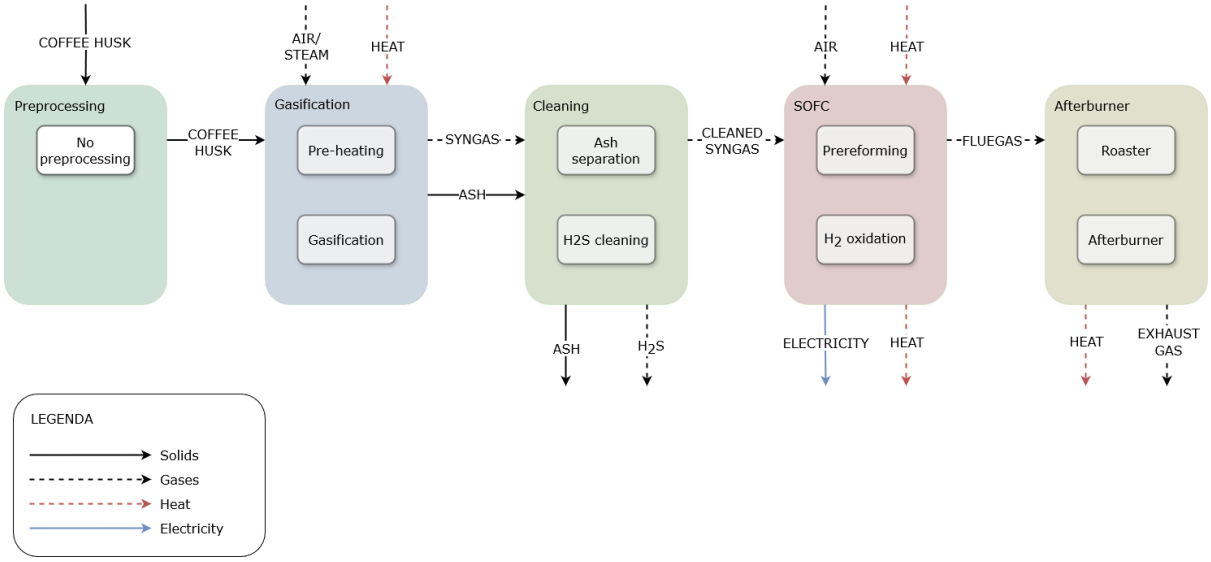

Figure 3: Block-flow diagram of a biomass power plant used to convert CPMR into electricity and heat to support the energy needs of a coffee processing plant in Wayanad, India.

3.3 Preprocessing

Preparing the biomass before gasification could have a substantial effect on the gasification performance and syngas composition. Preprocessing is generally done to change the moisture content of the biomass, clean the biomass of unfavorable compounds that could harm the catalyst or cause excessive tar formation during gasification, and control the particle size of the biomass. (Ruiz, Juárez, Morales, Muñoz, & Mendívil, 2013) The more intensive the biomass processing is, the more energy and cost-intensive the total process is. Therefore, avoiding preprocessing while allowing for good syngas outcomes would be preferable.

The moisture content of the biomass has an effect on the composition of the syngas produced in the gasifier. (Ruiz et al., 2013) Furthermore, the higher the moisture content is, the less stable the temperature in the gasifier is because the evaporation of moisture is an endothermic process. More energy will then be needed to keep the gasifier at a constant temperature. Additionally, temperature fluctuations within the reactor could lead to issues with fluidization (when applicable) and heavy coking of the reactor. (Motta, Miranda, Maciel Filho, & Wolf Maciel, 2018) A higher moisture content leads to a lower cold-gas efficiency (CGE) and higher heating values of the syngas. (Bonilla et al., 2019) The temperature within the gasifier remains relatively constant when the moisture content is lower than 15%. (Ruiz et al., 2013) To design a more or less constant syngas product, controlling the moisture content in the biomass is highly important. The moisture content of coffee husk is generally lower than 15 percent, with values in the literature averaging 10%. (Motta et al., 2018; Bonilla et al., 2019; Gouvea et al., 2009; Oliveira & Franca, 2015; de Oliveira et al., 2018) Therefore, for most gasification processes, the coffee husk will not have to be dried before use in a gasifier.

Another important parameter of biomass feedstocks for gasification is particle size. Generally, the larger the particle size is, the lower the biomass consumption rate and the lower the equivalence ratio (ER). (Ruiz et al., 2013) Reducing the particle size, generally done through grinding the biomass, increases the surface area and porosity of the biomass and breaks down lignin, which makes the biomass hard to decompose. Heat conduction from the gasifier into the biomass particles then becomes easier. The optimal particle size for gasification is dependent on the gasification process, the biomass type, and the requirements for syngas quality. (Anukam, Mamphweli, Reddy, Meyer, & Okoh, 2016) A disadvantage of the grinding of biomass as a

preprocessing method is that this size reduction is an energy intensive process and adds substantially to the energy needs of the biomass plant.

During the hulling process, where the coffee husk is removed from the green coffee bean, the husk material is already broken down. Therefore, the coffee husk does not have a uniform size distribution and varies up to a size of 9 millimeters. (de Oliveira et al., 2018; Bonilla et al., 2019) Furthermore, the biomass has a hollow semiellipsodial shape derived from the shape of the coffee cherry which makes its surface area larger and bulk density lower than those of other woody biomasses. (de Oliveira et al., 2018) The optimal particle size for pine bark was found to be between 2 and 6 millimeters. (Ruiz et al., 2013) However, pine bark has a higher volume-to-surface ratio than does coffee husk. Therefore, coffee husk seems to have a favorable particle size for gasification without grinding the material first. This finding is in line with multiple studies on the gasification of biomass that do not decrease the particle size before use. (Bonilla et al., 2019; de Oliveira et al., 2018)

A possible issue with gasification performance is the ash content of the biomass which could result in slagging and fouling of the gasifier. Poyilil, Palatel, and Chandrasekharan (2022) reported an ash content of 6.4% for coffee husk from Wayanad, which is relatively high in comparison with other types of biomass and other chemical composition analyses for coffee husk. Leaching of the biomass, a process in which the biomass is soaked in solvent to dissolve the salts in the biomass, among other (water-)soluble compounds, has the disadvantage that a drying step should be employed after leaching to reach the desired moisture content. (Yu et al., 2014) In other studies on the gasification of coffee husk, no such cleaning step has been deployed. (Bonilla et al., 2019; de Oliveira et al., 2018) Therefore, this form of preprocessing is not used in this study. When excessive slagging or fouling occurs, a form of cleaning can always be added to the biomass conversion process.

3.4 Gasification

This section describes the operating parameters used for the modeling and optimization of coffee husk gasification in Aspen Plus V12 ®. First, the assumptions that were used as a foundation for the model are described. Second, the Aspen Plus model, which was created to simulate energy generation from coffee husk, is discussed. Finally, the different operating parameters are explained: the gasification temperature, pressure, gasifying agent, and equivalence ratio.

3.4.1 Model assumptions

For the gasification model, the following assumptions were made (partially on the basis of the work of Pala et al. (2017)):

- The process is continuous (no batch processing)
- The process is steady state and isothermal
- The pressure and temperature are uniform in the gasifier chamber
- Gasification is performed at atmospheric pressure (1 bar)
- Tar formation is ignored, and the resulting char consists of ash only
- Ash is inert
- All the carbon from the biomass feed is converted (the carbon conversion efficiency (CCE) is 100%)
- All biomass-bound sulfur is transformed into H_2S gas

- Gases are considered ideal gases for the purposes of this study
- No heat loss is considered
- The compounds are in chemical equilibrium
- Nitrogen is inert (Abdul-Azeez, Suraj, Muraleedharan, & Arun, 2023)
- Pressure drops were neglected, both in the heaters and the gasifier

3.4.2 Model description

To calculate the thermodynamic properties of the conventional components, the Peng-Robinson equation of state with a Boston-Mathias modification (PR-BM) was chosen within Aspen Plus since this method is recommended for gas processing applications. Reasonable results could be expected for a wide range of temperatures and pressures when this method is used. (Pala et al., 2017)

Biomass is an unconventional input variable within Aspen Plus. The input variables for biomass are based on proximate and ultimate analyses of the biomass. For these input variables, the work of Poyilil et al. (2022) was used since they analyzed coffee husk from the Wayanad region. The proximate analysis was recorded on an air dry basis (ad) and resulted in a moisture content of 12.75%, a fixed carbon content of 14%, volatile matter content of 66.85%, and ash content of 6.4%. The ultimate analysis was performed on a dry ash-free basis (daf) and yielded a carbon content of 42.68%, a hydrogen content of 6.10%, an oxygen content of 48.88%, a nitrogen content of 1.92%, and a sulfur content of 0.42%. These numbers were slightly changed for the input in Aspen Plus to include the ash content in the ultimate analysis. The analysis of the chemical composition used is summarized in Table 4.

For the sulfanal analysis of the biomass feedstock in Aspen it was assumed that the total amount of sulfur belonged to organic compounds. For the particle size distribution, the size distribution from Bonilla et al. (2019) was used in the nonconventional mixed particle size model (MIXNCPSD), as shown in Table 4. To model the chemical properties of the biomass, the HCOALGEN model was used to determine the enthalpy parameters for the biomass with a user input for the heat of combustion based on the HHV of the biomass. For determination of the density of the biomass the DCOALIGT model was chosen.

In the Aspen Plus model, there are two input streams into the gasifier chamber, one for the biomass and the other for the gasification agent. Both streams are first heated to the gasification temperature within this model. The Aspen process model for the gasification step is shown in Figure 4. Typically, the biomass is directly fed into the gasifier, but since biomass is a non-conventional component in Aspen Plus, the biomass is first converted into conventional components based on the proximate and ultimate analysis of the biomass via a RYield reactor (DECOMP). After decomposition, the decomposed biomass components in the CONVEN stream are fed into the GASIFIER reactor.

A nonstoichiometric model was chosen for the gasification reaction based on the minimization of Gibbs free energy in a RGibbs reactor. Although this model shows more optimistic results than experimental results do, it is a good approach to model the upper limits of the gasification process with respect to conversion yields. The model gives good results with respect to the total hydrogen and carbon monooxide molar fractions. However, using a stoichiometric approach in Aspen Plus would yield results closer to the experimental reality. (Abdul-Azeez et al., 2023; Pilar González-Vázquez, Rubiera, Pevida, Pio, & Tarelho, 2021)

The gasification reaction of the Aspen Plus model is based on a total of nine different chemical reactions, such as carbon combustion, the water-gas shift (WGS) reaction and the Boudouard

Table 4: Chemical composition analysis of coffee husk from Wayanad based on the work of Poyilil et al. (2022). The particle size distribution was taken from Bonilla et al. (2019).

Proximate analysis	**daf wt%**	**ad wt%**
Moisture content	-	12.75
Fixed carbon (FC)	-	14
Volatile matter (VM)	-	66.85
Ash content	-	6.4
Ultimate analysis		
C	42.68	39.95
H	6.10	5.71
O	48.88	45.75
N	1.92	1.80
S	0.42	0.39
HHV	19.67 MJ/kg	
LHV	18.15 MJ/kg	
Bulk density	540 kg/m3	
Solid density	981.64 kg/m3	
Particle size distribution	**wt%**	
0.0-0.5 mm	13.15%	
0.5-1.0 mm	14.01%	
1.0-1.7 mm	20.54%	
1.7-2.0 mm	9.94%	
2.0-2.8 mm	20.60%	
2.8-4.0 mm	19.33%	
4.0-5.6 mm	2.33%	

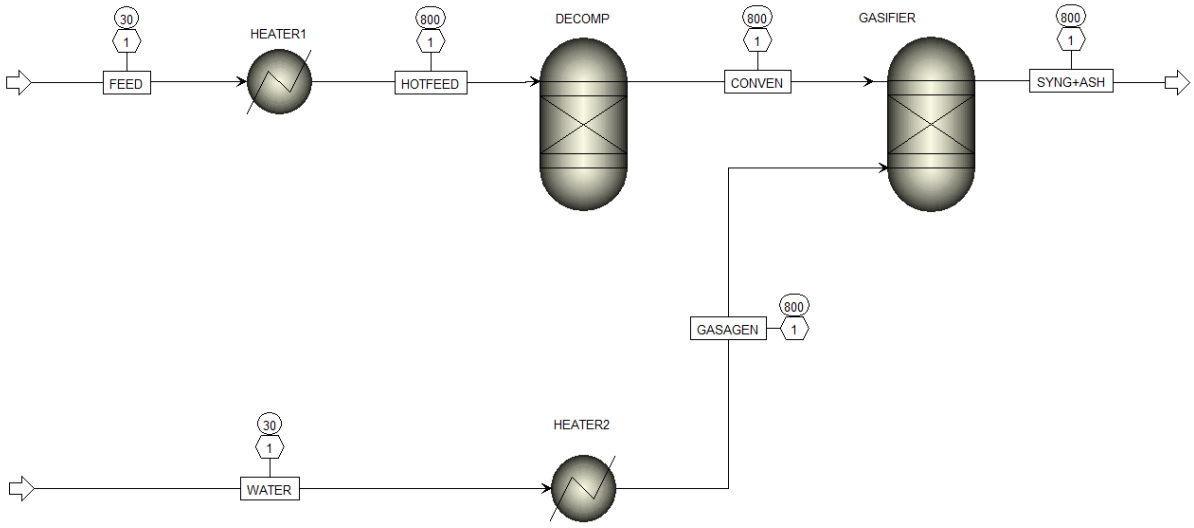

Figure 4: Process flow in Aspen Plus for the gasification of coffee husk including the heating of the biomass material in HEATER1, the decomposition of the biomass material to convert the nonconventional component into conventional components in DECOMP, the heating of water in HEATER2, and the gasification chamber in GASIFIER. The process model includes the temperature of the streams in degrees Celsius in the ovals and the pressure in bar in the hexagons above the streams.

reaction. A complete overview of the different chemical reactions that are included in the gasification model is shown in Table 15 of the Appendix.

In the following sections, the different operating parameters of coffee husk gasification are further discussed. These operation parameters were used as the basis of the process model in Aspen Plus and are outlined in Table 5.

3.4.3 Pressure

Atmospheric pressure was chosen to perform the coffee husk gasification. Higher pressures could be beneficial due to higher conversion efficiencies. The resulting syngas already being pressurized could benefit further processing of the gas. Although higher pressures have benefits, higher investment costs are incurred as well. Therefore, these higher pressures are often not economical for smaller scale operations. (Ruiz et al., 2013)

3.4.4 Temperature

According to de Oliveira et al. (2018), coffee husk gasification can be achieved from temperatures starting at 600 °C. However, good gasification performance has also been recorded with higher reaction temperatures. Based on a preliminary sensitivity analysis in Aspen Plus, temperatures between 600 and 1100 °C were tested (as shown in the sensitivity analysis results in Figure 9a). Based on these first tests, the optimal hydrogen molar fraction was determined at 800 °C. This optimal temperature for maximizing the hydrogen fraction in the syngas is in line with experimental and other modeling results from literature.(Begum, Rasul, Akbar, & Ramzan, 2013; Abdul-Azeez et al., 2023)

Table 5: Overview of the operating parameters used to model the coffee husk gasification of the biomass conversion model in Aspen Plus.

Operating parameter	Value
Biomass feed rate	1295 kg/h
Gasification temperature	800 °C
Pressure	1 bar
Gasifying agent	Steam
Steam/biomass ratio	0.1
Equivalence ratio	0.38

3.4.5 Gasifying agent and ratio

To identify the best gasifying agent, a preliminary sensitivity analysis in Aspen Plus was used to identify which gasifying agent (air, steam or a combination of both) yielded the best gasification results. Bonilla et al. (2019) recorded the optimal gasification conditions using an oxygen-steam mixture as a gasifying agent to optimize the H_2/CO ratio. Optimizing toward the hydrogen fraction in the syngas yielded optimal results using a 0.1 steam-to-biomass (S/B) ratio and no air. This 0.1 S/B ratio was used as a basis for the model.

3.4.6 Equivalence ratio (ER)

To understand the ER, both the S/B ratio and the stoichiometric ratio needed for complete decomposition of the biomass via steam should be understood. (Cerone & Zimbardi, 2021) The decomposition of the coffee husk feedstock can be described by Equation 2. To calculate the ER for steam gasification, the real steam-to-biomass ratio in the reaction is divided by the stoichiometric steam-to-biomass ratio, as shown in Equation 1. There are two sources of steam in the gasification reaction: the moisture content from the biomass and the steam from the gasification agent. Therefore, the total mass of steam in the gasification reactor is a combination of these two factors.

$$ER_{steam} = \frac{M_{H_2O}^{biomass} + M_{H_2O}^{steam}}{M_{H_2O}^{stoi}} \tag{1}$$

For the total mass of water needed for complete decomposition, the ultimate analysis composition of the coffee husk was used. Based on the molar mass of the different elements the structural formula for dry ash-free coffee husk is $C_{3.55}H_{6.05}O_{3.06}N_{0.14}S_{0.01}$. For total decomposition, 4.05 mol of water per mol of biomass is required on the basis of the 2X-Z molar fraction in Equation 2.

$$C_X H_Y O_Z + (2X - Z)H_2O \rightarrow (X)CO_2 + (\frac{Y}{2} + 2X - Z)H_2 \tag{2}$$

3.5 Syngas cleaning

Before the syngas can be fed into the SOFC, two reaction products from gasification need to be removed: ash and H_2S. Ash can lead to clogging and fouling of the system components and needs to be reduced to a few ppm to prevent this. (Radenahmad et al., 2020) H_2S gas is

generally allowed up to a maximum value of 1 ppm to protect the anode material of the SOFC. (Rahim et al., 2023) However, P. Aravind and de Jong (2012) reported that reducing the sulfur concentration of the syngas to a sub-ppm level (<10 ppm) is still acceptable for the oxidation performance of hydrogen in SOFCs with a Ni/GDC anode. A review from Rasmussen and Hagen (2010) on the use of an SOFC operating at a temperature of 850 °C fueled with biogas revealed that a maximum of 7 to 9 ppm H_2S was acceptable for a Ni-YSZ anode.

For the removal of ash, a hot-gas cleaning filter could be used to avoid the cooling of the product gas from gasification, which would decrease energy efficiency. (Radenahmad et al., 2020) The filter removes the solid ash particles from the product gas. For the purpose of this study, it was assumed that all ash could be removed through this method. In the Aspen model, this ash separation was achieved through a Separator block as shown in Figure 5.

There are multiple processes available for the removal of H_2S from syngas, which are typically divided into wet desulfurization and dry desulfurization. Wet desulfurization typically occurs at low temperatures and ambient pressures where dry desulfurization is performed at lower and higher temperatures. Traditionally, a wet process is used with a scrubber for large-scale commercial applications. (Rahim et al., 2023) Since the syngas produced during gasification has a high temperature, a high-temperature gas cleaning method is preferable for energy efficiency. Additionally, owing to the requirement for H_2S concentrations of less than 10 ppm, many of the absorptive solvents used in wet desulfurization are not usable for integration with an SOFC. Due to the attention given to thermochemical biomass conversion techniques like gasification, interest for high-temperature gas cleaning techniques increased over the past decade. (Rahim et al., 2023) Quite some of these techniques are still in their development phase and have drawbacks in terms of their reactivity with hydrogen and CO in the syngas and deactivation of the absorptive material. Additionally, some of the researched materials do not have the adsorptive qualities to integrate with an SOFC. (Rahim et al., 2023) A review on high-temperature desulfurization by P. Aravind and de Jong (2012) revealed that hot gas cleaning using a zinc titanate absorbant yielded <10 ppm sulfur levels after cleaning while being stable up to a temperature of 873 K and atmospheric pressure. A disadvantage of this method is that the remaining H_2S has an effect on methane reforming in the SOFC, but this effect is negligible for low methane contents in the syngas. (P. Aravind & de Jong, 2012) A dry process that results in high H_2S and CO_2 absorption rates for syngas is cryogenic distillation. (Li et al., 2022) But, since this cleaning method uses a low temperature, it has some of the same disadvantages as most wet cleaning methods.

Based on this brief review on cleaning options for the sulfur content, for this research, a zinc titanate absorption method was assumed at 600 °C (873 K) temperature and atmospheric pressure to minimize energy losses. For the purpose of this model, the remaining H_2S gas in the syngas was set to 5 ppm, which is in line with the experimental results of P. Aravind and de Jong (2012). The cooling of the syngas and the desulfurization of the syngas in the model are shown in the model overview in Figure 5.

3.6 SOFC

After the cleaning of the syngas to eliminate ash and the majority of the H_2S gas, the syngas is converted to electricity via a solid-oxide fuel cell (SOFC) to support the electricity need of the coffee processing unit. In this section, the Aspen model, which was created to estimate the potential of syngas for electricity production, is described. This includes: the model assumptions, the different components used in the Aspen software, and the electrochemical model for the calculation of the cell voltage and power output.

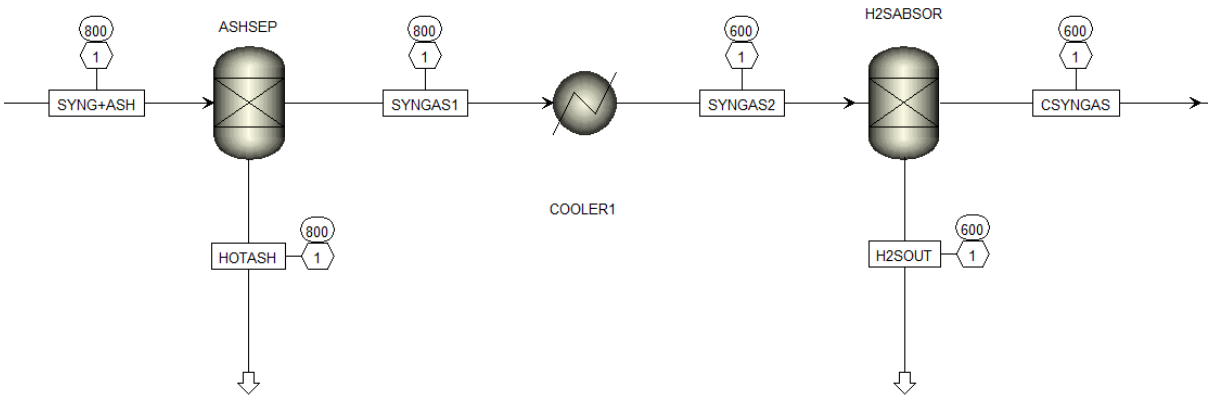

Figure 5: Process flow in Aspen Plus for the cleaning of the syngas produced through the gasification of coffee husk. First, the syngas is run through a separator block to remove the ash without the need for cooling of the syngas. Second, the gas is cleaned to remove H_2S from the syngas. Before cleaning, the syngas is cooled to 600 degrees Celsius through a COOLER block.

3.6.1 Model description

The SOFC simulation consists of a set of assumptions that shape the model. The following assumptions were made: (Sadeghi, Mehr, Zar, & Santarelli, 2018; Colpan, Dincer, & Hamdullahpur, 2007; Corigliano & Fragiacomo, 2020)

- The system operates in a steady-state condition
- The SOFC operates isothermally
- The system is in thermodynamic equilibrium
- All gases are treated as ideal gases
- Pressure drops along the SOFC are neglected
- The air inlet consists of 21% oxygen gas and 79% nitrogen gas
- There is no heat transfer between the SOFC and the outside environment
- There is no heat transfer between the input gases and the solid structure of the fuel cell
- Carbon formation on the anode was ignored due to a low methane content in the syngas
- All methane is converted to hydrogen and carbon monoxide gas on the anode through steam methane reforming (SMR)
- All carbon monoxide is converted to hydrogen and carbon dioxide through the water-gas shift (WGS) reaction

Due to the higher operating temperatures of SOFCs, the WGS reaction (Equation 4) where carbon monoxide and steam are converted to hydrogen and carbon dioxide is far more favorable than the electrochemical oxidation of carbon monoxide. (Gholaminezhad, Paydar, Jafarpur, & Paydar, 2017) Therefore, the electrochemical conversion of CO was ignored in this study. Another advantage is that methane in the syngas is converted into carbon dioxide and hydrogen gas through steam-methane reforming (see Equation 5) forming even more hydrogen gas that could be oxidized on the anode. Due to the formation of steam in this oxidation reaction of hydrogen (Equation 3), the WGS and SMR reactions shift to the product side. Therefore, all methane and carbon monoxide in the syngas was assumed to be reformed in the SOFC.

(Doherty, Reynolds, & Kennedy, 2010) Since both the WGS and SMR reactions produce hydrogen, which is consequently oxidized by the SOFC, the occurrence of carbon monoxide and methane in the syngas substantially increases the power output of the SOFC.

$$H_2 + \frac{1}{2}O_2 \rightarrow H_2O \tag{3}$$

$$CO + H_2O \rightleftharpoons H_2 + CO_2 \tag{4}$$

$$CH_4 + H_2O \rightleftharpoons 3H_2 + CO \tag{5}$$

To model these chemical reactions and the interrelations of these reactions, the reactions were divided into three different blocks. To model the prereforming of methane and carbon monoxide (WGS and SMR reactions), an RGibbs reactor was used (PREREFOR), as shown in Figure 6, in line with the work of Doherty et al. (2010). After prereforming, the gas is fed into the anode block where the hydrogen gas is being oxidized and the prereforming on the anode of the SOFC continues due to the formation of water in the oxidation reaction. The anode is an RStoic block where the three reactions (Equations 3 - 5) are used as inputs with a fuel utilization factor to predict the rate of hydrogen oxidation on the anode. Oxygen is supplied by the air stream (AIRIN), which is split in the cathode to supply the stoichiometric amount needed in the ANODE block. The stoichiometric amount of oxygen is based on the fuel utilization factor and the hydrogen, methane and CO fractions in the RESYNG stream. In the final block, an RGibbs reactor block (EQUILIBR) is used to consume the remaining methane and CO gas to allow the system to reach thermodynamic equilibrium. The complete SOFC model is shown in Figure 6.

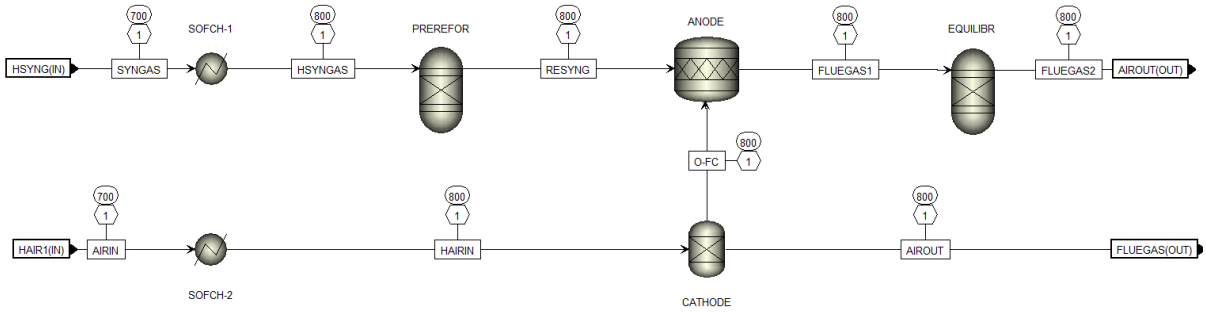

Figure 6: Process model in Aspen Plus of the SOFC. Since Aspen Plus does not contain an SOFC block, the fuel cell was modeled using: an RGIBBS reactor (PREREFOR) used for prereforming the syngas, an RStoic reactor (ANODE) for the stoichiometric oxidation of hydrogen and further reforming based on the chosen fuel utilization factor, and another RGibbs reactor to reform the remaining methane and carbon monoxide (EQUILIBR). The cathode of the fuel cell was modeled through a separator block (CATHODE) which split the incoming airflow (AIRIN) to supply the anode with a stoichiometric amount of oxygen for the reactions in the anode. Two heater blocks (SOFCH-1 and SOFCH-2) were used to model the isothermal operation of the fuel cell.

3.6.2 Temperature and pressure

The operating temperature and pressure are kept at 800 °C and 1 bar, as shown in Table 6, in line with operating conditions of SOFCs in literature. (Gholaminezhad et al., 2017; Ong, Lee, Hanna, & Ghoniem, 2016; Colpan et al., 2007) The operating temperature and pressure are equal to the gasification reaction which could benefit the heat integration of the complete

biomass conversion process. The two heater blocks (SOFCH-1 and SOFCH-2) are used to simulate the isothermal operation of the SOFC. Cooling of the SOFC was modeled through controlling the air inflow at the cathode side which is further discussed in Section 3.6.9. The temperature and pressure, together with the other operating parameters of the fuel cell, are shown in Table 6.

Table 6: Operating parameters of the SOFC using syngas from the gasification of coffee husk.

#	Parameter	Symbol	Value	Source
1	Operating temperature	T_{SOFC}	1073K	Gholaminezhad et al. (2017)
2	Pressure	p_{SOFC}	1 bar	Ong et al. (2016)
3	Fuel utilization	U_f	0.80	Chan, Ho, and Tian (2002)
4	Universal gas constant	R	8.314 J / mol·K	
5	Faraday constant	F	96485 C mol^{-1}	
6	Number of electrons	z	2	
7	Electron transfer coefficient	α	0.5	Gholaminezhad et al. (2017)
8	Preexponential factor anode	γ_{an}	2.051 $\cdot 10^9 Am^{-2}$	Buttler, Koltun, Wolf, and Spliethoff (2015)
9	Preexponential factor cathode	γ_{cat}	1.344 $\cdot 10^{10} Am^{-2}$	Buttler et al. (2015)
10	Activation energy anode	$E_{act,an}$	1.2 $\cdot 10^5 Jmol^{-1}$	Buttler et al. (2015)
11	Activation energy cathode	$E_{act,cat}$	1.0 $\cdot 10^5 Jmol^{-1}$	Buttler et al. (2015)
12	Limiting current density	j_l	18.000 A m^{-2}	Hernández-Pacheco, Singh, Hutton, Patel, and Mann (2004)
13	Electrolyte thickness	δ_E	6 μm	Elcogen (2024)
14	Current density	j	5000 A m^{-2}	Elcogen (2024)
15	Molar mass hydrogen	M_{H_2}	2.0159 g mol^{-1}	

3.6.3 Fuel utilization

The typical fuel utilization of an SOFC operated at a temperature of around 800 °C could reach values of up to 90%. However, starting from 80% and higher, the SOFC shows an increase in concentration polarisation. (Fang et al., 2015) For the purpose of this study, a fuel utilization of 0.80 was deemed realistic in line with the work of Chan et al. (2002). Additionally, since this study also analyzes the economic element of the biomass power plant, lower fuel utilization would require a larger cell stack since the produced current is dependent on the flow rate of the

syngas, which is fixed based on the biomass feed rate.

3.6.4 Reversible cell potential

The cell voltage of an SOFC is dependent on multiple factors. The maximum value for the voltage is given by the standard potential of the redox reactions occurring in the cell under open-circuit conditions, E_0. (Doherty et al., 2010; Choudhary & Sanjay, 2016) This standard potential is then adjusted by the reaction temperature and concentrations of the reactants and products as defined by the Nernst equation to obtain the reversible cell voltage, E_0 (see Equation 6).

$$E_{rev} = E_0 - \Delta E = E_0 - \frac{RT}{zF} \ln K_p = E_0 - \frac{RT}{zF} \ln \frac{p_{H_2O}}{p_{H_2} p_{O_2}^{0.5}} \tag{6}$$

Where R is the universal gas constant, T the reaction temperature, z the number of electrons in the reaction, and F the Faraday constant. The values for these constants can be found back in Table 6. The partial pressures of the different components of the oxidation reaction are found within the natural logarithm term of the Nernst equation.

The Nernst equation assumes a constant temperature and partial pressures on the electrode surface, whereas in reality, both the temperature and concentration are not constant over the length of the electrode surface. This is due to higher reaction rates at the beginning of the electrode due to higher concentrations of reactants and a temperature profile that increases over the length of the electrode due to the exothermic nature of the oxidation of hydrogen. Therefore, using the Gibbs free energy of the reactants and the products of the SOFC is a better measure of the cell voltage than is using the standard Nernst equation. The total Gibbs free energy of the input and output streams of the SOFC were determined using the molar enthalpy (ΔH), temperature (T) and molar entropy (S) of the different streams (i) times the total molar flow rate of the stream (M_i) as expresses in Equation 7.

$$\Delta G_{tot,i} = (\Delta H - T \cdot \Delta S) \cdot M_i \tag{7}$$

This Gibbs free energy of the different input and output streams and the amount of converted hydrogen were used to determine the Gibbs free energy per mol of hydrogen. Equation 8 shows this relation where the names of the different elements refer to the input and output streams as defined in Figure 6.

$$\Delta G = \frac{\Delta G_{FLUEGAS1} + \Delta G_{AIROUT} - \Delta G_{RESYNG} - \Delta G_{AIRIN}}{M_{f,H_2} \cdot U_{f,H_2} + M_{f,CO} \cdot U_{f,CO} + 3 \cdot M_{f,CH_4} \cdot U_{f,CH_4}} \tag{8}$$

Where M_f is the molar flow rate of hydrogen, carbon monoxide, and methane in the syngas and U_f is the fuel utilization factor of the SOFC. To calculate the reversible voltage from the Gibbs free energy of the reaction per mol of hydrogen, Equation 9 was used which shows the relation between the Gibbs free energy and the cell voltage.

$$E_{rev} = -\frac{\Delta G}{zF} \tag{9}$$

As mentioned earlier, this reversible cell potential is not the actual output voltage of an SOFC. There are multiple sources of voltage loss in the fuel cell that determine the eventual output voltage of the fuel cell. (Chan et al., 2002) These losses are dependent on the current density

of the individual cells of the SOFC stack. With low current densities, losses are mainly due to activation losses. With intermediate current densities Ohmic losses also start to influence the voltage output of the cell, and with higher current densities, the rate of reaction at the electrodes is high enough that a drop in the concentration of the reactants on the electrodes cause a voltage drop. To calculate the cell voltage, these losses need to be deducted from the open cell voltage, as shown in Equation 10. (Gholaminezhad et al., 2017; Hernández-Pacheco et al., 2004)

$$E_{cell} = E_{rev} - \eta_{act} - \eta_{ohm} - \eta_{conc} \tag{10}$$

Where η_{act} is the activation polarization, η_{ohm} is the ohmic polarization, and η_{conc} the concentration polarization. These different sources of overpotential are discussed in the following sections (Section 3.6.5 - 3.6.7).

3.6.5 Activation polarization

The activation polarization is an efficiency loss caused by the activation energies of the redox half reactions at the fuel cell anode and cathode and is a direct result of the kinetics at the electrode surface. (Hernández-Pacheco et al., 2004) Thus, the activation polarization should be divided into two terms: one for the anode and the other for the cathode as shown in Equation 11. (Corigliano & Fragiacomo, 2020)

$$\eta_{act} = \eta_{act,an} + \eta_{act,cath} \tag{11}$$

The activation polarization is a parameter for determining the current density as described by the Butler-Volmer equation shown by Equation 12.

$$j = j_0 \exp\left(\frac{\alpha \eta_{act} z F}{RT}\right) - \exp\left(-\frac{(1-\alpha)\eta_{act} z F}{RT}\right) \tag{12}$$

The subscript, i, refers to the electrode, j is the current density, j_0 is the exchange current density, and α is the electron transfer coefficient (see Table 6). At high activation polarization, the second part of the Butler-Volmer equation is much smaller than the first part. Neglecting this second part of the Butler-Volmer equation results in the Tafel equation. For low activation polarization, a linear simplified version of the Tafel equation can be used, which is shown in Equation 13. (Hernández-Pacheco et al., 2004) Both the high and the low activation polarization methods were compared to the outcome of the Butler-Volmer equation, and it was found that the low activation polarization relation deviated by a small but acceptable margin. This simplified relation was used in the electrochemical model of this study to estimate the activation polarization of the anode and the cathode.

$$\eta_{act,i} = \frac{RT}{zF} \cdot \frac{j}{j_{0,i}} \tag{13}$$

The exchange current density, j_0, is a parameter that reflects the rate of electron transfer in a given electrode material at zero current when the anodic and cathodic currents are in equilibrium. The higher this exchange current density is, the higher the electrochemical reaction rate, and the lower the activation losses. The exchange current density of the anode and cathode can be estimated via an Arrhenius type of expression, as shown in Equation 14. (Buttler et al., 2015)

$$j_{0,i} = \gamma_i \cdot \exp\left(-\frac{E_{act,i}}{RT}\right) \tag{14}$$

For this Arrhenius equation, both the preexponential factor, γ_i, and the activation energy, $E_{a,i}$, are specific for the type of electrode material, hence the subscript, i. These values were experimentally defined for a nickel anode, an yttria stabilized-zirconia (YSZ) electrolyte, and a YSZ/Lanthanum Strontium Manganite (LSM) cathode type of SOFC. The values were taken from Buttler et al. (2015) and are shown in Table 6.

3.6.6 Ohmic polarization

Ohmic polarization is a voltage drop caused by resistance encountered during the transport of charged particles through the electrodes, interconnections, and the electrolyte. (Hernández-Pacheco et al., 2004) The ohmic overpotential is a function of the current density, j, and the resistance over the different fuel cell components, R_k, where the subscript k is an indicator for the different components, like the interconnections, electrodes, and electrolyte (see Equation 15).

$$\eta_{ohm} = IR = j \cdot \sum R_k \tag{15}$$

Since the conductivity of electrons through the electrodes and interconnections is generally a multitude of orders of magnitude greater than that of O^{-2} ions moving through the electrolyte, this electron resistance was ignored. (Hauck, Herrmann, & Spliethoff, 2017) Multiple semiempirical definitions for the ohmic resistance of the electrolyte of a Ni-YSZ SOFC have been described in literature. In this study, the work of Buttler et al. (2015) was used since the equation depends on the thickness of the electrolyte layer, δ_E, and the operating temperature of the SOFC, T. This relation can be found in Equation 16.

$$\eta_{ohm} = j \cdot 2.99 \cdot 10^{-5} \cdot \delta_E \cdot \exp\left(\frac{10300}{T}\right) \tag{16}$$

This equation is comparable to the Arrhenius relation described by other authors.(Hernández-Pacheco et al., 2004; Hauck et al., 2017)

3.6.7 Concentration polarization

Concentration polarisation, also known as diffusion polarization, is caused by the low concentration of reactants on the electrode interface in comparison to the bulk phase due to diffusion limitations at high reaction rates that generally occur at a fuel utilization higher than 80 percent. (Hernández-Pacheco et al., 2004) This effect could occur on both electrodes, although Chan, Khor, and Xia (2001) mentioned that no significant concentration polarization could yet be observed on the cathode at the limiting current density on the anode. Therefore this polarization factor on the cathode was ignored. The reason that diffusion could become a limiting factor and cause a voltage drop is the intricate behavior of gas molecules during mass transport through the pores of the electrode material. The diffusion of the reactants is therefore related to the design of the electrode with respect to its porosity, tortuosity, the pore size, and permeability. Hernández-Pacheco et al. (2004) used the Dusty Gas Model to determine the diffusion of reactants through a porous electrode material. A simpler method was used by Chan et al. (2002) based on an logarithmic growth in the diffusion polarization toward the limiting current density, j_l, which is roughly the behavior seen experimentally. For the purpose of this model, this simpler approach was chosen with the limiting current density from Hernández-Pacheco et

al. (2004), as shown in Table 6, since the effect of the concentration polarization was expected to be limited with the chosen fuel utilization.

The function used for concentration polarization is similar to the second part of the Nernst equation, which is temperature- and concentration-dependent (see Equation 17). (Chan et al., 2002) The Nernst equation is based on the concentration of the reactants on the surface of the electrode being equal to the bulk concentration, and the equation for concentration polarization corrects for this concentration difference.

$$\eta_{conc} = -\frac{RT}{zF} \cdot \ln\left(1 - \frac{j}{j_l}\right) \tag{17}$$

3.6.8 Power

The power output of the SOFC is dependent on the cell potential, as defined in the previous section, and the amount of hydrogen converted on the surface of the anode which determines the number of electrons released in the redox reaction. The amount of hydrogen oxidized at the anode is dependent on the amount of hydrogen in the syngas after prereforming and the fuel utilization as shown by Equation 18.

$$P_{SOFC} = \frac{z \cdot F \cdot M_f^{H_2} \cdot U_f}{3600} \cdot E_{cell} \tag{18}$$

3.6.9 Air ratio

The air inflow at the cathode side of the SOFC is described by the air ratio, λ_{air}: the amount of air supplied compared with the stoichiometric amount needed. (Gholaminezhad et al., 2017) To allow for isothermal operation of the SOFC, the air inlet should actively cool the SOFC during operation due to the exothermal nature of the reactions occurring on the anode (the SMR reaction is endothermic, but the syngas consists of only a small fraction of methane).

The air inlet temperature was set to 100 °C lower than the operational temperature of the SOFC. (Choudhary & Sanjay, 2016; Colpan et al., 2007) A lower temperature would cause unwanted effects like temperature gradients causing thermal stress in the cathode, electrolyte and anode. A lower inlet temperature impacts diffusion of oxygen ions at the inlet of the cathode and, therefore, the reaction rate. (Zhao et al., 2024)

The amount of heat generated in the SOFC is caused by the WGS, SMR and oxidation of hydrogen, as modeled in blocks PREREFOR, ANODE, and EQUILIBR, together with the heat generated owing to the cell overpotentials. (Djamel, Hafsia, Bariza, Hocine, & Kafia, 2013) This heat was compensated by cooling the SOFC through the lower temperate syngas and air being fed into the SOFC. The amount of air that is being fed into the SOFC is determined via a Design-Spec block (HEATBALA) in Aspen, where the total heat of the SOFC is set to zero by changing the air inlet flow rate.

3.7 Heat

In this section, the heating needs, heat recycling, and sources of heat loss are discussed. The aim of the model is to supply the heat needed for the roasting of coffee in the coffee processing unit and minimize heat loss throughout the system, thereby optimizing the overall energy efficiency of the biomass plant.

The flue gas released from the SOFC still contains hydrogen gas since the fuel utilization was set to a value lower than one. This residual hydrogen gas was used to generate heat by combining

the outgoing streams of the SOFC and using an afterburner. Using either an afterburner or a combined heat and power (CHP) approach is often chosen for this type of biomass power plant to increase energy output in the form of heat and/or electricity. (Doherty et al., 2010; Chan et al., 2002; Sadeghi et al., 2018) The combination of the output streams of the SOFC (FLUEGAS and AIROUT) and the burning off of the flue gas is shown in the AFTERBUR block in Figure 7.

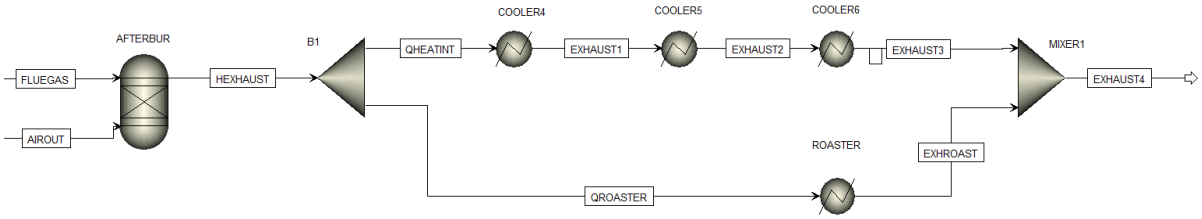

Figure 7: Process flow in Aspen Plus for heat integration of the model. The fluegas is first burned off by combining the two output streams of the SOFC (FLUEGAS and AIROUT) into an adiabatic RGibbs block. The exhaust gas (HEXHAUST) is then split to use the heat in the flue gas for the heating of the different input streams and to supply heat for coffee roasting in the ROASTER block. The other stream is used for the steam used during gasification (COOLER4), the heating of the syngas before injection in the SOFC (COOLER5), and the air used in the SOFC (COOLER6). The two streams are combined to leave the system as exhaust gas (EXHAUST4).

When leaving the afterburner chamber, the flue gas was split into two separate streams (QHEATINT and QROASTER; see Figure 7). This split was designed to prevent temperature crossover in the modeled network of heat exchangers. The temperature difference between the cold and hot streams should be at least 10 °C to prevent temperature crossover in the heat exchanger. (Doherty et al., 2010) The QROASTER stream provided heat for the roasting process. To assess the amount of heat necessary for roasting, the equivalent of the heat normally provided by the LPG was used. For the total throughput of the processing plant, a total of 277 kg of LPG is used per hour as established earlier. The heating value chosen for the LPG was 50 MJ/kg. (World Nuclear Association, 2020) This heating value results in an energy need of 3.85 MWh per hour for the roasting process during the operating hours of the coffee processing plant. A Heater block was used to model the heat transfer from the flue gas to the coffee roaster drum through a heat exchanger as shown in the ROASTER block of the Aspen model in Figure 7. The net duty of this Heater block was set to precisely the heat normally provided through the LPG: 3.85 MW.

The heat in the other flue gas stream (QHEATINT) was used to:

- Heat the water used as gasifying agent in the gasifier to 800 °C in the COOLER4 block
- Heat the syngas after gas cleaning before it enters the SOFC to 700 °C in the COOLER5 block
- Heat the air used on the cathode side of the SOFC to 700 °C via the COOLER6 block.

In the process model, only the gasification process needs an additional energy input during operation of the plant (energy use during ramp-up is disregarded). The assumption was made that this heat is supplied through an electric arc furnace (EAF) powered by the electricity generated in the SOFC. All other energy inputs can be covered through reusing heat that is being emitted elsewhere in the process, as shown in Table 7.

There are multiple sources of heat loss in the system: the ash content that is removed, the H_2S that is bonded to the column of zinc titanate during desulfurization, the heat emitted during the cooling of the syngas before desulfurization, and the heat in the exhaust gas at the end of

Table 7: Heat integration performed in the coffee husk biomass energy plant to optimize the energy efficiency of the plant. The steam used for biomass gasification is heated using heat from the exhaust gas after the use of an afterburner (HEATER2). The same exhaust gas is used to heat the air going into the SOFC (HEATER4) and to heat the syngas before it enters the SOFC (HEATER3). Part of the heat in the exhaust gas is used for coffee roasting.

Block	Type	IN	OUT	Description
HEATER1, DECOMP, GASIFIER	Input	Electric arc furnace	-	Power input for gasifier using an electric arc furnace
HEATER2	Input	COOLER4	-	Heat required to create steam for gasification
HEATER3	Input	COOLER5	-	Heating of syngas before entering the SOFC
HEATER4	Input	COOLER6	-	Heating of air entering the SOFC
COOLER4	Output	-	HEATER2	Heat exchanger to heat the steam used during gasification
COOLER5	Output	-	HEATER3	Heat exchanger to heat the syngas before the SOFC
COOLER6	Output	-	HEATER4	Heat exchanger used for air entering the SOFC
ROASTER	Output	-	Coffee roaster	Heat used for the coffee roasting process

the process. A visualization of the complete process flow including these sources of heat loss can be found in Figure 19 in the Appendix.

3.8 Economic model

To assess the bottom-line profitability of the use of coffee husks for energy generation, a financial assessment was performed. One widely used measure for the financial performance of an energy project is the levelized cost of electricity (LCOE). The LCOE is an indicator of the real costs of a project per unit of energy generated, or, phrased differently, the minimum sales price of electricity to break even with the project. With this measurement, there is one generic way of comparing energy projects with each other even when the overall cost structure, cash flow, and lifetime of the projects are completely different. Hence, it is a method to compare apples with apples in terms of financial performance of an energy project. (CFI, 2024a) The LCOE is dependent on the net present value (NPV) of a project. If a project has a positive NPV, the project's revenues are higher than the costs and the initial investment; therefore, the project should be accepted from a financial viewpoint. (HBR, 2004; Malek, Kawsary, & Hasanuzzaman, 2022; CFI, 2024b)

One of the problems with discounted cash-flow (DCF) based valuation models, like the LCOE,

is that they often undervalue the projects they are used on. This ultimately results in lower investment in projects that are innovative but uncertain as well due to lack of track records or a history of similar initiatives. This high uncertainty causes the DCF model to work with a high discount rate and therefore a lower present value of future revenue. (HBR, 2004; Glantz & Kissell, 2014) It does not consider the fact that uncertainty about a project's profitability could result in higher future revenues as well. (Glantz & Kissell, 2014) This is a risk for renewable energy initiatives since the technologies used often have limited track records and are used on a scale that has not been applied before. Furthermore, future revenues are heavily dependent on intermittent energy sources which are difficult to predict. Therefore, using a DCF-based valuation method for projects related to sustainable technology could slow investment and ultimately result in lower adoption of more sustainable energy alternatives.

Other project valuation methods show a more optimistic valuation for projects. The real options analysis (ROA) is one of these options, although it is often overlooked by companies since this method tends to overvalue projects, especially projects where future revenue is quite uncertain. This method is also misused to oversell projects. (HBR, 2004) The ROA and DCF methods are not mutually exclusive. Where a DCF usually undervalues a project, the ROA method could show the real potential of a project. When the DCF sees a higher discount rate with higher project risk, the value of an option increases with uncertainty and shows the potential for a higher project profit. (HBR, 2004; Glantz & Kissell, 2014)

In this research, the DCF approach will be used since this approach enables comparison with other energy projects. Another reason to not use the more optimistic ROA is that if the DCF approach already results in positive investment advice, that is, if the project has a positive NPV, there would not be a need for additional valuation. The last reason is that the ROA method requires quite arbitrary input variables in order to value an asset that is based on historical prices of the underlying assets. With innovative projects such as the one described in this study, these are often not available. (HBR, 2004)

To calculate the NPV for the costs of the project, for every year, t, of the economic lifetime of the investment, the total costs (TC) of the project are divided by the compounded cost of capital in that given year. The sum of all these discounted yearly costs minus the initial investment in year zero (I_0) results in the NPV of the costs of the project (see Equation 19).

$$NPV_{cost} = \sum_{t=1}^{n} \frac{TC_t}{(1+r)^t} - I_0 \tag{19}$$

To derive the LCOE, the NPV should be divided by the total discounted electricity output generated from the project, as shown in Equation 20. (CFI, 2024a) This electricity output is dependent on the electricity produced by the SOFC minus the electricity needed for the EAF, which keeps the gasifier at the operating temperature.

$$LCOE = \frac{NPV}{\sum_{t=1}^{n} \frac{E_t}{(1+r)^t}} \tag{20}$$

In the following sections, the attributes for the calculation of the LCOE are described based on the project investment for the biomass energy plant in Wayanad. These assumptions and input parameters for the economic analysis are summarized in Table 8.

Table 8: Overview of the assumptions made for the economic analysis of the biomass energy plant in Wayanad.

Parameter	Value	Source
Project lifetime	30 years	Tera, Zhang, and Liu (2024)
Capacity factor	0.247 (90 days for 24 hours a day)	
Plant scale	1295 kg/hour	
Construction period	1 year	
Financing	100% loan	
Long-term Lending Interest Rate India	8.57%	Worldbank (2022)
Corporate tax rate India	25%	PwC Worldwide Tax Summaries (2024)
Discount rate	6.43%	PwC Worldwide Tax Summaries (2024)
Inflation	4%	Statista (2024)
$CEPCI^{2024}$	800.7	Towering Skills (2024)
Lang factor	3.63	Tera et al. (2024)
Wholesale electricity price	55 $/MWh	IEA (2023)
Commercial LPG price Wayanad	1.07 $/kg	Good Returns (2024)
OpEx factor	1.5%	
Ash disposal	60 $/tonne	Permana, Fagioli, De Lucia, Rusirawan, and Farkas (2024)
Biomass	0 $/tonne	
Water	0 $/tonne	
Transportation costs	0 $/tonne	

3.8.1 Model assumptions

The biomass plant operates during the harvest season (December, January, and February) for a period of 90 days. Within these 90 days, the plant is assumed to run for 24 hours a day. All maintenance on the plant is performed outside of this period. This operation for 2160 hours a year means that the plant has a capacity factor of 0.247. The plant processes 1295 kilograms of coffee husk per hour. All model assumptions are shown in Table 8.

To correctly discount the costs and electricity generated by the plant, a project lifetime should be chosen. Since there are few to no commercially operated SOFCs that have operated for decades, the project lifetime is based on assumptions from the literature. For this project a lifetime of 30 years was chosen. (Tera et al., 2024) The project was assumed to be built in year zero of the project and starts to generate electricity and heat in year one.

3.8.2 Cost of capital

A discount rate was used to discount future cash flows back to their present value. (CFI, 2024a) The discount rate is an arbitrary cost parameter because its value is hard to predict over the full lifetime of the investment project. It does, however, have a substantial effect on the financial analysis and therefore the outcome of the investment decision. To determine the discount rate, companies often use the weighted average cost of capital (WACC) as a proxy rate. (Investopedia, 2024) As the name suggests, this WACC is the weighted average costs of all the different funding sources of a project as shown in Equation 21.

$$WACC = \frac{E}{V} * c_e * \frac{D}{V} * c_d * (1 - T) \tag{21}$$

Where E is the total amount of equity financing in the project, V the total amount of financing, D is the amount of debt financing, c_e is the cost of equity, c_d is the cost of debt, and T is the corporate tax rate.

For this project, the assumption is that it will be fully funded through loan financing due to the involvement of the Worldbank in the Climate Smart Coffee Program. For the cost of debt, the long-term lending interest rate in India from 2022, the latest year available in the data of the Worldbank, was used. This interest rate was 8.57 percent. (Worldbank, 2022) Since there is only loan financing, the WACC is equal to this long-term lending interest rate, which is compensated by the corporate tax rate since these interest payments are tax deductible. India has a corporate tax rate of 25 percent; therefore, the WACC amounts to 6.43 percent.

3.8.3 Capital expenditures (CapEx)

The initial investment costs, or capital costs, of the biomass plant were determined through evaluation of the costs of the different system components. These components were priced via cost equations, Z_i, adjusted by the Chemical Engineering Plant Cost Index (CEPCI). The CEPCI is an index used to adjust the plant construction cost from the reference year to the current year to adjust for changes in prices over the years. The CEPCI is an important tool for economic analyses in the chemical process industry. (Chemical Engineering, 2024) Equation 22 shows the relation used to calculate the capital costs of a certain component on the basis of the reference year of the cost equation, the CEPCI of the reference year and the CEPCI of the current year. The CEPCI of the current year is shown in Table 8 and is equal to 800.7 (March 2024). (Towering Skills, 2024)

$$Z_i = Z_i^0 \cdot \frac{CEPCI_{2024}}{CEPCI^0} \tag{22}$$

Where Z_i^0 represents the costs of component i in the base year and Z_i represents the component costs in the current year.

The total capital costs of the system were determined through the costs of the individual components indexed by a Lang factor as shown by Equation 23. This Lang factor scales the costs of the components to include costs for piping, engineering, assembly, safety, site equipment, quality control, commissioning, and connection to the grid, among others. (European Commission, 2019) This is an arbitrary cost component, and values reported in literature range from 1.62 for an electrolysis and methanation plant to 5 as a standard for petrochemical installations. (European Commission, 2019) Since Tera et al. (2024) performed an economical analysis for a system quite similar to the biomass plant described in this study, the same Lang factor of 3.63 was used, as shown in Table 8.

$$Z_{tot} = \sum Z_i \cdot f_{Lang} \tag{23}$$

For the costs of the different components of the system, cost equations from literature are used that are dependent mainly on the mass flow or surface area of the system component. These are shown in Table 9, including their CEPCIs and reference years. The costs for the mixers and splitters were neglected owing to their low attribution to the overall costs and were assumed to be part of the Lang factor correction. The costs for the gasifier are mainly based on the feed rate of the biomass in kilograms per hour. For the SOFC, the costs are dependent on the total surface area of the SOFC and the operating temperature. The cost equation of the SOFC used by Tera et al. (2024) has been changed to calculate the surface area on the basis of the output current and current density instead of the cell area and number of cells. For the heat exchangers, the overall surface area A_{heatx} was calculated using the input and output temperatures of the hot and cold streams, the net duty of the heater Q, and the heat transfer coefficient U, as expressed in Equations 24 and 25. (PDH Online, 2020)

$$A_{heatx} = \frac{Q}{U \cdot \Delta T_m} \tag{24}$$

$$\Delta T_m = \frac{(T1 - t2)(T2 - t1)}{\ln(\frac{T1-t2}{T2-t1})} \tag{25}$$

Where ΔT_m is the log mean temperature difference, $T1$ the inlet of the hot stream, $T2$ the outlet of the hot stream, $t1$ the inlet of the cold stream, and $t2$ the outlet of the cold stream. The heat transfer coefficient used was 20 W.m^{-2}.K^{-1}, an average value for a nonpressurized gas heat exchanger. (Engineering Toolbox, 2003)

For the cost equation of the afterburner shown in Table 9, the mass flow of the stream exiting of the afterburner m_{ab} is taken as an input variable in kilograms per second. The cost equation is dependent on a pressure drop. In the current system model, pressure drops were neglected; therefore, it was assumed that the ingoing pressure was equal to 1.15 bar and that the outgoing pressure was 1 bar. The last component taken into account in the capital cost calculation is the inverter responsible for inverting the output voltage of the SOFC towards the voltage of the electricity grid. This cost equation is dependent on the electrical work in Watt, W_{SOFC}.

3.8.4 Operational expenditures (OpEx)

The OpEx of the biomass plant consists of all costs to operate the plant. These costs can be divided into fixed and variable costs. Fixed costs include fixed labor costs (long-term contracts), maintenance costs, insurance, and land leases, among others. The variable costs scale with the output of the biomass plant and consists of unplanned maintenance and flexible labor costs, among others. These O&M costs are often expressed as a percentage of the CapEx and range from 1 to 6%. (IRENA, 2012, 2022; Guo, Zhang, Zhang, & Bi, 2024) Due to the low capacity factor (the plant runs for 3 months a year) it was assumed that the operating expenditures were 1.5 percent (see Table 8).

Other operational expenditures are fuel costs, i.e., the costs of the coffee husk material. As established in Chapter 2, there is currently no economical way of dealing with the coffee husk; therefore, it was assumed that the coffee husk could be used at zero cost (there are no opportunity costs). The biomass plant operates at the same location as the coffee processing plant, and no costs for transport are incurred. This availability of biomass at the location of the plant and the zero costs of the biomass are substantial financial advantages of the bioenergy plant. IRENA

Table 9: Cost equations of the different components of the coffee husk energy plant including their reference year and the corresponding CEPCI factor from that reference year. The costs of mixers and splitters were neglected due to their relatively small contribution to the overall capital costs of the system.

Part	Cost equation	Year	CEPCI	Reference
Gasifier (incl. cleaning of syngas)	$Z_g = 1600 \cdot (m_{bio,dry})^{0.67}$	2012	590.8	Abedinia et al. (2024)
SOFC	$Z_{SOFC} = \frac{I}{j} \cdot (2.97T - 1907)$	2007	525.4	Tera et al. (2024)
Heater/cooler/ exchanger	$Z_{heatx} = 130 \cdot (\frac{A_{heatx}}{0.093})^{0.78}$	2005	468.2	Tera et al. (2024)
Afterburner	$Z_{AB} = (\frac{46.08 \cdot m_{AB}}{0.995 - P_{out}/P_{in}}) \cdot [1 + exp(0.018T_{AB} - 26.4)]$	1994	368	Abedinia et al. (2024)
Inverter	$Z_{inv} = 10^5 \cdot (\frac{W_{SOFC}}{500})^{0.7}$	2002	396	Abedinia et al. (2024)

(2022) reported that the costs for feedstock account for 20% to 50% of the LCOE of bioenergy plants without the costs for transportation. Another input stream of the biomass plant is the water used for gasification. Due to the low S/B ratio of 0.1, these costs were also set to zero. Finally, the ash produced during the cleaning of the syngas after gasification needs to be disposed of. The costs of ash disposal was assumed to be \$60/ton. (Permana et al., 2024)

Energy from the biomass plant replaces the electricity and LPG used during the processing of the coffee beans and therefore results in cost savings. These cost savings are included in the DCF model as negative costs. For the electricity use, the wholesale price of electricity in India was used. An average of these electricity prices was taken from the first quarter of 2019 to the first quarter of 2024 which resulted in a price of 55.7 \$/MWh as shown in Table 8. (IEA, 2023) For the cost savings on LPG, the LPG price in Wayanad from July 2024 was used: 1698 INR per 19 kilogram of LPG. (Good Returns, 2024) To calculate this price in terms of the USD price per kilogram, the exchange rate of the day of writing was used. This resulted in the LPG price of 1.07 \$/kg, as shown in Table 8.

All the operational costs were indexed on a yearly basis with the inflation rate and therefore steadily increased over the lifetime of the project. Statista (2024) predicted that the inflation in India would converge to a value of 4 percent by 2029. Therefore, for this study, this value of 4 percent will be used for the inflation. The discounted cash flow model used to calculate the LCOE of the bioenergy project can be found in Table 16 of the Appendix.

4 Results

In this chapter, the outcomes of the technical and financial models used to assess the potential of a biomass conversion plant using coffee husk as a feedstock are presented. The results are structured as follows. First, the outcomes of the gasification model are presented in Section 4.1. Second, the modeling results for the SOFC are explained in Section 4.2. The results from heat integration and the overall system performance are discussed in Section 4.3. Third, the results of the financial analysis are presented in Section 4.4. Finally, a sensitivity analysis of the main model parameters is discussed in Section 4.5.

4.1 Gasification

To understand the performance of a gasifier, multiple performance factors can be included: the composition of the syngas, the carbon conversion efficiency (CCE), and the cold gas efficiency (CGE). Owing to the subsequent use of an SOFC, the composition of the syngas is is less important than the overall energy contained in the syngas. H_2, CO, and CH_4 can be oxidized and/or reformed in the SOFC. Therefore, the need for a high H_2/CO ratio in the syngas for an SOFC is lower than for a methanation reactor. Additionally, the CCE within the model was assumed to be 100% because of the minimisation of the Gibbs free energy of the reactions during gasification. Hence, the main performance parameter for the gasification process is the CGE. For the calculation of the CGE, the lower heating value (LHV) of the feed was compared to that of the cleaned syngas. This relation is shown in Equation 26.

$$CGE = \frac{LHV_{syn}}{LHV_{feed}} \tag{26}$$

With an S/B ratio of 0.1, resulting in an equivalence ratio of 0.38, the cold-gas efficiency of the gasifier was 0.79 on the basis of an LHV of the cleaned syngas of 14.34 MJ/kg. The resulting syngas after gas cleaning had a H_2/CO molar ratio of 1.29. Table 10 provides an overview of all the gasification performance indicators.

Table 10: Main performance parameters of the modeled steam gasification of coffee husk. The model results were compared with the experimental results of coffee husk gasification from literature, although these studies used different operation conditions than those chosen in this study.

Parameter	**Value**	**de Oliveira et al. (2018)**	**Bonilla et al. (2019)**
Temperature	800 °C	800 °C	550 °C
Gasifying agent	Steam	Air	Air/O_2
Steam/biomass ratio (S/B)	0.1		
Equivalence ratio (ER)	0.38	0.12	1.5-5.6
HHV_{syngas}	11.2 MJ/Nm^3	7.76 MJ/Nm^3	7.63-8.84 MJ/Nm^3
LHV_{syngas}	14.34 MJ/kg		
Cold-gas efficiency (CGE)	0.79		0.55-0.82
H_2/CO	1.29		

Comparing these results with those of other studies looking on the gasification of coffee husk is not straightforward since studies on coffee husk gasification are rare and use different operating parameters. de Oliveira et al. (2018) used air gasification with an ER of 0.12 which resulted in an HHV of 7.76 MJ/Nm^3, substantially lower than the HHV of 11.20 MJ/Nm^3 reported in this study. The same can be said of the HHV for air/oxygen gasification performed at 550 °C by Bonilla et al. (2019). The higher HHV of this study could be explained by the complete carbon conversion, whereas the other studies assumed char and/or tar formation. Although the CGE of 0.79 is relatively high compared with values in literature, it is still in the range achieved by Bonilla et al. (2019).

The cleaned syngas consisted of 48.17% hydrogen gas, 37.27% carbon monoxide, 7.15%, and 6.06% carbon dioxide as shown in Table 11. Methane, nitrogen, and hydrogen sulfide were present in parts per million range.

Table 11: Chemical composition of the produced syngas before gas cleaning. Hydrogen and carbon monoxide were the largest fractions in the produced syngas.

Compound	**mol %**	**Compound**	**mol %**
H_2	48.17	CH_4	0.34
CO	37.27	N_2	0.84
H_2O	7.15	H_2S	0.16
CO_2	6.06		

4.2 SOFC

After gasification and gas cleaning, the produced syngas was fed into the SOFC at 700 °C on the anode side, whereas air at the same temperature was fed into the cathode side. The difference between the inlet stream temperature and SOFC operating temperature was used to cool the SOFC during operation and allow for isothermal operation. The air inflow was therefore scaled to supply the needed cooling to the SOFC. This resulted in an air ratio of 31.6, the amount of air supplied compared with the stoichiometric amount needed for the reactions on the anode. This amount of air is relatively high compared with the air ratios mentioned in the literature, which are in the range of 7-8.5. (Gholaminezhad et al., 2017) A high air ratio has serious implications for the outcome of the model with respect to heat integration and the economic model due to the sizing of heat exchangers.

The reversible cell voltage was calculated on the basis of the Gibbs free energy of the input and output streams to include voltage drops caused by concentration and temperature differences on the surface of the anode. The reversible cell voltage was 948 mV. The overpotentials caused by activation barriers (78.2 mV on the anode and 1.3 mV on the cathode), ionic resistance (13.2 mV) and diffusion limitations (15.0 mV) resulted in a decrease in the reversible cell voltage of 108 mV. The cell voltage of the SOFC was therefore 840 mV. All the results from the SOFC model are shown in Table 12.

The total current of the SOFC is dependent on the amount of hydrogen oxidized and directly related to the coffee husk feed rate and the syngas composition. For the SOFC design, the number of SOFC cells depends on the total current, the current density and the area of the individual cell. The total current from the hydrogen in the syngas was 3190.8 kA. With a cell potential of 840 mV, this resulted in a power output of the SOFC of 2681 kW, or 2,070 Wh per kilogram of biomass input. Since the gasifier was heated using an EAF requiring 241 kW to keep the gasifier at 800 °C, the net power output of the biomass power plant was 2,440 kW.

Table 12: Results of the reforming and oxidation of syngas produced from coffee husk using an SOFC at a temperature of 800 °C and a pressure of 1 bar.

Parameter	**Symbol**	**Value**
Air ratio	λ_{air}	31.6
Reversible cell voltage	E_{rev}	948 mV
Overpotential	η	108 mV
- Anode activation	$\eta_{act,an}$	78.2 mV
- Cathode activation	$\eta_{act,cat}$	1.3 mV
- Ohmic	η_{ohm}	13.2 mV
- Concentration	η_{conc}	15.0 mV
Cell potential	E_{cell}	840 mV
Current	I	3190.8 kA
Power output	P	2681 kW
Energy/kilogram of biomass		2,070 Wh
Net power output		2440 kW
Electrical efficiency	η_{elec}	0.886
Energy efficiency	η_{energy}	0.4996

To assess the performance of the SOFC, the electrical and energy efficiency was used as a metric. The electrical efficiency was calculated via the reversible cell voltage and the cell potential, as expressed in Equation 27. The electrical efficiency of the SOFC was 88.6%.

$$\eta_{elec} = \frac{E_{cell}}{E_{rev}} \tag{27}$$

The energy efficiency of the SOFC was calculated via the lower heating value (LHV) of the syngas and the electrical power output (see Equation 28).

$$\eta_{elec} = \frac{P}{LHV \cdot m_{syngas}/3.6} \tag{28}$$

Where LHV is the lower heating value of the syngas in MJ per kg, m_{syngas} is the mass flow of the syngas in kg per hour and P is the electrical power output of the SOFC. This equation yields an energy efficiency of 50%.

Validation of the results for the SOFC model is not straightforward. Experimental and modeling results for SOFC performance using syngas are available, but the operating conditions and syngas compositions in the literature are often substantially different than those of the coffee husk-derived syngas modeled in this study. Abedinia et al. (2024) reported a cell voltage for an SOFC at an operating temperature of 1073 K of approximately 0.9 V for syngas derived from municipal solid waste (MSW), which is comparable to this study.

4.3 Heat & overall efficiency

Due to the use of heat exchangers and integration with the coffee roasting process, the majority of heat produced within the biomass plant could be reused. All heaters in the process are provided with recycled heat. Thus, the heat losses in the model are from the cleaning steps (ash separation and desulfurization), the cooling of the syngas before desulfurization, and the exhaust gas that leaves the system at a temperature of 82 °C. Since the coffee processing unit is only operational for 10 hours a day, whereas the biomass plant operates for 24 hours a day, the heat for roasting is lost in the 14-hour window in the day when the coffee processing plant is not operational. The results of the heat losses and the energy efficiency of the biomass plant can be found in Table 13 and are discussed in the following paragraphs.

Table 13: Total energy input and outputs of the biomass plant and the total system efficiencies compared with results from literature.

Parameter	**Energy per hour**	**Jia, Abudula, Wei, Sun, and Shi (2015)**
Heating value coffee husk	6,528.31 kW	
Heat coffee roasting	3,846.15 kW	
Electricity		
EAF gasifier	241.41 kW	
Coffee processing unit	896.00 kW	
Residual power output	1,543.97 kW	
Efficiency		
Electrical efficiency	0.41	0.40
Energy efficiency	0.62	0.45

The power output of the biomass plant is dependent on the electrical output of the SOFC minus the electrical power used by the EAF. Part of the electrical power output (896 kW) is used in the coffee processing unit but does not affect the electrical efficiency of the biomass plant itself. It affects only the residual power output, which is the power available to supply back to the electricity grid. This residual power output is 1,544 kW during operation of the coffee processing unit. Outside of the 10 hours per day operation all electricity produced by the biomass plant, 2440 kW, is available for other uses. Using Equation 29, the total electrical efficiency of the biomass plant was 41%. This electrical performance is comparable to the work of Jia et al. (2015), who developed a similar model with a gasification-SOFC-afterburner setup and similar operating conditions using woody biomass as a feedstock.

$$\eta_{elec} = \frac{P_{SOFC} - P_{gasifier}}{\cdot LHV_{feed}/3.6 \cdot m_{feed}} \tag{29}$$

Where P_{SOFC} is the power output of the SOFC, $P_{gasifier}$ is the electrical power required for the gasifier EAF, LHV_{feed} the lower heating value of the coffee husk in MJ/kg, and m_{feed} the feed rate of the coffee husk in kilograms per hour.

The overall system efficiency is dependent on the electrical output of the SOFC and the heat that is used for the roasting process, together with the useful power output of the biomass plant. Part of the electrical power produced is used to heat the gasifier via an EAF, so this electrical power

should be deducted from the total power produced by the SOFC. The heat for the roasting process is the same amount of heat that is normally produced by burning LPG, a total of 3846 kW per hour (see Table 13). The biomass plant produces electricity and heat for 24 hours a day during the 90-day window of the harvest season, while the coffee roasting is performed when the coffee processing plant is operating for 10 hours per day. To calculate the total efficiency of the process over a given year, these differences in operation should be considered since the heat for coffee roasting is released in the exhaust gas when the coffee roaster is not operational. Taking these considerations (see Equation 30) into account the total energy efficiency of the process was 0.62. This is substantially higher than the efficiency of 0.45 reported by Jia et al. (2015). The higher system efficiency is due mainly to the integration with the coffee roaster, which makes the system more efficient than a system with just an afterburner. Sadeghi et al. (2018) reported a total system efficiency of 0.79 although that was based on a gasifier-SOFC-CHP setup. This result shows that with an extension of the biomass plant with a CHP plant, the system efficiency might be even higher.

$$\eta_{total} = \frac{24 \cdot (P_{SOFC} - P_{gasifier}) + 10 \cdot P_{roaster}}{24 \cdot LHV_{feed}/3.6 \cdot m_{feed}} \tag{30}$$

Where $P_{roaster}$ the heating power necessary for the roasting process.

4.4 Financial

To assess the financial feasibility of the biomass plant an economic model was created based on a discounted cash flow of the costs of the plant to calculate the LCOE. The LCOE can then be used to compare the financial performance of the coffee husk power plant with that of other energy plants. The total capital expenditures derived from the cost equations laid out in Section 3.8 and the chosen Lang factor of 3.63 was $ 24.1 million. To understand the costs per amount of output, the total CapEx was divided by the total electricity output of the SOFC. The residual heat was seen as an energy loss with no value and therefore not included in the CapEx per kW output. The total CapEx per kW of output was $8,984. The results of the financial model, including CapEx, are shown in Table 14.

IRENA (2022) reported that gasification as a technology is still in a development phase, from which it can be concluded that the use of an SOFC for bioenergy is in its infancy stage. Immature technologies typically have higher capital and operating costs than more traditional technologies used for bioenergy plants, such as direct combustion. Data from IRENA (2022) on bioenergy projects in India for the 0.5-5 MW scale output reveal a cost range of around $500-$6500 per kW. However, most of the bioenergy projects are concentrated around the $1000-$1500 per kW range. These data are an average for the different feedstocks reported, but the data show that for agricultural and vegetal waste in India (like coffee husk), most projects could be realized for less than $2000 per kW.

The largest contributor to the capital expenditures of the biomass plant comes from the heat exchangers with approximately half of the component costs coming from the four heat exchangers in the system (see Figure 8). This is largely due to the high air ratio needed for isothermal operation of the SOFC. For operation with a high air ratio, a large volume of air needs to be heated and the heat from this large volume of air is later recycled through the use of a heat exchanger (HX3). The SOFC comes in second with respect to capital expenditures, accounting for 31% of the total costs for the system components. The gasifier only contributed 4% of the total component costs.

The main economic parameter for the comparison of the costs of the biomass energy plant to those of other energy projects is the LCOE. The LCOE of the biomass energy plant was

Table 14: An overview of the economic performance of the biomass plant assessed through a discounted cash flow to calculate the NPV for the costs and the resulting LCOE. The savings on electricity and LPG in the coffee processing unit are seen as negative costs.

Parameter	Costs	Literature	Reference
CapEx	$ 24,089,210		
CapEx/kW	$ 8,984	$ 500 - $ 6500	IRENA (2022)
OpEx	$ 361,338/year		
Ash removal	$ 9,364/year		
Fuel costs	$ 0/year		
LPG savings	$ -266,795/year		
Electricity savings	$ -44,890/year		
NPV_{costs}	$ 25,282,923		
NPV_{power}	56130 MWh		
LCOE	$ 0.45/kWh	$ 0.93/kWh	Permana et al. (2024)

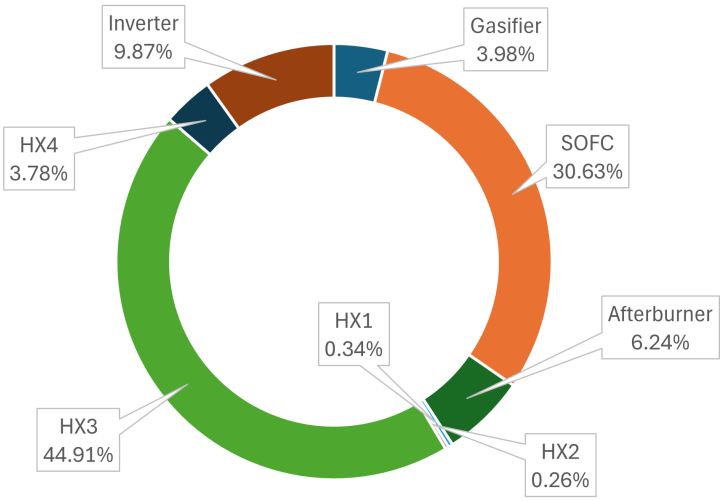

Figure 8: Distribution of the different system component costs in the CapEx, with the largest contributor being the heat exchanger for the recycling of heat from the air going into the cathode side of the SOFC.

$0.45/kWh. On average, bioenergy projects in India have the lowest costs per kWh in the world with an average LCOE for bioenergy of just $0.06/kWh, which is even lower than that of new fossil fuel projects. (IRENA, 2022) The SOFC project is a multitude more expensive than this average for bioenergy in India. However, most bioenergy in India is produced through direct combustion or the production of ethanol for the transport sector. Therefore, this average LCOE is not a good comparison for the costs of similar gasification-SOFC biomass plants as discussed within this study. Corigliano, Lorenzo, and Fragiacomo (2021) reported that for a hybrid SOFC-gas turbine setup the LCOE was between $0.09 and $0.14/kWh. Another hybrid setup combining an SOFC with an organic Rankine cycle (ORC) in Italy reported an LCOE of $0.93/kWh.

4.5 Sensitivity analysis

In the previous sections, the results of the gasification-SOFC model were described and compared with those in the literature. In this section, the main operating parameters and model assumptions are tested to understand how critical these parameters are for the performance of the system and to optimize the operating conditions of the plant. Since the biomass plant as a whole should be optimized and not just the individual components, a sensitivity analysis will be used to optimize the performance of the system as a whole with respect to power output and economic viability. For the sensitivity analysis of the technical input parameters and CapEx, the sensitivity analysis function in Aspen Plus was used.

4.5.1 Gasification temperature

Coffee husk gasification can already be achieved at temperatures of 600 °C. Therefore, a sensitivity analysis was performed on the gasification temperature to optimize the composition of the syngas, the cold-gas efficiency of the gasification process, the overall energy efficiency, and the CapEx of the biomass plant. A sensitivity analysis towards the power output of the plant was also performed, but no notable differences in power output were detected. This result confirms that SOFCs have quite a low selectivity toward the different molar fractions in the syngas. The results of the analysis are shown in Figure 9.

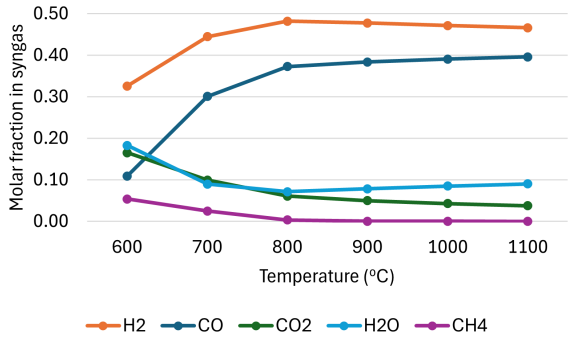

(a) Molar fractions of species in the syngas

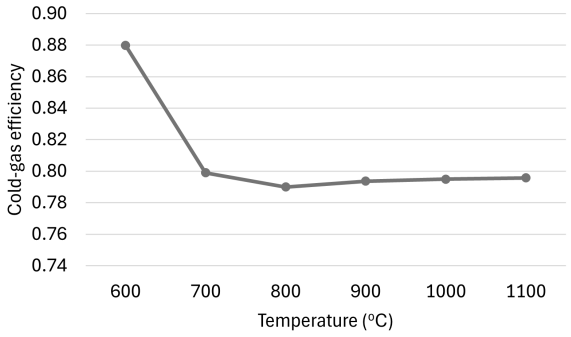

(b) Cold-gas efficiency (CGE)

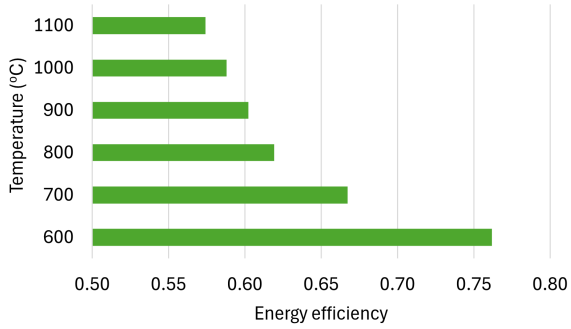

(c) Overall energy efficiency of the biomass plant

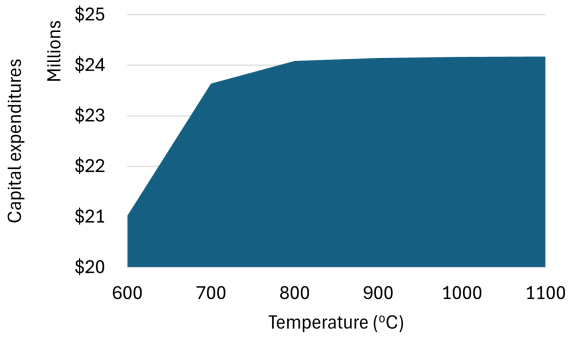

(d) Capital expenditures for biomass plant

Figure 9: Sensitivity analyses of the gasification temperature between 600 and 1100 °C to optimize the performance of the biomass plant. With a) the molar fractions of the main compounds in the syngas (hydrogen, carbon monoxide, carbon dioxide, water, and methane), b) the cold-gas efficiency of the gasifier that yields the best result at low gasification temperatures, c) the overall energy efficiency of the biomass plant which is highest at the lowest gasification temperature, and d) the capital expenditures of the biomass plant which is lowest at the 600 °C gasification temperature.

The gasification temperature has a positive effect on the formation of hydrogen and carbon

monoxide in the syngas, whereas the carbon dioxide, water, and methane content decrease with rising temperatures, as shown by Figure 9a. These results are in line with the reaction enthalpies of the different reactions during gasification (as shown in Table 15 in the Appendix), which predict this shift in reaction equilibrium with increasing temperature. Since the SOFC reforms both methane and carbon monoxide, higher concentrations of methane in the syngas have no negative impact on the overall system performance. A higher methane content results in a higher cold-gas efficiency of the syngas as shown in Figure 9b. The lower energy requirement that comes with a lower gasification temperature results in an increase in overall system efficiency and a decrease in CapEx due to a lower need for heat recycling (Figure 9c and 9d, respectively).

4.5.2 Steam/biomass ratio (S/B)

The steam-to-biomass (S/B) ratio of the primary process was chosen based on a preliminary sensitivity analysis to optimize the syngas composition. Previous sections showed that an optimization toward a high H_2/CO ratio in the syngas that enters the SOFC does not seem as effective for the system performance as, for example, in a Fischer-Tropsch reaction. (Pala et al., 2017) Therefore, the decision to choose an S/B ratio of 0.1 was challenged through this sensitivity analysis. The S/B ranged from 0.1 to 0.5, and the effects on the CGE, cell voltage, overall energy efficiency and CapEx of the biomass plant were assessed. The results are shown in Figure 10.

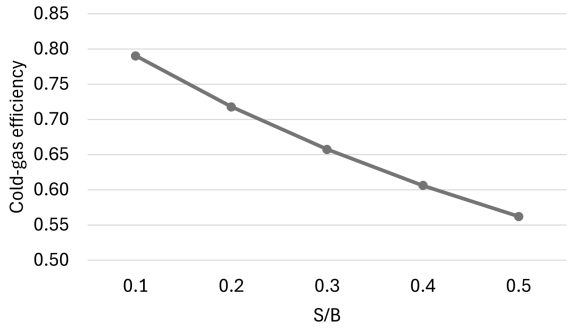

(a) Cold-gas efficiency of the gasification process

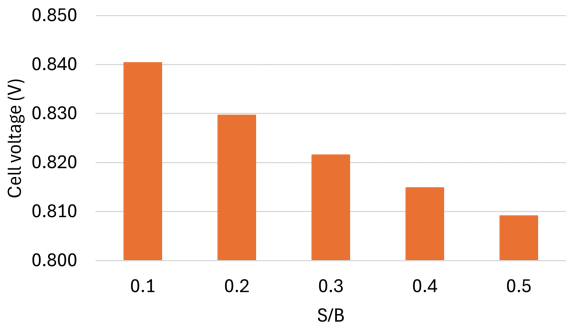

(b) Cell voltage of the SOFC

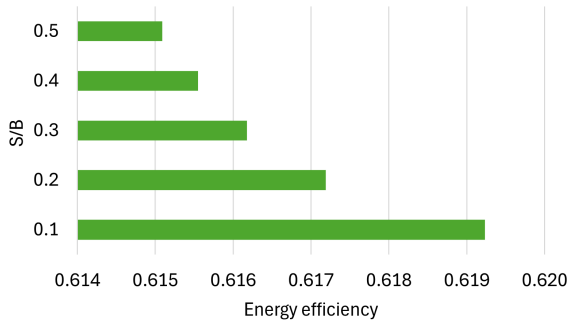

(c) Overall energy efficiency of the biomass plant

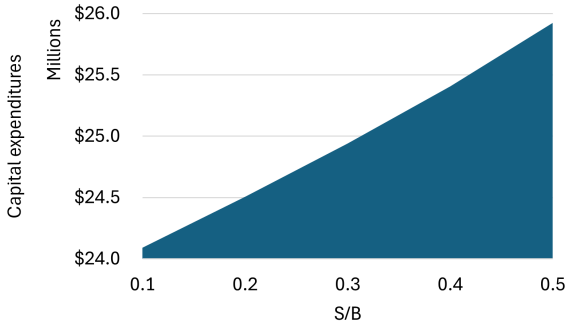

(d) Capital expenditures for biomass plant

Figure 10: Sensitivity analyses of the S/B ratio of the gasification process, which ranged from 0.1-0.5. With a) the cold-gas efficiency of the gasification reactor which decreased by more than 20% with a higher S/B ratio; b) the cell voltage of the SOFC, which showed only limited variations; c) the overall energy efficiency of the biomass plant, which was highest at the chosen S/B ratio of 0.1, although the effect was limited; and d) the capital expenditures of the biomass plant, which were lowest at the 0.1 S/B ratio.

The analysis revealed that increasing the S/B ratio had a negative effect on all four outcomes from which the CGE was most substantial, with a decrease from 0.79 to 0.56 (see Figure 10a). Only a limited effect on the cell voltage and overall energy efficiency of the biomass plant was observed (Figure 10b and 10c, respectively).

4.5.3 SOFC temperature

Changing the SOFC temperature could have a substantial effect on the heat integration of the biomass plant because of the high air ratio. A lower temperature results in the use of smaller heat exchangers and a lower capital cost. However, a lower SOFC temperature could also have a negative impact on the performance of the SOFC due to lower ion diffusivity. The SOFC operating temperature ranged between 700 °C and 900 °C with intervals of 50 degrees to assess the effects on the cell voltage and CapEx. The results are shown in Figure 11.

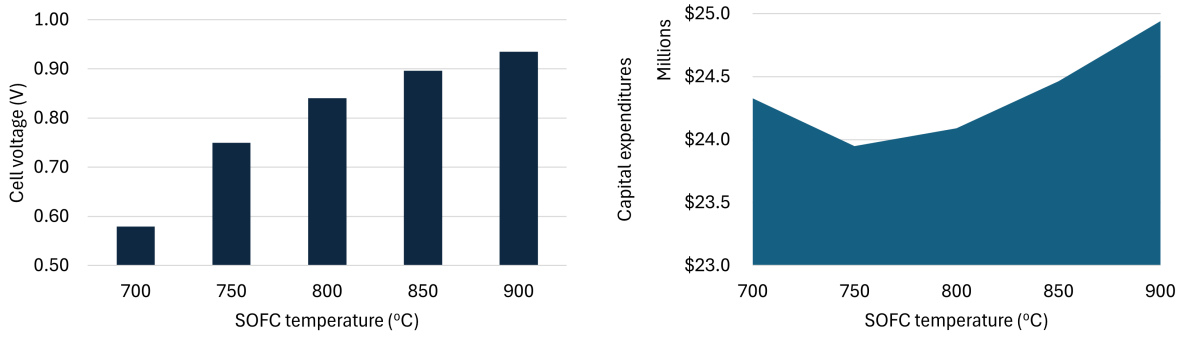

(a) Cell voltage of the SOFC

(b) Capital expenditures for biomass plant

Figure 11: Sensitivity analyses of the SOFC operating temperature with a range of 700 °C and 900 °C with intervals of 50 degrees. With a) the cell voltage of the SOFC, which increased with temperature; and b) CapEx, which was lowest at 750 °C and highest at 900 °C. However, with a higher voltage and therefore power output of the SOFC, the CapEx per kWh of electricity decreases with increasing operating temperature.

The idea that the SOFC temperature affects the CapEx substantially seems to be false. From the chosen temperature of 800 °C, the CapEx deviates by a maximum of 3.5% (see Figure 11b). Nevertheless, lowering the temperature does have a negative effect on the cell voltage of the SOFC (Figure 11a). Increasing the temperature to 900 °C increases the voltage and the efficiency of the SOFC but results in a higher CapEx. When the CapEx per kWh of electricity produced is considered, these costs decrease with higher operating temperatures since the CapEx increases by 3.5%, whereas the power output increases by 11.3% at 900 °C. Based on the model created in Aspen Plus, running the SOFC at a higher temperature positively impacts all the performance metrics analyzed.

4.5.4 Fuel utilization

A higher fuel utilization results in a higher hydrogen oxidation rate and therefore a higher current output of the SOFC. Within this analysis, the impacts on the cell voltage, system efficiencies, and CapEx of the plant were assessed. A fuel utilization greater than 0.8 could lead to higher degrees of concentration polarization as discussed earlier. One large driver of the CapEx is the cost of the heat exchangers, which are driven mostly by recycling the heat from the air going in and out on the cathode side of the SOFC. A lower fuel utilization would produce less heat and might result in a different air ratio for cooling the SOFC. However, the air ratio shows only minor fluctuations when the fuel utilization is changed and was therefore omitted from

this sensitivity analysis. The effects of changing the fuel utilization from 0.5 to 0.9 on the SOFC cell voltage, electrical efficiency, overall efficiency, and CapEx were evaluated. The results from this evaluation are shown in Figure 12.

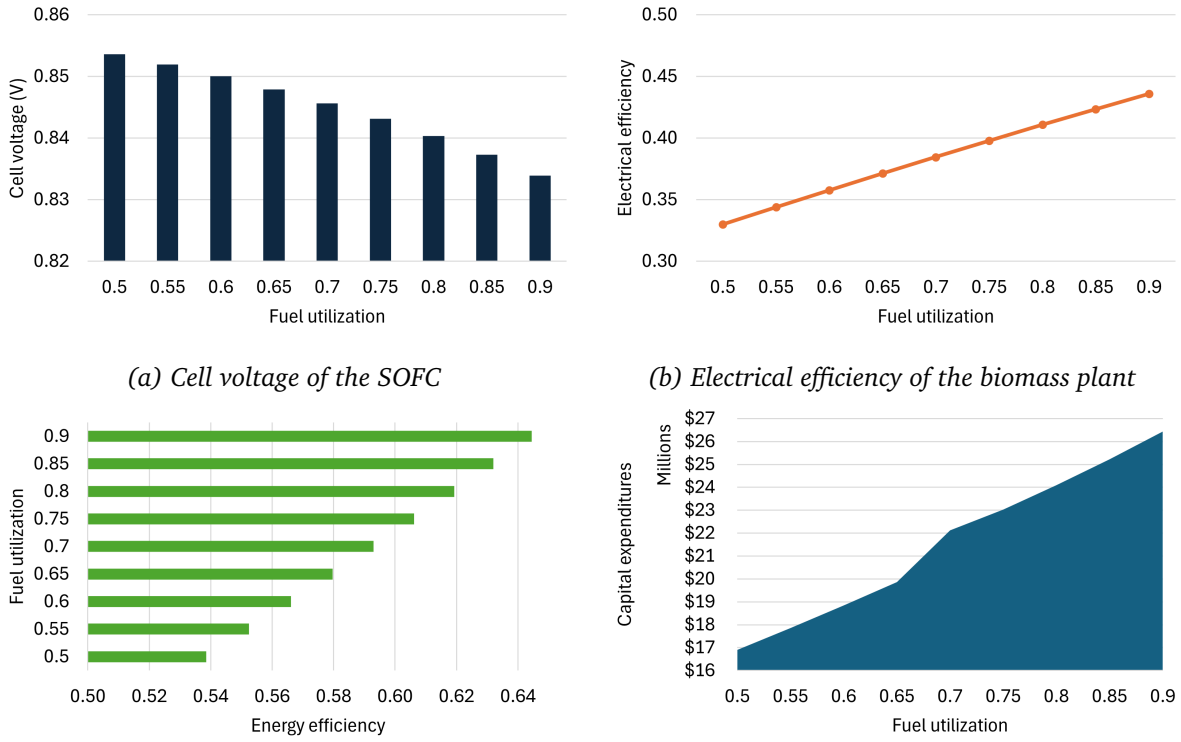

(a) Cell voltage of the SOFC

(b) Electrical efficiency of the biomass plant

(c) Overall energy efficiency of the biomass plant

(d) Capital expenditures for the biomass plant

Figure 12: Sensitivity analyses of the fuel utilization (FU) of the SOFC with a range between 0.5 and 0.9 with intervals of 0.05. With a) the cell voltage of the SOFC, which decreases with increasing FU but has limited effects; b) the electrical efficiency; c) the energy efficiency of the biomass plant, which is inversely related to the voltage and increase with increasing FU; and d) the CapEx, which increases with increasing FU.

With a higher fuel utilization, the voltage output of the SOFC drops; however, the effects are only 20 mV between fuel utilizations of 0.5 and 0.9, as shown in Figure 12a. In the previous sections, the voltage output of the SOFC, the power output, and the efficiencies of the system all exhibited similar behavior since the current of the system remained unchanged. However, with higher fuel utilization, a higher current is achieved, which seems to have a positive effect on the power output of the SOFC and the electrical and overall system efficiency, as shown in Figure 12b and Figure 12c. Although the efficiencies of the system improve with increasing fuel utilization, the CapEx of the system increases as well; both in absolute terms as in CapEx per kWh of electrical output (Figure 12b). Nevertheless, since the power output increases with higher fuel utilization, the LCOE of the plant decreases.

4.5.5 Current density

The last technical parameter analyzed was the current density, which is one of the main performance indicators of the SOFC. The higher the current density is, the lower the total stack area needed to process the syngas feed, decreasing the overall size of the SOFC and therefore the purchasing costs of the SOFC. This does not directly mean that the CapEx will decrease since other factors impact the capital costs of the system as well. For the current density, the cell voltage and the CapEx per kWh were chosen as the main performance indicators to be tested in

the sensitivity analysis. The results are shown in Figure 13.

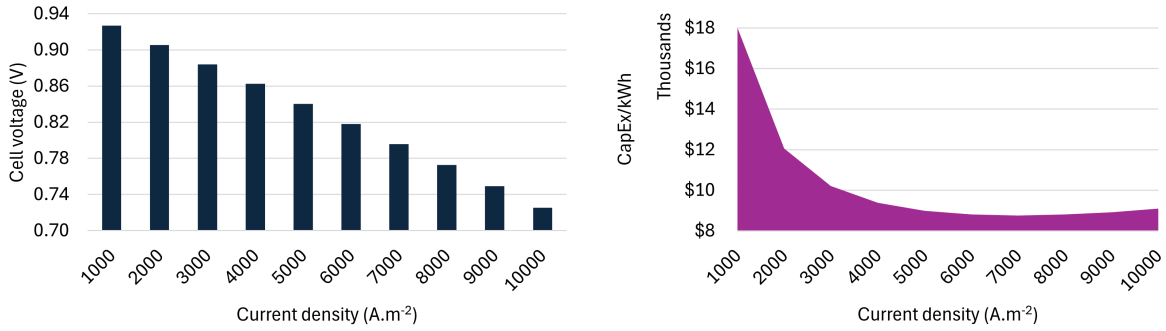

(a) Cell voltage (V) of the SOFC

(b) Capital expenditures for the biomass plant

Figure 13: Sensitivity analyses of the current density of the SOFC with a range between 1000 and 10000 A.m^{-2}. With a) the cell voltage of the SOFC, which decreases with higher current density; and b) the CapEx per kWh, which decreases steeply between current densities of 1,000 and 5,000, reaches its lowest value of 8,757 $/kWh at a current density of 7,000 and increases toward the highest current density of 10,000.

With increasing current density, the total voltage output decreases from a cell voltage of 927 mV at 1000 Ampere to 725 mV at 10,000 Ampere, as shown in Figure 13a. A lower current density requires a larger SOFC for the same power output, explaining the higher capital costs at low current densities, as shown in Figure 13b. The increase in CapEx per kWh stops after a current density of 7000A and increases slightly afterwards. This is probably due to a further decrease in voltage, which directly impacts the power output and thereby increases the CapEx/kWh.

4.5.6 System optimization

Implementing all the process parameters with either the highest power output or the lowest CapEx would result in a gasification temperature of 600 °C, an S/B ratio of 0.1, an SOFC operating temperature of 900 degrees, a fuel utilization of 0.5, and a current density of 7000. Since the sensitivity analyses were performed separately, the interrelations between the different parameters were not analyzed. The interrelation between the optimal process parameters could lead either to further optimization of the performance or, more likely, to negative interrelations affecting the overall performance of the biomass plant. Combining the optimal results of the sensitivity analysis results in a power output of 2,146 kW, a CapEx of $ 17.5 million, and an LCOE of $ 347.72 per MWh.

The LCOE of this optimized state has decreased, but the power output is lower and the energy losses in the system have increased because the gasifier is producing heat at 600 °C instead of being in need of heating from an EAF.

4.5.7 Economic model

In the economic model, arbitrary assumptions were made that influence the outcome of the LCOE. Since both the economic and the technical model are agnostic about the equipment used and the sizing of, for example, the gasifier reactor and the stack design of the SOFC, the model is based on cost equations for the different components and averages of costs found in literature. This sensitivity analysis aims to show the effects of the chosen inflation, the Lang factor, the OpEx percentage, and the days of operation per year as proxies for the capacity factor of the plant. The results of the analysis of inflation and the Lang factor are shown in Figure 14, the other economic parameters are presented in Figure 15.

The inflation percentage was used to index both the operational costs of the 30-year lifetime of the plant and the cost savings on electricity and LPG from the fact that these sources are now supplied through the biomass plant. When the inflation rate ranged from 2 to 6%, a shift in the LCOE of 445.75 $/MWh to 457.03 $/MWh was observed. Tripling inflation results in an increase in the LCOE of 2.6% (see Figure 14a).

The Lang factor was used as an index for the component costs to include all other costs such as auxiliary equipment and permits. This factor was set to 3.63, which is the factor used by Tera et al. (2024) for the economic assessment of a biomass plant. The values reported in the literature range from just lower than 2 to approximately 5 for petrochemical projects. Therefore, the Lang factor in this analysis ranged from 2-5 with intervals of 0.5. The results show a significant shift in the LCOE from 199.25 $/MWh to 661.55 $/MWh. A shift of 250% in the Lang factor (from 2 to 5) has an impact of 332% on the LCOE (as shown in Figure 14b).

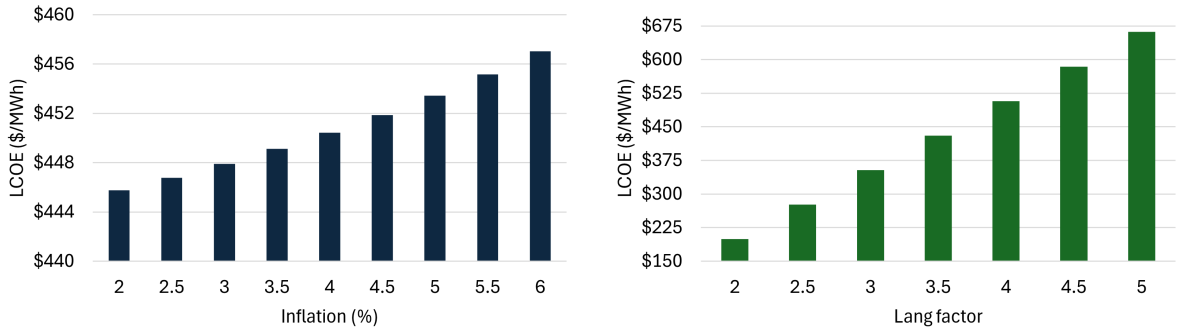

(a) Inflation percentage

(b) Lang factor

Figure 14: Sensitivity analysis of the a) inflation toward the LCOE; and b) the Lang factor toward the LCOE. The LCOE increases with a higher inflation, although this effect is limited to a maximum of 2.5 percent between an inflation of 2 and 6 percent. The Lang factor has a greater impact on the LCOE, increasing by more than 300 percent with a change in the Lang factor from 2 to 5.

The operational expenditures are modeled as a fixed percentage of the CapEx. These operational costs often range between 1% and 6%. In the sensitivity analysis, these values were chosen with an interval of 1%. The shift in OpEx more than doubled the LCOE ($ 407.03 at 1% and $ 841.05 at 6%), with an almost linear relation, shown in Figure 15.

The capacity factor, defined through the days of operation of the plant, had the largest impact on the financial performance of the biomass plant (see Figure 15). This analysis kept the OpEx of the plant fixed; however, in reality it would be logical that these expenditures would grow with the capacity factor. In terms of costs, only the ash disposal costs increased with the number of days in operation per year. The higher the capacity factor is, the higher the electricity output of the plant and the lower the LCOE. With 300 days of operation, the capacity factor was 0.82, which is in line with the maximum capacity factors of biomass plants in India. (IRENA, 2022) Changing the capacity factor to 300 days per year yields a reduction in LCOE of 73%.

Finally, the impact of changing the discount rate was assessed by varying the discount rate from 5 to 10%. The results are shown in Figure 15. A linear relation between the discount rate, in the form of the WACC, and the LCOE can be seen where the LCOE almost doubles from 383.81 $/MWh to 645.49 $/MWh when the WACC is doubled from 5 to 10%. The sensitivity towards the WACC is an interesting outcome for the decision of the loan-to-equity ratio of the financing of the biomass plant. Currently, the WACC, and therefore the discount rate, is based on 100 percent loan financing. When equity is used to finance the biomass project, the WACC will change, which will impact the LCOE of the project directly.

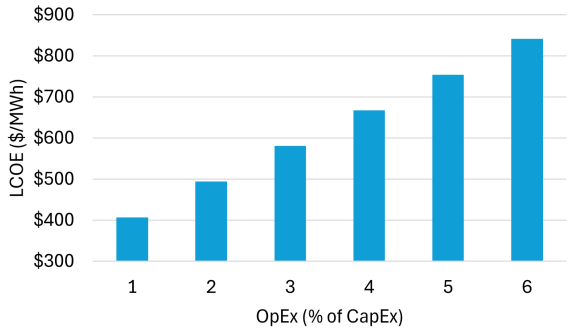

(a) Operational expenditures as a percentage of CapEx

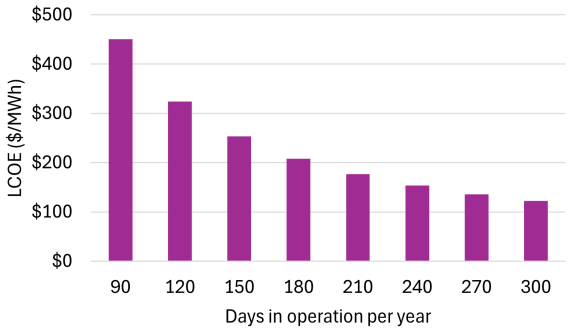

(b) Number of days of operation per year

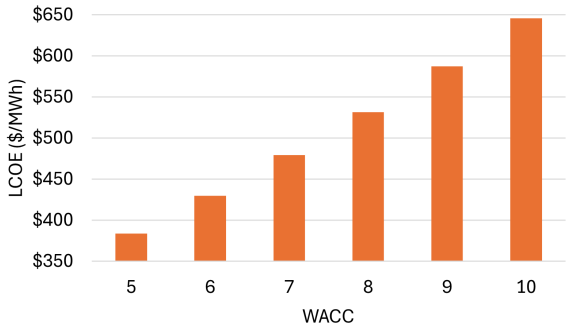

(c) Discount factor expressed as the WACC

Figure 15: Sensitivity analysis of the economic part of this study with respect to a) OpEx as a percentage of CapEx, which shows linear growth in LCOE; b) the capacity factor of the plant expressed as the number of days of operation per year, which shows a steep decline in the LCOE between 90 and 180 days of operation while declining less steeply toward 300 days of operation; and c) the WACC or discount factor chosen for the model, which almost doubles between 5 percent and 10 percent to a value of 645 $/MWh.

5 Discussion

The methodology is based on a number of assumptions to create a technical and economic model for the coffee husk power plant. The technical model represents the upper margins of performance of the biomass conversion process and is agnostic about the type of equipment used, i.e. the type of gasifier and the size and materials of the SOFC stack. The financial model is based on this same agnostic approach with respect to the equipment used and uses generic cost equations and arbitrary input parameters to analyze the economic performance of the biomass plant. Therefore, a critical assessment is performed to challenge these model assumptions.

In this section, the most critical assumptions that were made to build the model for the biomass plant are discussed. The assumptions on the operation of the biomass plant in relation to the coffee processing unit are given in Section 5.1. Second, the model design for gasification and gas cleaning is discussed in Section 5.2. In Sections 5.3 and 5.4, the SOFC and heat integration are critically assessed, and finally, in Section 5.5, the economic model is evaluated.

5.1 Plant operation

For the biomass plant operation, it was assumed that the plant operates for a fixed period of 90 days per year, parallel with the harvest season and the operation of coffee processing units in Wayanad. This harvest season is heavily dependent on the weather in a given year and could be shorter or longer in reality. Also, the start of the monsoon season is an important factor since coffee cherries are dried under ambient conditions after harvest before they are processed to produce green coffee beans. As seen in the sensitivity analysis, the capacity factor of the biomass plant is an important factor for the economic viability of the biomass plant. When the harvest season is shorter in a given year, it impacts the economic viability of the plant. The assumption that the operation of the biomass plant is parallel with the harvest season substantially impacts the financial viability of the plant. If the capacity factor of the plant aligns with that of average bioenergy plants in India according to the data of IRENA (2022), the LCOE could be quartered following the sensitivity analysis results.

The assumption was that the biomass plant operates continuously, 24 hours in a day, and is fed with the biomass residues produced during coffee processing. In this scenario, the biomass plant only has to provide electricity and heat for the coffee processing unit for 10 hours a day. During the other 14 hours of the day, the heat produced is lost to the environment and negatively impacts the efficiency of the plant substantially. The electricity that is not utilized in the coffee processing plant should find another destination. Currently, the assumption is that the electricity can be sold to the grid, but this assumption is by no means a certain.

The overall model of the plant does not include any pressure drops over the different components and piping in the system. Adding pressure losses and pumps to compensate for these losses would impact the overall system efficiency and costs of the biomass plant. However, an argument could be made that the current Lang factor would cover the costs for these pumps as well and that the addition of pumps would have limited to no effect on the CapEx of the plant.

5.2 Gasification & gas cleaning

In the gasification model, an RGibbs reactor was used in Aspen Plus, which models coffee husk gasification by minimizing the Gibbs free energy of the gasification reactions. This results in complete carbon conversion in the reaction and no char formation. Additionally, tar formation was disregarded, and nitrogen was assumed to be inert. The current Aspen Plus model describes the theoretical upper limits of the gasification reaction. In reality, the performance of the gasifier

would be not as efficient, and the conversion to syngas would be lower since there would be a tar and char fraction after gasification. However, the experimental results show that CGE values as high as those in the current model can be achieved. As mentioned earlier, a stoichiometric model, as described by Pilar González-Vázquez et al. (2021), would yield results closer to the experimental reality of the gasification process, and the use of such a model would further improve the biomass conversion model.

The current gasification reaction uses steam as the gasifying agent based on a preliminary analysis toward optimizing the hydrogen fraction in the syngas. However, another gasifying agent could yield better results. Compared with other options, steam is a gasifying agent that is easy to implement and readily available. This could be another reason for the use of steam.

5.3 SOFC

For the SOFC, the largest caveat in the validity of the model would be the large air ratio that is needed to run the SOFC isothermally. The incoming air cannot be more than 100 degrees cooler than the operating temperature of the SOFC, which results in a large energy need to heat the incoming air. When this heat is recycled via heat exchangers, the needed size of these heat exchangers contributes to more than 40% of the component costs of the biomass plant.

In addition, Aspen Plus does not contain an SOFC block to model the performance of a fuel cell. Therefore, the fuel cell model used generic blocks, possibly affecting the modeling results and their reliability compared with experimental findings. The use of the Gibbs free energy of the reactions in the ANODE block instead of the Nernst equation to determine the reversible cell voltage partly compensates for some of the imprecision of the model.

The overpotentials were determined via generic relations based on experimental results that approximate the values for the overpotentials. For the activation overpotential, the simplified version of the Tafel equation that yields good results for low activation polarizations could be improved upon by using the Buttler-Volmer equation. For the concentration polarization, a simplified relation of Chan et al. (2001) was used to mimic the approximate logarithmic relation between the current density and concentration overpotential caused by the diffusion of the molecules through the pores of the electrodes. However, this simplified method provides a good approximation of the concentration overpotential, especially at low current densities.

For the operation conditions of the SOFC, literature was used to determine the optimal parameters. The syngas described in the literature has a different composition than that used in this research. Additionally, the operating conditions used for the coffee husk conversion system were slightly different from those reported in the literature. Thus, without experimental validation of the model, assessing the viability of the SOFC model will be difficult.

Another factor that should be included in the operation of an SOFC is the lower flexibility of its operation compared with that of a PEM electrolyser. Due to the long warm-up period needed before the SOFC becomes fully operational and the heat required to perform this warm-up, switching off the SOFC often is neither economical nor easy to integrate into the coffee processing unit. Therefore, the decision was made to continually run the SOFC even when the coffee processing unit does not require any energy input.

5.4 Heat

For heat integration, an afterburner was used to burn the remaining hydrogen gas exiting the SOFC. In literature, the choice is often made to use an SOFC with a combined heat and power (CHP) plant. The CHP generates heat that could still be used for the roasting of the coffee, heat recycling, and additional electrical power. This gasification-SOFC-CHP approach would be an

interesting approach for comparison with the current afterburner implementation to determine which approach would lead to better system efficiency.

Another limitation of the current model is that no exergy loss from the system components and piping to the environment through conduction has been taken into account. It was assumed that the system is perfectly isolated and in thermodynamic equilibrium. Furthermore, the heat exchangers were assumed to be perfectly isolated and the heat transfer performance was assumed to be optimal. With these assumptions, no additional heat input was needed since heating of the input streams and gasifier is supplied through the waste heat and produced electricity, respectively. The effect of accounting for additional heat losses on the overall system efficiency should be determined. A substantial amount of heat is still discarded as waste. This wasted heat could also be used to further improve the heat integration of the system when more sources of exergy loss are included in the model.

Finally, it was assumed that the heat from the heat exchanger could be used for the roasting of the coffee. The heat supplied for roasting is equal to the amount of heat normally generated through the burning of LPG in the coffee roaster. However, whether this heat can be integrated into existing coffee roasting equipment at coffee processing plants in Wayanad should be further researched.

5.5 Economic model

From all the assumptions made in this study, the ones in the economic assessment of the biomass plant might be most arbitrary. The cost equations and the CEPCI factor are used to transform the costs of the equipment in a given year to the current year. This CEPCI factor includes factors such as inflation, commodity prices, and overall selling prices of equipment on the basis of a large dataset of relevant transaction data. (Chemical Engineering, 2024) However, this index is a generic index for all components and does not include cost reductions of certain technologies due to maturation and scaling up of the production of that technology. For certain components, like heat exchangers, which are already mature systems, the CEPCI system might be a good approach. A SOFC is not yet mature technology as even gasifiers were seen as new kids on the bioenergy block by IRENA (2022). These technologies could see drastic price reductions following Wright's Law, as seen with other renewable energy technologies such as photovoltaics and wind turbines. (Our World in Data, 2023) In addition to the CEPCI factor, the use of these cost equations could generally be questioned. Since the technological model was agnostic about the type of gasifier or SOFC used, a generic approach to pricing using these cost equations was a logical choice.

A Lang factor was used to scale the component costs to the CapEx of the study. The Lang factor includes costs for piping, electrical work, and permits, among other factors. This Lang factor ranges between 1.8 and 5 in literature. A more favorable Lang factor could directly shift the economic model from financially impossible to economically viable. A real assessment of all the different capital costs would shed light on the 'real' Lang factor of the system.

Other arbitrary assumptions were made in the financial model, like: the inflation rate, the OpEx percentage, and the discount rate. The limited sensitivity of the model to the inflation rate makes the inflation assumption relatively safe. The OpEx percentage and discount rate do show large fluctuations in their sensitivity analyses. The operational expenditures need further definition of the different costs to obtain a better idea of the size of this cost component. The discount rate is always a vulnerability of the discounted cash flow method. Using the WACC as a discount rate already grounds the discount rate toward the real time value of money. However, the current WACC is based on the assumption that the full CapEx of the biomass plant is financed through loans. In reality, the WACC will also be dependent on the cost of equity.

6 Conclusions & Recommendations

This study created a blueprint for the use of coffee processing mill residues (CPMR) to support the energy needs of coffee processing units in the district of Wayanad in the state of Kerala in India. The evaluation of the available biomass residues of the dry coffee process and their current uses revealed that coffee husk was the most potent material to use for biomass conversion to energy because of its availability: coffee husk is the largest residue with 40% of the weight of the dried coffee cherry. Additionally, the current uses for coffee husk are limited, and no economical use for managing this residue is available thus far. The coffee husk has a generally low moisture content of approximately 12%, a relatively small particle size, and a low bulk density. Therefore, gasification was the most suitable biomass conversion technique to use for the coffee husk material. A solix oxide fuel cell (SOFC) was used to convert the syngas from gasification to electricity and heat: the two energy sources needed during dry coffee processing including roasting and grinding.

To optimize the biomass energy system, a two-step gas cleaning process was integrated to prepare the syngas produced during gasification for injection into the SOFC. These cleaning steps removed the ash content of the syngas and lowered the hydrogen sulfide fraction to a concentration lower than 10 ppm to protect the anode plates of the SOFC against degradation. After the syngas was reformed and oxidized in the SOFC, an afterburner was used to produce additional heat. The heat from the exhaust gas was used for coffee roasting to replace the currently used liquefied petroleum gas (LPG). The residual exhaust gas was deployed for heating the input streams of the biomass conversion plant: the steam used as a gasifying agent, the syngas before it entered the SOFC, and the air supplied to the cathode side of the SOFC.

The biomass plant was modeled in Aspen Plus to assess the potential of coffee husk in the biomass conversion process. The SOFC produced a power output of 2,681 kW with a cell voltage of 840 mV and a current of 3,190 kA based on a biomass feedrate of 1,295 kilograms per hour. From this electrical power output, 241 kW was needed to heat the gasifier via an electric arc furnace (EAF) to allow for a constant operating temperature in the gasifier. The coffee processing plant has an electrical energy need of 896 kW. Therefore, the electricity produced from the coffee husk exceeds the energy needed during coffee processing. The residual electrical power output of the biomass plant is 1,544 kW during coffee processing and 2440 kW when the coffee processing unit is not operational. On the basis of this residual electrical output and the total coffee production in Wayanad of 61,000 tonnes of green coffee beans, the potential of this method for electricity production in Wayanad would amount to 93.4 GWh of electricity. This substantial surplus of energy could be used for other purposes, such as supporting local communities, or selling to the electricity grid. Taking heat integration into account, the overall energy efficiency of the plant was 62%. The majority of the exergy loss of the system came from the heat in the exhaust gas, which was assumed to be released into the environment.

To assess the economic viability of the biomass plant, a discounted cash-flow method was used to calculate the levelized cost of electricity (LCOE). For the calculation of capital expenditures (CapEx), cost equations from literature were used for the components of the energy plant, including a CEPCI factor to index these costs to the current year. A Lang factor of 3.63 was applied to these component costs to include additional costs for piping, land, and electrical connections, among others. This method yielded a CapEX of $ 24.1 million or $ 8,984 per kW. Compared with those of other bioenergy projects in India, these costs are relatively high. This is probably due to the innovative nature of the project, the chosen method of assessing capital costs, and the uncertainty about the costs associated with these types of innovative projects and arbitrary input variables. For the calculation of the LCOE, cash-flows were produced with a project lifetime of 30 years, including operational expenditures estimated at 1.5% of the CapEx, fuel costs being zero, costs for ash disposal, and savings on electricity and LPG realized through

this project as negative costs. All costs were indexed on a yearly basis by an inflation rate of 4%. This resulted in an LCOE of $ 0.45 per kWh. The LCOE is substantially higher than the average cost for bioenergy in India. However, the LCOE is in line with similar system designs in literature. The higher LCOE is probably due to the innovative nature of the plant's design. When technology such as the SOFC matures, technology prices could fall following Wright's Law.

A sensitivity analysis of the technical parameters of this study revealed better operation conditions: a lower gasification temperature, higher SOFC temperature, lower fuel utilization, and higher current density. The outcome of these optimized operation conditions resulted in an LCOE of $ 0.35 per kWh. The sensitivity analysis of the economic model showed substantial fluctuations with LCOE values approaching $ 0.12 per kWh under more favorable conditions. Increasing the capacity factor of the plant from 90 days per year to 300 days per year would be a game changer for its economic viability; and feasible when biomass is available year round, not just during the harvest season.

The LCOE of the plant of $ 0.45 per kWh is substantially higher than the average cost for bioenergy in India. However, with changes in operating conditions, a higher capacity factor, and more favorable cost parameters, the coffee husks biomass plant could become a viable option to make coffee processing more sustainable by reducing carbon emissions and waste generation. Moreover, the use of coffee husks for bioenergy could support local smallholder coffee farmers in improving the quality of their coffee, making coffee farming more profitable and resilient in the future.

For further improvements to this feasibility study, the following recommendations should be taken into consideration:

- The system model can be improved by including pressure drops, including exergy losses caused by pump efficiency, heat loss through system components, piping and nonoptimal efficiency of the heat exchangers, and changing the modeling approach of the gasifier to a stoichiometric model that provides results closer to experimental reality.
- Designing the system on the basis of a selection of technologies, such as a fluidized bed gasifier, contrary to the current model which is agnostic about the type of gasifier and SOFC used. This adds to the precision of the technical model and the accuracy of the economic model compared to the current system of cost equations combined to a Lang factor.
- Extending the sensitivity analysis with the interrelationship between the different input parameters to find the optimal operating conditions for the biomass plant.
- Improving the capacity factor of the biomass plant. Following the sensitivity analysis, this parameter has the highest potential to lower the LCOE of the plant.
- Heat produced and released into the environment through the exhaust gas could be integrated into coffee cultivation. The drying of harvested coffee cherries before further processing occurs under ambient conditions and is sensitive to rainfall and high humidity causing fungal growth and other degradation of the cherries. These conditions cause lower yields and lower quality coffee. Heat from the biomass plant could be used in the mechanical drying of these cherries, shortening the period needed for drying and providing more overall process control. Thus, resulting in higher yields and higher quality coffee beans.
- This residual heat could be used to dry the coffee husk (and potentially other biomass sources) to store biomass for a longer period of time. This allows longer operation of the

biomass plant, increasing the capacity factor of the plant and substantially lowering the LCOE as seen in the results of this study.

- Researching the technical possibilities to use other coffee mill processing residues, such as defective cherries, defective green beans, and peaberries, as feedstocks for energy generation in the same biomass plant. Additionally, whether the use of these alternative biomass sources for bioenergy is economically more favorable than their current use should be studied.
- Conducting further research on the combination of the designed biomass plant with a combined heat and power (CHP) plant. This design is often described in literature and generally achieves higher overall system efficiencies than the current afterburner does. (Hasanzadeh, Chitsaz, Mojaver, & Ghasemi, 2021; Sadeghi et al., 2018)
- The coffee processing plant used in this research to base the feedrate of the biomass on, Perfetto Naturals, processes more crops than just coffee. Investigating these other crops and the biomass residues produced could scale up the biomass power plant, and, more importantly, might allow the plant to be operational outside the harvest season of the coffee cherries.
- Add carbon capture and sequestration to the biomass conversion process to make the plant carbon-negative. (Anukam et al., 2016)
- A substantial amount of electricity currently produced is not needed during coffee processing and is sold to the electricity grid. However, this makes the assumption that this electricity could always be sold to the grid for a market price. This electrical power could be put to better use by supporting local communities in their energy needs, making them less dependent on the electricity grid and providing more energy security.
- Solar assistance might supply the heat for the gasification currently supplied by an electric arc furnace, either through photovoltaics or through concentrated solar power (CSP) directly into the gasifier chamber.
- Aristizábal-Marulanda et al. reported that side products from CPMRs could be used to create four different categories of products through a biorefinery concept: bioenergy, biofuels, bioactive compounds, and chemical compounds. A biorefinery has the potential to further decrease the waste produced during coffee processing and produce more valuable outputs than just electricity and heat.

Appendix

Coffee cultivation in India

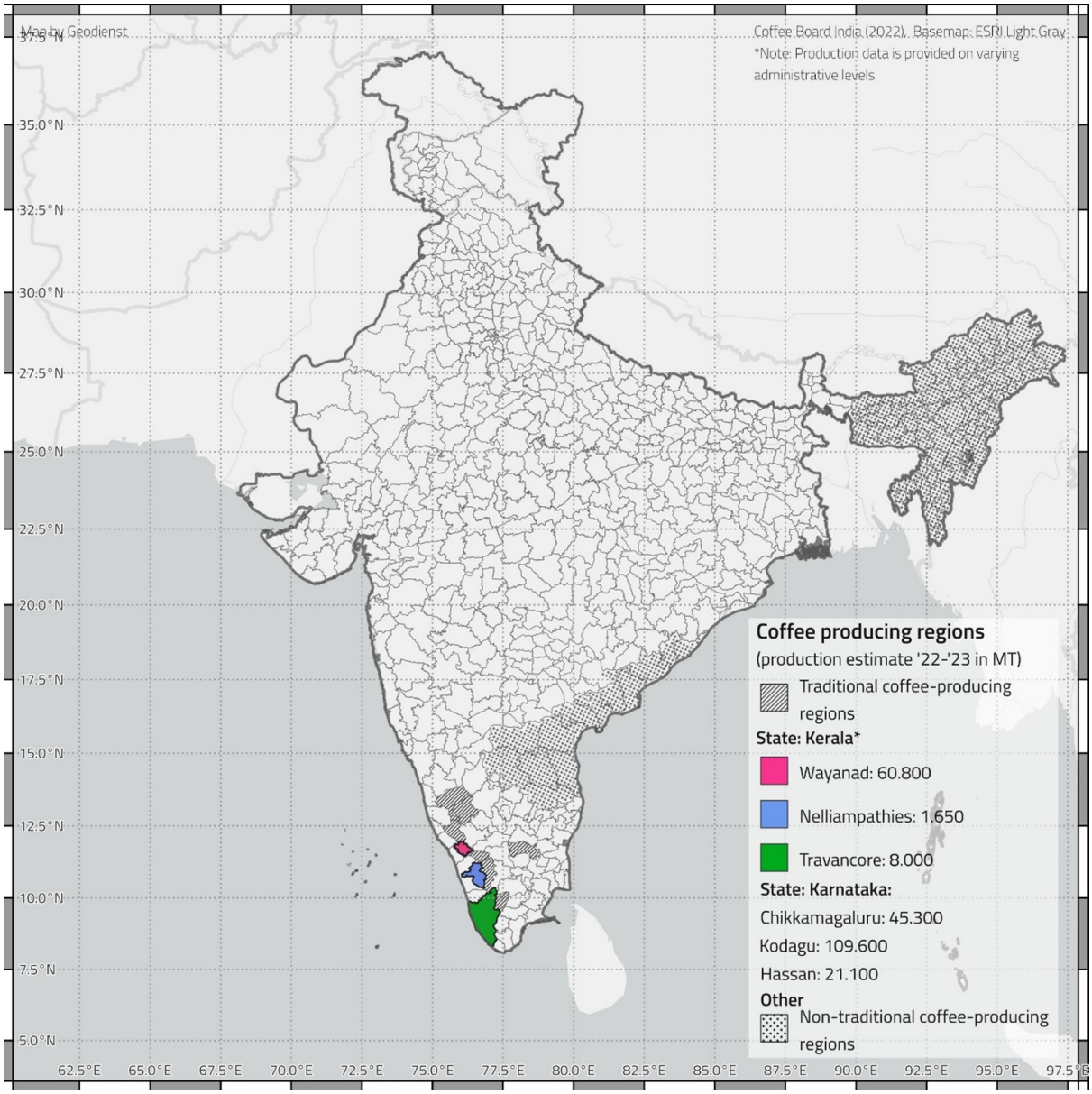

Figure 16: Map of India with the district of Wayanad highlighted in pink with the total production of 60,800 metric ton of coffee in the season 2022/2023. (Iglesias, 2023)

Alternative processing methods

Semi-dry process

Within the semi-dry process the dry and wet processing methods are combined. Other names for the same process are honey, semi-washed, or the decascado process. (Febrianto & Zhu, 2023) Coffee cherries are depulped like in the wet process but not fermented. After depulping they are directly dried before hulling. Due to the drying with the mucilage still around the coffee bean, a honey-like aroma is added to the coffee bean, hence the name. (Bastian et al., 2021) The mucilage contains primarily carbohydrates like saccharides and pectin which cause this sweet aroma. Within the semi-dry process there are certain levels of categories based on the amount of mucilage left on the coffee bean after depulping resulting in white, yellow, red and black honey coffee, where white means no mucillage and black up to 80 percent of mucillage on the coffee bean. This naming refers to the colour of the coffee bean after drying. While drying the beans, an aerobic fermentation process takes place in the coffee bean as well comparable to that of the dry process. Based on the amount of mucillage still left on the bean, the drying could take up to 4 weeks, just like the dry process. (Febrianto & Zhu, 2023) Drying with only the mucillage around the coffee bean compared to the full cherry like in the dry process results in a coffee bean lower in chlorogenic acid, and lower in trigonelline than both the dry and wet process. Due to the sweeter quality in the honey process it is often used for espresso. (Bastian et al., 2021)

Other processing methods

Other, more niche, types of coffee processing exist which are often variations on the two main methods. These methods take influences from other industries to optimize the flavour of the coffee beans. From these emerging processing methods, carbonic maceration, anaerobic fermentation, and digestion processing are the most known ones. (de Melo Pereira et al., 2019; Várady et al., 2022) Other examples methods include wine coffee beans and Burundian coffees that use different fermentation techniques to give a unique taste to the coffee bean. (Febrianto & Zhu, 2023) These alternative processing methods often use an extensive fermentation process of the coffee cherry that still covers the coffee bean resulting in a significant change in the taste of the coffee bean in comparison to the more traditional methods. Subsequently, these methods also affect the occurrence of antioxidant activities in the green coffee bean which are related to health benefits as mentioned earlier. (Várady et al., 2022) Therefore, in the search towards higher quality coffee, farmers and coffee processing companies are experimenting more and more with these different processing techniques.

With anaerobic fermentation, either wet parchment coffee from the wet processing or the whole coffee cherries before the dry processing starts are fermented in anaerobic conditions. The coffee beans are placed in a bioreactor either with or without a starter culture for the fermentation. The fermentation therefore is done with micro-organisms naturally occurring in the coffee beans or with an added culture which would give more control over the fermentation process. The fermentation usually takes somewhere between 16 to 90 hours. This additional fermentation compared to the standard wet or dry process adds important flavour precursors that result in a higher volatile content after roasting contributing to aromas like chocolate, caramel and fruity notes. These are important for the sensory quality of the coffee. The type of micro-organism that becomes dominant during the fermentation process has an important impact on the development of certain tasting notes, so control over these type of cultures is important for quality control and consistent results after anaerobic fermentation. (Febrianto & Zhu, 2023)

With carbonic masceration the coffee cherries are being fermented under a CO_2 rich environment as a preparation step for either the dry processing, wet processing or semi-dry process.

This technique is found in wine making as well. Coffee cherries are stored in a bioreactor, which can be everything from a metal reactor to a plastic bag, where the air is removed and CO_2 is added to create a CO_2 rich environment. The reactor is then placed in an incubator for 24 to 120 hours in temperatures ranging from 18 to 38 °C. Due to this environment the riping process of the coffee fruit is delayed and the fermentation causes a change in the chemical composition of the green coffee bean and thereby a change in the sensory profile of the coffee. Carbonic masceration was found to increase the alkaloids, phenolics, acids, and sugars in Arabica coffee which subsequently improved its sensory score in coffee tasting tests. (Febrianto & Zhu, 2023) This chemical shift in the coffee bean could be even more interesting for increasing the quality of Robusta coffees since it seems to add certain qualities to the green coffee bean that are missing in Robusta coffee.

One of the most (in)famous forms of coffee processing resulting in the most expensive coffees in the world are processed through an animal fermentation. In this form of processing, the coffee cherries are fed to certain animals. The digested coffee beans are subsequently processed by collection of the animal faeces and washing and drying to end up with the green coffee bean. (Tsai, Chang, Huang, Lin, & Chen, 2023; Febrianto & Zhu, 2023) These coffee beans have a unique sensory experience, are low-volume and labor-intensive, and therefore have a high price. The high quality of this coffee is often explained by the fact that animals in the wild only eat the best and ripest cherries, which is basically the optimal harvesting condition. The cherries are consumed whole and digested for up to 70 hours, without destroying the cherry. The microbiome in the gut of these animals affect the coffee bean in a unique way contributing to the sensory experience in the cup. (Febrianto & Zhu, 2023) However, the digestion method is controversial due to the animal cruelty involved in higher volume production of the coffee where the animals are caged and fed only with the coffee cherry with the civet cat being the most known example. (Tsai et al., 2023) Other examples of animals used within the digestion method are elephants, the jacu bird and certain types of monkeys. (Febrianto & Zhu, 2023)

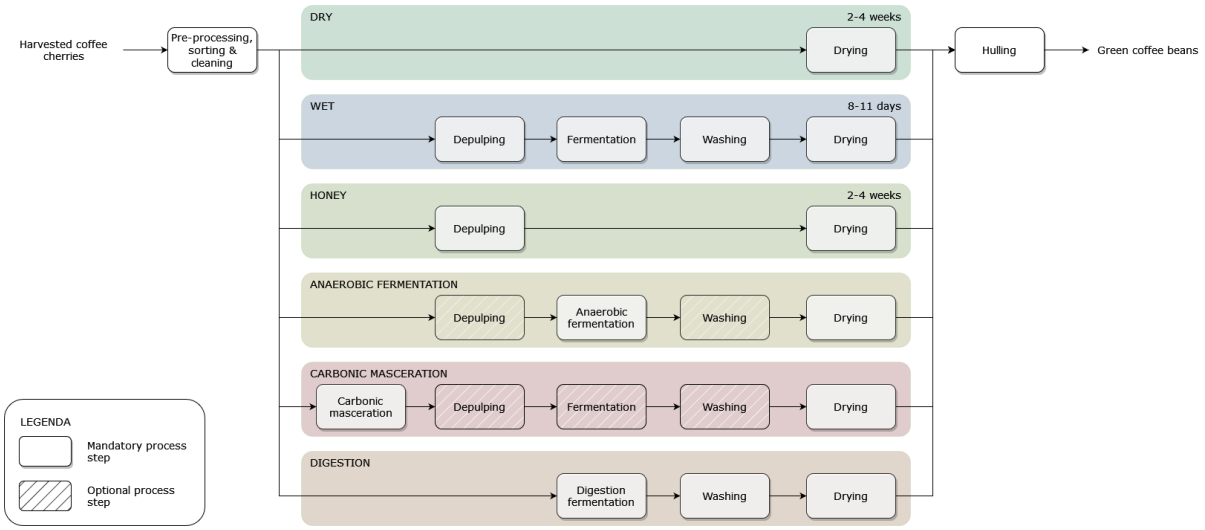

Figure 17: Differences between the dry, wet, honey, anaerobic fermentation, carbonic masceration, and digestion processing of harvested coffee cherries including the process duration. All processes eventually result in the green coffee bean after hulling of the processed coffee bean.

Coffee processing units in Wayanad

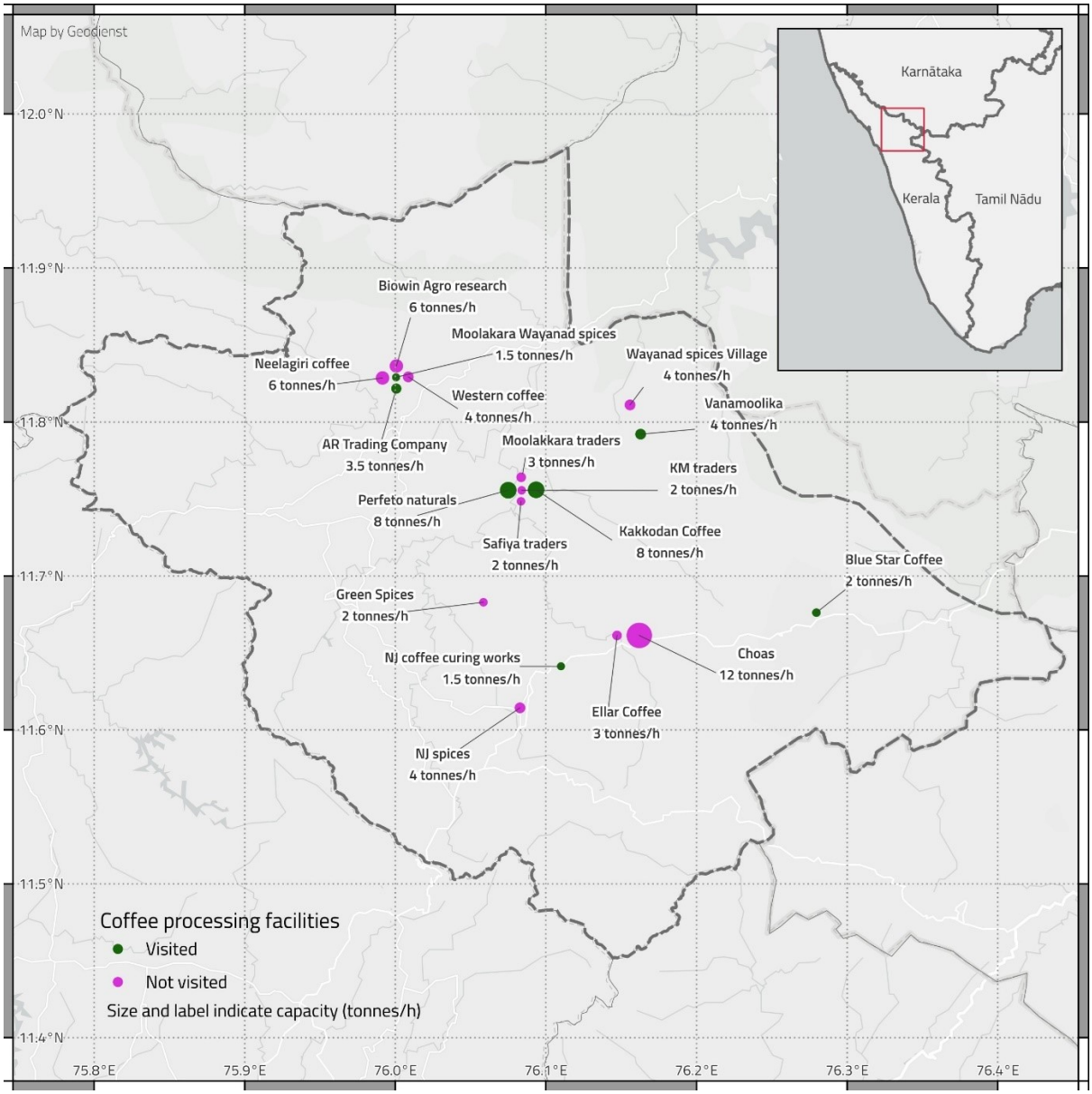

Figure 18: Coffee processing units in the district of Wayanad in Kerala, India. Iglesias (2023) visited some of the coffee processing units which are indicated on the map.

Chemical reactions during gasification

Table 15: Chemical reactions included in the gasification model. (Ruiz et al., 2013; Pala et al., 2017; Pilar González-Vázquez et al., 2021)

#	Chemical reaction	Name	ΔH^0_{298K} (kJ/mol)
R-1	$C + O_2 \leftrightarrow CO_2$	Carbon combustion	-393.0
R-2	$C + \frac{1}{2} O_2 \leftrightarrow CO$	Partial oxidation of carbon	-112.0
R-3	$C + CO_2 \leftrightarrow 2\ CO$	Boudouard	+172.0
R-4	$C + H_2O \leftrightarrow CO + H_2$	Water-gas	+131.0
R-5	$CO + H_2O \leftrightarrow CO_2 + H_2$	Water-gas shift	-41.0
R-6	$C + H_2 \leftrightarrow CH_4$	Methanation of carbon	-74.0
R-7	$H_2 + \frac{1}{2} O_2 \leftrightarrow H_2O$	Hydrogen partial combustion	-242.0
R-8	$CH_4 + H_2O \leftrightarrow CO_2 + 3\ H_2$	Steam methane reforming	+206.0
R-9	$H_2 + S \leftrightarrow H_2S$	H_2S formation	-20.2

Process model in Aspen Plus

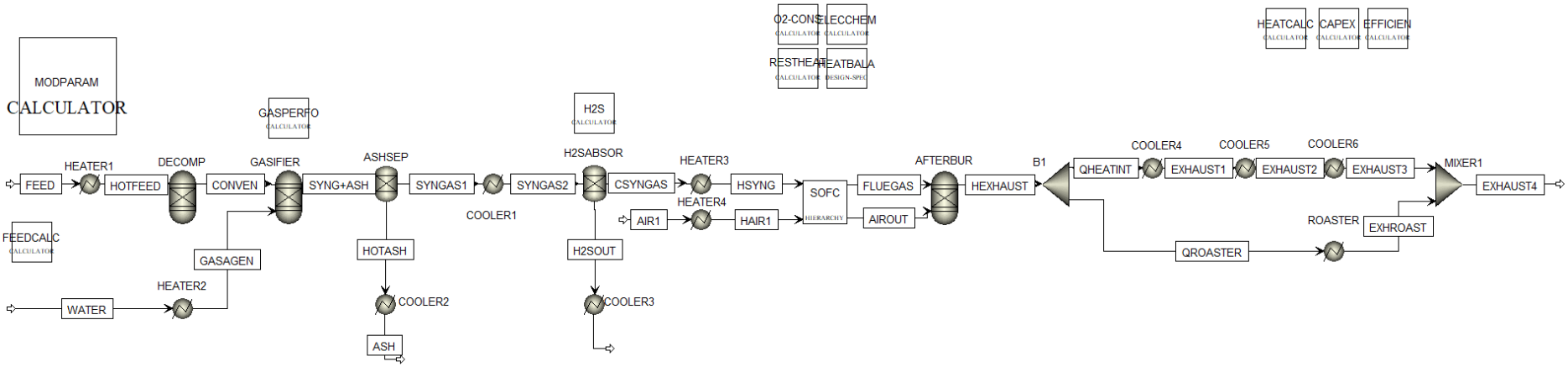

Figure 19: Complete model visualization in Aspen Plus of the biomass conversion process using coffee husk as a feedstock including the Calculator and DesignSpec blocks for system customization regarding the electrochemistry of the SOFC and the different system efficiencies and costs.

Table 16: Discounted cash flows and energy output over the first 10 years of the 30 year lifetime of the coffee husk energy plant modelled in this study.

	Year											
	0	**1**	**2**	**3**	**4**	**5**	**6**	**7**	**8**	**9**	**10**	...
Costs (x1000)												
Investment	$24,089.2	-	-	-	-	-	-	-	-	-	-	...
Operational costs	-	$375.8	$390.8	$406.5	$422.7	$439.6	$457.2	$475.5	$494.5	$514.3	$534.9	...
Ash disposal	-	$9.7	$10.1	$10.5	$11.0	$11.4	$11.8	$12.3	$12.8	$13.3	$13.9	...
LPG savings	-	$-277.5	$-288.6	$-300.1	$-312.1	$-324.6	$-337.6	$-351.1	$-365.1	$-379.7	$-394.9	...
Electricity savings	-	$-46.7	$-48.5	$-50.5	$-52.5	$-54.6	$-56.8	$-59.1	$-61.4	$-63.9	$-66.4	...
Total	$24,089.2	$61.4	$63.8	$66.4	$69.0	$71.8	$74.7	$77.7	$80.8	$84.0	$87.4	...
Discount rate	100.00%	93.6%	87.6%	81.9%	76.7%	71.7%	67.1%	62.8%	58.8%	55.0%	51.5%	...
Present value	$24,089.2	$57.4	$55.9	$54.4	$52.9	$51.5	$50.1	$48.8	$47.5	$46.2	$45.0	...
NPV of costs	$25,282.9											
Energy												...
Net output (MWh)	-	4464	4464	4464	4464	4464	4464	4464	4464	4464	4464	...
Present value (MWh)	-	4177	3909	3657	3422	3202	2996	2804	2624	2455	2297	...
NPV of energy	56130	MWh										
LCOE	**450.43**	$/MWh										

References

Abdul-Azeez, K., Suraj, P., Muraleedharan, C., & Arun, P. (2023, March). Aspen plus simulation of biomass gasification: a comprehensive model incorporating reaction kinetics, hydrodynamics and tar production. *Process Integration and Optimization for Sustainability*, *7*(1), 255–268.

Abedinia, O., Shakibi, H., Shokri, A., Sobhani, B., Sobhani, B., Yari, M., & Bagheri, M. (2024). Optimization of a syngas-fueled sofc-based multigeneration system: Enhanced performance with biomass and gasification agent selection. *Renewable and Sustainable Energy Reviews*, *199*, 114460. Retrieved from https://www.sciencedirect.com/science/article/pii/S1364032124001837 doi: https://doi.org/10.1016/j.rser.2024.114460

Adams, M. R., & Dougan, J. (1987). Waste products. In R. J. Clarke & R. Macrae (Eds.), *Coffee: Volume 2: Technology* (pp. 257–291). Dordrecht: Springer Netherlands. Retrieved from https://doi.org/10.1007/978-94-009-3417-7_9 doi: 10.1007/978-94-009-3417-7_9

Alves, R. C., Rodrigues, F., Antónia Nunes, M., Vinha, A. F., & Oliveira, M. B. P. (2017). Chapter 1 - state of the art in coffee processing by-products. In C. M. Galanakis (Ed.), *Handbook of coffee processing by-products* (p. 1-26). Academic Press. Retrieved from https://www.sciencedirect.com/science/article/pii/B9780128112908000013 doi: https://doi.org/10.1016/B978-0-12-811290-8.00001-3

Anukam, A., Mamphweli, S., Reddy, P., Meyer, E., & Okoh, O. (2016). Pre-processing of sugarcane bagasse for gasification in a downdraft biomass gasifier system: A comprehensive review. *Renewable and Sustainable Energy Reviews*, *66*, 775-801. Retrieved from https://www.sciencedirect.com/science/article/pii/S1364032116304762 doi: https://doi.org/10.1016/j.rser.2016.08.046

Aravind, P., & de Jong, W. (2012). Evaluation of high temperature gas cleaning options for biomass gasification product gas for solid oxide fuel cells. *Progress in Energy and Combustion Science*, *38*(6), 737-764. Retrieved from https://www.sciencedirect.com/science/article/pii/S0360128512000214 doi: https://doi.org/10.1016/j.pecs.2012.03.006

Aravind, P. V., Champatan, V., Gopi, G., Vijay, V., Smit, C., Pande, S., ... Nampoothiri, K. U. K. (2022). Negative emissions at negative cost-an opportunity for a scalable niche. *Frontiers in Energy Research*, *10*. Retrieved from https://www.frontiersin.org/articles/10.3389/fenrg.2022.806435 doi: 10.3389/fenrg.2022.806435

Aristizábal-Marulanda, V., Chacón-Perez, Y., & Cardona Alzate, C. A. (2017). Chapter 3 - the biorefinery concept for the industrial valorization of coffee processing by-products. In C. M. Galanakis (Ed.), *Handbook of coffee processing by-products* (p. 63-92). Academic Press. Retrieved from https://www.sciencedirect.com/science/article/pii/B9780128112908000037 doi: https://doi.org/10.1016/B978-0-12-811290-8.00003-7

Arya, S. S., Venkatram, R., More, P. R., & Vijayan, P. (2022, February). The wastes of coffee bean processing for utilization in food: a review. *Journal of Food Science and Technology*, *59*(2), 429-444.

Barreto Peixoto, J. A., Silva, J. F., Oliveira, M. B. P. P., & Alves, R. C. (2023). Sustainability issues along the coffee chain: From the field to the cup. *Comprehensive Reviews in Food Science and Food Safety*, *22*(1), 287-332. Retrieved from https://ift.onlinelibrary.wiley.com/doi/abs/10.1111/1541-4337.13069 doi: https://doi.org/10.1111/1541-4337.13069

Bastian, F., Hutabarat, O. S., Dirpan, A., Nainu, F., Harapan, H., Emran, T. B., & Simal-Gandara, J. (2021). From plantation to cup: Changes in bioactive compounds during coffee processing. *Foods*, *10*(11). Retrieved from https://www.mdpi.com/2304-8158/10/11/2827 doi: 10.3390/foods10112827

Baêta, B. E. L., de Miranda Cordeiro, P. H., Passos, F., Gurgel, L. V. A., de Aquino, S. F., & Fdz-Polanco, F. (2017). Steam explosion pretreatment improved the biomethaniza-

tion of coffee husks. *Bioresource Technology*, *245*, 66-72. Retrieved from https://www.sciencedirect.com/science/article/pii/S0960852417314244 doi: https://doi.org/10.1016/j.biortech.2017.08.110

Begum, S., Rasul, M. G., Akbar, D., & Ramzan, N. (2013). Performance analysis of an integrated fixed bed gasifier model for different biomass feedstocks. *Energies*, *6*(12), 6508–6524. Retrieved from https://www.mdpi.com/1996-1073/6/12/6508 doi: 10.3390/en6126508

Bonilla, J., Gordillo, G., & Cantor, C. (2019). Experimental gasification of coffee husk using pure oxygen-steam blends. *Frontiers in Energy Research*, *7*. Retrieved from https://www.frontiersin.org/articles/10.3389/fenrg.2019.00127 doi: 10.3389/fenrg.2019.00127

Borrelli, R. C., Esposito, F., Napolitano, A., Ritieni, A., & Fogliano, V. (2004, March). Characterization of a new potential functional ingredient: coffee silverskin. *J Agric Food Chem*, *52*(5), 1338–1343.

Buttler, A., Koltun, R., Wolf, R., & Spliethoff, H. (2015). A detailed techno-economic analysis of heat integration in high temperature electrolysis for efficient hydrogen production. *International Journal of Hydrogen Energy*, *40*(1), 38-50. Retrieved from https://www.sciencedirect.com/science/article/pii/S0360319914028511 doi: https://doi.org/10.1016/j.ijhydene.2014.10.048

Cardoen, D., Joshi, P., Diels, L., Sarma, P. M., & Pant, D. (2015). Agriculture biomass in india: Part 1. estimation and characterization. *Resources, Conservation and Recycling*, *102*, 39-48. Retrieved from https://www.sciencedirect.com/science/article/pii/S0921344915300227 doi: https://doi.org/10.1016/j.resconrec.2015.06.003

Cerone, N., & Zimbardi, F. (2021). Effects of oxygen and steam equivalence ratios on updraft gasification of biomass. *Energies*, *14*(9). Retrieved from https://www.mdpi.com/1996-1073/14/9/2675 doi: 10.3390/en14092675

CFI. (2024a). *Levelized Cost of Energy (LCOE)*. Retrieved 2024-01-18, from https://corporatefinanceinstitute.com/resources/valuation/levelized-cost-of-energy-lcoe/

CFI. (2024b). *Net Present Value (NPV)*. Retrieved 2024-01-21, from https://corporatefinanceinstitute.com/resources/valuation/net-present-value-npv/

Chan, S., Ho, H., & Tian, Y. (2002). Modelling of simple hybrid solid oxide fuel cell and gas turbine power plant. *Journal of Power Sources*, *109*(1), 111-120. Retrieved from https://www.sciencedirect.com/science/article/pii/S0378775302000514 doi: https://doi.org/10.1016/S0378-7753(02)00051-4

Chan, S., Khor, K., & Xia, Z. (2001). A complete polarization model of a solid oxide fuel cell and its sensitivity to the change of cell component thickness. *Journal of Power Sources*, *93*(1), 130-140. Retrieved from https://www.sciencedirect.com/science/article/pii/S0378775300005565 doi: https://doi.org/10.1016/S0378-7753(00)00556-5

Chemical Engineering. (2024). *The Chemical Engineering Plant Cost Index ®*. Retrieved 2024-06-28, from https://www.chemengonline.com/pci-home

Choudhary, T., & Sanjay. (2016). Computational analysis of ir-sofc: Transient, thermal stress, carbon deposition and flow dependency. *International Journal of Hydrogen Energy*, *41*(24), 10212-10227. Retrieved from https://www.sciencedirect.com/science/article/pii/S0360319916308552 doi: https://doi.org/10.1016/j.ijhydene.2016.04.016

Colpan, C. O., Dincer, I., & Hamdullahpur, F. (2007). Thermodynamic modeling of direct internal reforming solid oxide fuel cells operating with syngas. *International Journal of Hydrogen Energy*, *32*(7), 787-795. Retrieved from https://www.sciencedirect.com/science/article/pii/S0360319906005374 (Fuel Cells) doi: https://doi.org/10.1016/j.ijhydene.2006.10.059

Corigliano, O., & Fragiacomo, P. (2020). Extensive analysis of sofc fed by direct syngas at different anodic compositions by using two numerical approaches. *Energy Conver-*

sion and Management, *209*, 112664. Retrieved from https://www.sciencedirect.com/science/article/pii/S0196890420302028 doi: https://doi.org/10.1016/j.enconman.2020.112664

Corigliano, O., Lorenzo, G. D., & Fragiacomo, P. (2021). Techno-energy-economic sensitivity analysis of hybrid system solid oxide fuel cell/gas turbine. *AIMS Energy*, *9*(5), 934-990. Retrieved from https://www.aimspress.com/article/doi/10.3934/energy.2021044 doi: 10.3934/energy.2021044

Cruz-O'Byrne, R., Piraneque, N., Aguirre, S., & Ramirez-Vergara, J. (2020, 10). Microorganisms in coffee fermentation: A bibliometric and systematic literature network analysis related to agriculture and beverage quality (1965-2019). *Coffee Science*, *15*, e151773. doi: 10.25186/.v15i.1773

Custom Market Insights. (2024, January). *India Coffee Market 2024–2033*. Retrieved 2024-08-05, from https://www.custommarketinsights.com/report/india-coffee-market/

Davis, A. P., Gole, T. W., Baena, S., & Moat, J. (2012, November). The impact of climate change on indigenous arabica coffee (coffea arabica): Predicting future trends and identifying priorities. *PLOS ONE*, *7*(11), 1-13. Retrieved from https://doi.org/10.1371/journal.pone.0047981 doi: 10.1371/journal.pone.0047981

de Melo Pereira, G. V., de Carvalho Neto, D. P., Magalhães Júnior, A. I., Vásquez, Z. S., Medeiros, A. B., Vandenberghe, L. P., & Soccol, C. R. (2019). Exploring the impacts of postharvest processing on the aroma formation of coffee beans – a review. *Food Chemistry*, *272*, 441-452. Retrieved from https://www.sciencedirect.com/science/article/pii/S0308814618314663 doi: https://doi.org/10.1016/j.foodchem.2018.08.061

de Oliveira, J. L., da Silva, J. N., Martins, M. A., Pereira, E. G., & da Conceição Trindade Bezerra e Oliveira, M. (2018). Gasification of waste from coffee and eucalyptus production as an alternative source of bioenergy in brazil. *Sustainable Energy Technologies and Assessments*, *27*, 159-166. Retrieved from https://www.sciencedirect.com/science/article/pii/S2213138817302655 doi: https://doi.org/10.1016/j.seta.2018.04.005

Djamel, H., Hafsia, A., Bariza, Z., Hocine, B. M., & Kafia, O. (2013). Thermal field in sofc fed by hydrogen: Inlet gases temperature effect. *International Journal of Hydrogen Energy*, *38*(20), 8575-8583. Retrieved from https://www.sciencedirect.com/science/article/pii/S0360319913000566 doi: https://doi.org/10.1016/j.ijhydene.2013.01.004

Doherty, W., Reynolds, A., & Kennedy, D. (2010). Computer simulation of a biomass gasification-solid oxide fuel cell power system using aspen plus. *Energy*, *35*(12), 4545-4555. Retrieved from https://www.sciencedirect.com/science/article/pii/S0360544210002598 (The 3rd International Conference on Sustainable Energy and Environmental Protection, SEEP 2009) doi: https://doi.org/10.1016/j.energy.2010.04.051

Dong, W., Hu, R., Chu, Z., Zhao, J., & Tan, L. (2017). Effect of different drying techniques on bioactive components, fatty acid composition, and volatile profile of robusta coffee beans. *Food Chemistry*, *234*, 121-130. Retrieved from https://www.sciencedirect.com/science/article/pii/S0308814617307410 doi: https://doi.org/10.1016/j.foodchem.2017.04.156

dos Santos, L. C., Adarme, O. F. H., Baêta, B. E. L., Gurgel, L. V. A., & de Aquino, S. F. (2018). Production of biogas (methane and hydrogen) from anaerobic digestion of hemicellulosic hydrolysate generated in the oxidative pretreatment of coffee husks. *Bioresource Technology*, *263*, 601-612. Retrieved from https://www.sciencedirect.com/science/article/pii/S0960852418306977 doi: https://doi.org/10.1016/j.biortech.2018.05.037

Duque-Dussán, E., Figueroa-Varela, P. A., & Sanz-Uribe, J. R. (2023, October 5). Peaberry shape and size influence on different coffee postharvest processes. *Journal of Food Process Engineering*, *n/a*(n/a), e14461. Retrieved from https://onlinelibrary.wiley.com/doi/abs/10.1111/jfpe.14461 doi: https://doi.org/10.1111/jfpe.14461

Elcogen. (2024). *Solid Oxide Fuel Cells - SOFC Technical Data.* Retrieved 2024-5-11, from https://elcogen.com/products/solid-oxide-fuel-cells/

Engineering Toolbox. (2003). *Heat Exchangers - Overall Heat Transfer Coefficients.* Retrieved 2024-07-02, from https://www.engineeringtoolbox.com/heat-transfer-coefficients-exchangers-d_450.html

European Commission. (2019, February 28). *Innovative large-scale energy storage technologies and power-to-gas concepts after optimization.* Retrieved from https://ec.europa.eu/research/participants/documents/downloadPublic?documentIds=080166e5c58ae3ff&appId=PPGMS

Fang, Q., Blum, L., Peters, R., Peksen, M., Batfalsky, P., & Stolten, D. (2015). Sofc stack performance under high fuel utilization. *International Journal of Hydrogen Energy*, *40*(2), 1128-1136. Retrieved from https://www.sciencedirect.com/science/article/pii/S0360319914032285 doi: https://doi.org/10.1016/j.ijhydene.2014.11.094

Febrianto, N. A., & Zhu, F. (2023). Coffee bean processing: Emerging methods and their effects on chemical, biological and sensory properties. *Food Chemistry*, *412*, 135489. Retrieved from https://www.sciencedirect.com/science/article/pii/S030881462300105X doi: https://doi.org/10.1016/j.foodchem.2023.135489

Foreign Agricultural Service. (2023, May 12). *Coffee Annual - 2023, country India.* Retrieved from https://fas.usda.gov/data/india-coffee-annual-7

Franca, A. S., & Oliveira, L. S. (2008). Chemistry of defective coffee beans. *Food chemistry research developments*, *4*(1), 105–138.

Fu, X., Li, G., Hu, F., Huang, J., Lou, Y., Li, Y., ... Cheng, J. (2023, feb 27). Comparative transcriptome analysis in peaberry and regular bean coffee to identify bean quality associated genes. *BMC Genomic Data*, *24*(1), 12. Retrieved from https://doi.org/10.1186/s12863-022-01098-y doi: 10.1186/s12863-022-01098-y

Gholaminezhad, I., Paydar, M. H., Jafarpur, K., & Paydar, S. (2017). Multi-scale mathematical modeling of methane-fueled sofcs: Predicting limiting current density using a modified fick's model. *Energy Conversion and Management*, *148*, 222-237. Retrieved from https://www.sciencedirect.com/science/article/pii/S0196890417305307 doi: https://doi.org/10.1016/j.enconman.2017.05.071

Glantz, M., & Kissell, R. (2014). Chapter 1 - introduction to multi-asset risk modeling—lessons from the debt crisis. In M. Glantz & R. Kissell (Eds.), *Multi-asset risk modeling* (p. 1-19). San Diego: Academic Press. Retrieved from https://www.sciencedirect.com/science/article/pii/B9780124016903000019 doi: https://doi.org/10.1016/B978-0-12-401690-3.00001-9

Good Returns. (2024). *LPG Price in Kerala (3rd July 2024).* Retrieved 2024-07-03, from https://www.goodreturns.in/lpg-price-in-kerala-s18.html

Gouvea, B. M., Torres, C., Franca, A. S., Oliveira, L. S., & Oliveira, E. S. (2009, sep 01). Feasibility of ethanol production from coffee husks. *Biotechnology Letters*, *31*(9), 1315-1319. Retrieved from https://doi.org/10.1007/s10529-009-0023-4 doi: 10.1007/s10529-009-0023-4

Guo, S., Zhang, J., Zhang, H., & Bi, Y. (2024). Multi-criteria study and optimization of an innovative combined scheme utilizing compressed air energy storage for a modified solid oxide fuel cell-driven gas turbine power plant fueled by biomass feedstock. *Energy Conversion and Management*, *314*, 118731. Retrieved from https://www.sciencedirect.com/science/article/pii/S0196890424006721 doi: https://doi.org/10.1016/j.enconman.2024.118731

Hami, M., & Mahmoudimehr, J. (2023). When to switch from heat-up to start-up in the warming-up process of a solid oxide fuel cell: A numerical study and multi-objective planning. *Journal of Power Sources*, *585*, 233656. Retrieved from https://www.sciencedirect.com/science/article/pii/S0378775323010327 doi: https://doi

.org/10.1016/j.jpowsour.2023.233656
Hasanzadeh, A., Chitsaz, A., Mojaver, P., & Ghasemi, A. (2021). Stand-alone gas turbine and hybrid mcfc and sofc-gas turbine systems: Comparative life cycle cost, environmental, and energy assessments. *Energy Reports*, *7*, 4659-4680. Retrieved from https://www.sciencedirect.com/science/article/pii/S2352484721005151 doi: https://doi.org/10.1016/j.egyr.2021.07.050
Hauck, M., Herrmann, S., & Spliethoff, H. (2017). Simulation of a reversible sofc with aspen plus. *International Journal of Hydrogen Energy*, *42*(15), 10329-10340. Retrieved from https://www.sciencedirect.com/science/article/pii/S0360319917303579 doi: https://doi.org/10.1016/j.ijhydene.2017.01.189
HBR. (2004, December). *Making Real Options Really Work* . Retrieved 2024-01-19, from https://hbr.org/2004/12/making-real-options-really-work
Hejna, A. (2021). Potential applications of by-products from the coffee industry in polymer technology – current state and perspectives. *Waste Management*, *121*, 296-330. Retrieved from https://www.sciencedirect.com/science/article/pii/S0956053X20307078 doi: https://doi.org/10.1016/j.wasman.2020.12.018
Hernández-Pacheco, E., Singh, D., Hutton, P. N., Patel, N., & Mann, M. D. (2004). A macro-level model for determining the performance characteristics of solid oxide fuel cells. *Journal of Power Sources*, *138*(1), 174-186. Retrieved from https://www.sciencedirect.com/science/article/pii/S0378775304007098 doi: https://doi.org/10.1016/j.jpowsour.2004.06.051
Hoseini, M., Cocco, S., Casucci, C., Cardelli, V., & Corti, G. (2021). Coffee by-products derived resources. a review. *Biomass and Bioenergy*, *148*, 106009. Retrieved from https://www.sciencedirect.com/science/article/pii/S0961953421000465 doi: https://doi.org/10.1016/j.biombioe.2021.106009
IEA. (2023). *Quarterly average wholesale prices for selected regions, 2019-2025*. Retrieved 2024-07-02, from https://www.iea.org/data-and-statistics/charts/quarterly-average-wholesale-prices-for-selected-regions-2019-2025
IEA. (2024, February 7). *India could triple its biofuel use and accelerate global deployment*. Retrieved 2024-07-21, from https://www.iea.org/commentaries/india-could-triple-its-biofuel-use-and-accelerate-global-deployment
Iglesias, S. (2023). *Carbon emissions and energy efficiency of Robusta coffee processing*. Unpublished PhD thesis.
International Coffee Organization. (2024, June). *Coffee market report june 2024*. https://www.icocoffee.org/documents/cy2023-24/cmr-0624-e.pdf. (Accessed: 2024-08-05)
Investopedia. (2024, June 13). *Cost of Capital vs. Discount Rate: What's the Difference?* Retrieved 2024-06-25, from https://www.investopedia.com/ask/answers/052715/what-difference-between-cost-capital-and-discount-rate.asp
IRENA. (2012). *RENEWABLE ENERGY TECHNOLOGIES: COST ANALYSIS SERIES - Biomass for Power Generation*. Retrieved from https://www.irena.org/-/media/Files/IRENA/Agency/Publication/2012/RE_Technologies_Cost_Analysis-BIOMASS.pdf
IRENA. (2022). *Renewable power generation costs in 2022*. Retrieved from https://www.irena.org/-/media/Files/IRENA/Agency/Publication/2023/Aug/IRENA_Renewable_power_generation_costs_in_2022.pdf?rev=cccb713bf8294cc5bec3f870e1fa15c2
Janissen, B., & Huynh, T. (2018). Chemical composition and value-adding applications of coffee industry by-products: A review. *Resources, Conservation and Recycling*, *128*, 110-117. Retrieved from https://www.sciencedirect.com/science/article/pii/S0921344917303154 doi: https://doi.org/10.1016/j.resconrec.2017.10.001
Jayachandra, T., Venugopal, C., & Anu Appaiah, K. (2011). Utilization of phytotoxic agro waste— coffee cherry husk through pretreatment by the ascomycetes fungi mycotypha for biomethanation. *Energy for Sustainable Development*, *15*(1), 104-108. Retrieved from

https://www.sciencedirect.com/science/article/pii/S0973082611000032 doi: https://doi.org/10.1016/j.esd.2011.01.001

Jia, J., Abudula, A., Wei, L., Sun, B., & Shi, Y. (2015). Thermodynamic modeling of an integrated biomass gasification and solid oxide fuel cell system. *Renewable Energy*, *81*, 400-410. Retrieved from https://www.sciencedirect.com/science/article/pii/S0960148115002128 doi: https://doi.org/10.1016/j.renene.2015.03.030

Klingel, T., Kremer, J. I., Gottstein, V., Rajcic de Rezende, T., Schwarz, S., & Lachenmeier, D. W. (2020). A review of coffee by-products including leaf, flower, cherry, husk, silver skin, and spent grounds as novel foods within the european union. *Foods*, *9*(5). Retrieved from https://www.mdpi.com/2304-8158/9/5/665

Kumar, N., & Goel, N. (2019). Phenolic acids: Natural versatile molecules with promising therapeutic applications. *Biotechnology reports*, *24*, e00370. doi: https://doi.org/10.1016/j.btre.2019.e00370

Li, H., Zhang, R., Wang, T., Sun, X., Hou, C., Xu, R., ... Tang, Z. (2022). Simulation of h2s and co2 removal from igcc syngas by cryogenic distillation. *Carbon Capture Science Technology*, *3*, 100012. Retrieved from https://www.sciencedirect.com/science/article/pii/S2772656821000129 doi: https://doi.org/10.1016/j.ccst.2021.100012

Liu, W., Liu, C., Gogoi, P., & Deng, Y. (2020). Overview of biomass conversion to electricity and hydrogen and recent developments in low-temperature electrochemical approaches. *Engineering*, *6*(12), 1351-1363. Retrieved from https://www.sciencedirect.com/science/article/pii/S2095809920303039 doi: https://doi.org/10.1016/j.eng.2020.02.021

Malek, A. A., Kawsary, M., & Hasanuzzaman, M. (2022). Chapter 10 - economic assessment of solar thermal energy technologies. In M. Hasanuzzaman (Ed.), *Technologies for solar thermal energy* (p. 293-322). Academic Press. Retrieved from https://www.sciencedirect.com/science/article/pii/B9780128239599000040 doi: https://doi.org/10.1016/B978-0-12-823959-9.00004-0

Martuscelli, M., Esposito, L., Di Mattia, C. D., Ricci, A., & Mastrocola, D. (2021, June). Characterization of coffee silver skin as potential food-safe ingredient. *Foods*, *10*(6), 1367. doi: https://doi.org/10.3390/foods10061367

Ministry of Commerce and Industry. (2022). *Coffee Board India.* Retrieved 2024-08-05, from https://coffeeboard.gov.in/coffee-statistics.html

Motta, I. L., Miranda, N. T., Maciel Filho, R., & Wolf Maciel, M. R. (2018). Biomass gasification in fluidized beds: A review of biomass moisture content and operating pressure effects. *Renewable and Sustainable Energy Reviews*, *94*, 998-1023. Retrieved from https://www.sciencedirect.com/science/article/pii/S1364032118304805 doi: https://doi.org/10.1016/j.rser.2018.06.042

Murthy, P. S., & Madhava Naidu, M. (2012). Sustainable management of coffee industry by-products and value addition—a review. *Resources, Conservation and Recycling*, *66*, 45-58. Retrieved from https://www.sciencedirect.com/science/article/pii/S0921344912000894 doi: https://doi.org/10.1016/j.resconrec.2012.06.005

Myhrvold, N. (2023, January 20). *coffee roasting.* Retrieved 2024-08-05, from https://www.britannica.com/topic/coffee-roasting

National Coffee Association of U.S.A., Inc. (2023). *What is Coffee?* Retrieved 2023-11-16, from https://www.ncausa.org/About-Coffee/What-is-Coffee

NLWorks. (2023). *India Climate Smart Coffee.* Retrieved 2024-01-03, from https://nl-works.com/program/climate-smart-coffee-consortium/

Oliveira, L. S., & Franca, A. S. (2015). Chapter 31 - an overview of the potential uses for coffee husks. In V. R. Preedy (Ed.), *Coffee in health and disease prevention* (p. 283-291). San Diego: Academic Press. Retrieved from https://www.sciencedirect.com/science/article/pii/B9780124095175000310 doi: https://doi.org/10.1016/B978-0-12-409517-5.00031-0

Ong, K. M., Lee, W. Y., Hanna, J., & Ghoniem, A. F. (2016). Isolating the impact of co concentration in syngas mixtures on sofc performance via internal reforming and direct oxidation. *International Journal of Hydrogen Energy*, *41*(21), 9035-9047. Retrieved from https://www.sciencedirect.com/science/article/pii/S0360319916300490 doi: https://doi.org/10.1016/j.ijhydene.2016.03.107

Our World in Data. (2023, April 18). *Learning curves: What does it mean for a technology to follow Wright's Law*. Retrieved 2024-07-19, from https://ourworldindata.org/learning-curve

Pala, L. P. R., Wang, Q., Kolb, G., & Hessel, V. (2017). Steam gasification of biomass with subsequent syngas adjustment using shift reaction for syngas production: An aspen plus model. *Renewable Energy*, *101*, 484-492. Retrieved from https://www.sciencedirect.com/science/article/pii/S0960148116307790 doi: https://doi.org/10.1016/j.renene.2016.08.069

Passos, F., Cordeiro, P. H. M., Baeta, B. E. L., de Aquino, S. F., & Perez-Elvira, S. I. (2018). Anaerobic co-digestion of coffee husks and microalgal biomass after thermal hydrolysis. *Bioresource Technology*, *253*, 49-54. Retrieved from https://www.sciencedirect.com/science/article/pii/S0960852417322162 doi: https://doi.org/10.1016/j.biortech.2017.12.071

PDH Online. (2020). *Shell and Tube Heat Exchangers - Basic Calculations*. Retrieved 2024-07-02, from https://www.pdhonline.com/courses/m371/m371content.pdf

Permana, D. I., Fagioli, F., De Lucia, M., Rusirawan, D., & Farkas, I. (2024). Energy, exergy, environmental and economy (4e) analysis of the existing of biomass-orc plant with capacity 150 kwe: A case study. *Energy Conversion and Management: X*, *23*, 100646. Retrieved from https://www.sciencedirect.com/science/article/pii/S2590174524001247 doi: https://doi.org/10.1016/j.ecmx.2024.100646

Pilar González-Vázquez, M., Rubiera, F., Pevida, C., Pio, D. T., & Tarelho, L. A. (2021). Thermodynamic analysis of biomass gasification using aspen plus: Comparison of stoichiometric and non-stoichiometric models. *Energies*, *14*(1). Retrieved from https://www.mdpi.com/1996-1073/14/1/189

Poisson, L., Blank, I., Dunkel, A., & Hofmann, T. (2017). Chapter 12 - the chemistry of roasting—decoding flavor formation. In B. Folmer (Ed.), *The craft and science of coffee* (p. 273-309). Academic Press. Retrieved from https://www.sciencedirect.com/science/article/pii/B9780128035207000128 doi: https://doi.org/10.1016/B978-0-12-803520-7.00012-8

Poltronieri, P., & Rossi, F. (2016). Challenges in specialty coffee processing and quality assurance. *Challenges*, *7*(2). Retrieved from https://www.mdpi.com/2078-1547/7/2/19

Poyilil, S., Palatel, A., & Chandrasekharan, M. (2022, July). Physico-chemical characterization study of coffee husk for feasibility assessment in fluidized bed gasification process. *Environmental Science and Pollution Research*, *29*(34), 51041–51053.

PwC Worldwide Tax Summaries. (2024, May 15). *India: Corporate - Taxes on corporate income*. Retrieved 2024-06-25, from https://taxsummaries.pwc.com/india/corporate/taxes-on-corporate-income

Radenahmad, N., Azad, A. T., Saghir, M., Taweekun, J., Bakar, M. S. A., Reza, M. S., & Azad, A. K. (2020). A review on biomass derived syngas for sofc based combined heat and power application. *Renewable and Sustainable Energy Reviews*, *119*, 109560. Retrieved from https://www.sciencedirect.com/science/article/pii/S1364032119307683 doi: https://doi.org/10.1016/j.rser.2019.109560

Rahim, D. A., Fang, W., Wibowo, H., Hantoko, D., Susanto, H., Yoshikawa, K., ... Yan, M. (2023). Review of high temperature h2s removal from syngas: Perspectives on downstream process integration. *Chemical Engineering and Processing - Process Intensification*, *183*, 109258. Retrieved from https://www.sciencedirect.com/science/article/pii/

S0255270122004615 doi: https://doi.org/10.1016/j.cep.2022.109258
Rasmussen, J. F. B., & Hagen, A. (2010). The effect of h2s on the performance of sofcs using methane containing fuel. *Fuel Cells*, *10*(6), 1135-1142. Retrieved from https://onlinelibrary.wiley.com/doi/abs/10.1002/fuce.201000012 doi: https://doi.org/10.1002/fuce.201000012
Ruiz, J., Juárez, M., Morales, M., Muñoz, P., & Mendívil, M. (2013). Biomass gasification for electricity generation: Review of current technology barriers. *Renewable and Sustainable Energy Reviews*, *18*, 174-183. Retrieved from https://www.sciencedirect.com/science/article/pii/S1364032112005631 doi: https://doi.org/10.1016/j.rser.2012.10.021
Sadeghi, M., Mehr, A., Zar, M., & Santarelli, M. (2018). Multi-objective optimization of a novel syngas fed sofc power plant using a downdraft gasifier. *Energy*, *148*, 16-31. Retrieved from https://www.sciencedirect.com/science/article/pii/S0360544218301385 doi: https://doi.org/10.1016/j.energy.2018.01.114
Saenger, M., Hartge, E.-U., Werther, J., Ogada, T., & Siagi, Z. (2001). Combustion of coffee husks. *Renewable Energy*, *23*(1), 103-121. Retrieved from https://www.sciencedirect.com/science/article/pii/S0960148100001063 doi: https://doi.org/10.1016/S0960-1481(00)00106-3
Said, N. S. M., Abdullah, S. R. S., Ismail, N. Hasan, H. A., & Othman, A. R. (2023). Integrating treatment processes of coffee processing mill effluent for reclamation of secondary resources. *Journal of Cleaner Production*, *386*, 135837. Retrieved from https://www.sciencedirect.com/science/article/pii/S0959652622054117 doi: https://doi.org/10.1016/j.jclepro.2022.135837
Setter, C., Silva, F., Assis, M., Ataíde, C., Trugilho, P., & Oliveira, T. (2020). Slow pyrolysis of coffee husk briquettes: Characterization of the solid and liquid fractions. *Fuel*, *261*, 116420. Retrieved from https://www.sciencedirect.com/science/article/pii/S0016236119317740 doi: https://doi.org/10.1016/j.fuel.2019.116420
Seufert, V., Austin, S. E., Badami, M. G., Turner, S., & Ramankutty, N. (2023). The diversity of organic farmer motivations and livelihoods in the global south – a case study in kerala, india. *Geoforum*, *138*, 103670. Retrieved from https://www.sciencedirect.com/science/article/pii/S0016718522002548 doi: https://doi.org/10.1016/j.geoforum.2022.103670
Statista. (2024, April). *India: Inflation rate from 1987 to 2029*. Retrieved 2024-06-25, from https://www.statista.com/statistics/271322/inflation-rate-in-india/
Tera, I., Zhang, S., & Liu, G. (2024). A conceptual hydrogen, heat and power polygeneration system based on biomass gasification, sofc and waste heat recovery units: Energy, exergy, economic and emergy (4e) assessment. *Energy*, *295*, 131015. Retrieved from https://www.sciencedirect.com/science/article/pii/S0360544224007874 doi: https://doi.org/10.1016/j.energy.2024.131015
Towering Skills. (2024). *Cost Indices*. Retrieved 2024-06-28, from https://toweringskills.com/financial-analysis/cost-indices/#chemical-engineering-plant-cost-index-cepci
Tsai, J.-J., Chang, C.-C., Huang, D.-Y., Lin, T.-S., & Chen, Y.-C. (2023). Analysis and classification of coffee beans using single coffee bean mass spectrometry with machine learning strategy. *Food Chemistry*, *426*, 136610. Retrieved from https://www.sciencedirect.com/science/article/pii/S0308814623012281 doi: https://doi.org/10.1016/j.foodchem.2023.136610
USDA Foreign Agricultural Service. (2024). *Production - Coffee*. Retrieved 2024-08-05, from https://fas.usda.gov/data/production/commodity/0711100
Várady, M., Tauchen, J., Fraňková, A., Klouček, P., & Popelka, P. (2022). Effect of method of processing specialty coffee beans (natural, washed, honey, fermentation, maceration)

on bioactive and volatile compounds. *LWT*, *172*, 114245. Retrieved from https://www.sciencedirect.com/science/article/pii/S002364382201180X doi: https://doi.org/10.1016/j.lwt.2022.114245

World Nuclear Association. (2020, November 18). *Heat Values of Various Fuels*. Retrieved 2024-5-21, from https://world-nuclear.org/information-library/facts-and-figures/heat-values-of-various-fuels

Worldbank. (2022). *Lending Interest Rate*. Retrieved 2024-06-25, from https://data.worldbank.org/indicator/FR.INR.LEND?skipRedirection=true&view=map

Wu, H., Gu, J., BK, A., Nawaz, M. A., Barrow, C. J., Dunshea, F. R., & Suleria, H. A. (2022). Effect of processing on bioaccessibility and bioavailability of bioactive compounds in coffee beans. *Food Bioscience*, *46*, 101373. Retrieved from https://www.sciencedirect.com/science/article/pii/S2212429221004983 doi: https://doi.org/10.1016/j.fbio.2021.101373

Yu, C., Thy, P., Wang, L., Anderson, S., VanderGheynst, J., Upadhyaya, S., & Jenkins, B. (2014). Influence of leaching pretreatment on fuel properties of biomass. *Fuel Processing Technology*, *128*, 43-53. Retrieved from https://www.sciencedirect.com/science/article/pii/S0378382014002835 doi: https://doi.org/10.1016/j.fuproc.2014.06.030

Zhao, B., Jian, H., Qian, Y., Zhuge, W., Zhang, Y., & Zeng, Z. (2024). Analyzing the thermal and electrical performance of a tubular sofc with inserts by mass transfer coefficients. *Applied Thermal Engineering*, *242*, 122536. Retrieved from https://www.sciencedirect.com/science/article/pii/S1359431124002047 doi: https://doi.org/10.1016/j.applthermaleng.2024.122536